MARTIN MARIETTA ENERGY SYSTEMS LIBRARIES
3 4456 0059980 4

ORNL-5438

Nitrogen Oxide Absorption into Water and Dilute Nitric Acid in an Engineering-Scale Sieve-Plate Column—Description of a Mathematical Model and Comparison with Experimental Data

R. M. Counce

[redacted]

OAK RIDGE NATIONAL LABORATORY
CENTRAL RESEARCH LIBRARY
CIRCULATION SECTION
4500N ROOM 175
LIBRARY LOAN COPY
DO NOT TRANSFER TO ANOTHER PERSON
If you wish someone else to see this report, send in name with report and the library will arrange a loan.

OAK RIDGE NATIONAL LABORATORY
OPERATED BY UNION CARBIDE CORPORATION · FOR THE DEPARTMENT OF ENERGY

Printed in the United States of America. Available from
the Department of Energy,
Technical Information Center
P.O. Box 62, Oak Ridge, Tennessee 37830
Price: Printed Copy $8.00; Microfiche $3.00

This report was prepared as an account of work sponsored by an agency of the United States Government. Neither the United States Government nor any agency thereof, nor any of their employees, contractors, subcontractors, or their employees, makes any warranty, express or implied, nor assumes any legal liability or responsibility for any third party's use or the results of such use of any information, apparatus, product or process disclosed in this report, nor represents that its use by such third party would not infringe privately owned rights.

ORNL-5438
Dist. Category UC-79c

Contract No. W-7405-eng-26

ADVANCED FUEL RECYCLE PROGRAM

NITROGEN OXIDE ABSORPTION INTO WATER AND DILUTE NITRIC ACID IN AN ENGINEERING-SCALE SIEVE-PLATE COLUMN — DESCRIPTION OF A MATHEMATICAL MODEL AND COMPARISON WITH EXPERIMENTAL DATA

R. M. Counce
Chemical Technology Division

This report was prepared as a thesis and submitted to the faculty of the Graduate School of the University of Tennessee in partial fulfillment of the degree of Master of Science in the Department of Chemical, Metallurgical, and Polymer Engineering.

Date Published: September 1978

OAK RIDGE NATIONAL LABORATORY
Oak Ridge, Tennessee 37830
operated by
UNION CARBIDE CORPORATION
for the
DEPARTMENT OF ENERGY

MARTIN MARIETTA ENERGY SYSTEMS LIBRARIES
3 4456 0059980 4

ACKNOWLEDGEMENTS

This work was performed in the Chemical Technology Division under the auspices of the Advanced Fuel Recycle Program of the Oak Ridge National Laboratory.* The author is grateful for the interest of D. E. Ferguson, Division Director, W. D. Burch, Program Director, and W. S. Groenier, Manager of Engineering Research, whose support made this work possible.

The author wishes to acknowledge the numerous helpful suggestions of the Master's Committee from the Chemical, Metallurgical, and Polymer Engineering Department of the University of Tennessee: J. J. Perona (Chairman), J. M. Holmes, and J. S. Watson. Additionally, the author wishes to acknowledge the helpful suggestions of W. D. Holland and W. S. Groenier of the Chemical Technology Division. The assistance of E. C. Brantley, S. M. Gibson, and E. R. Johns of the Chemical Technology Division during the experimental phase of this study is also appreciated.

Special appreciation is expressed to M. S. Stewart of the Chemical Technology Division and R. H. Powell and R. V. Clark of the Information Division for their help in producing this manuscript.

*This report incorporates excerpts from previously issued documents, ORNL/TM-5910 and ORNL/TM-5921.

ABSTRACT

The study reported here is concerned with the absorption of gaseous NO_x compounds into water and dilute HNO_3 in a three-stage sieve-plate column with plates designed for high gas-liquid interfacial area. The performance of the column was measured while several operating parameters were varied. A mechanistic model was developed and presented to explain the observed phenomena.

The results of the study indicate the importance of three mechanisms in the absorption of gaseous NO_x compounds: (a) the absorption of NO_2^*, which results in the production of liquid HNO_3 and HNO_2; (b) the dissociation of the liquid HNO_2 into HNO_3 and gaseous NO; and (c) the gas-phase oxidation of NO to NO_2.

A useful model was developed to explain the absorption of NO_x compounds based on the above mechanisms. This model is presented and discussed.

TABLE OF CONTENTS

CHAPTER		PAGE
I.	INTRODUCTION AND SIGNIFICANCE	1
II.	LITERATURE REVIEW	3
	The NO_2-N_2O_4 Equilibrium	4
	The Absorption of NO_2^* into Water and Dilute HNO_3 Accompanied by Reaction with H_2O	5
	Reactions Involving Aqueous HNO_2	20
	The Oxidation of NO	23
	Reactions Involving N_2O_3	26
	Multiple-Plate and Packed Absorbers	26
	Literature Summary	30
III.	DEVELOPMENT OF THE MODEL	32
	A Mathematical Simulation of the NO_2-N_2O_4 Equilibrium	33
	The Local Absorption Rate of N_2O_4 into Water	34
	A Model for N_2O_4 Absorption in the Froth on the Sieve Plates	36
	A Model for the Dissociation of Liquid HNO_2 in the Froth on the Sieve Plates	43
	A Model for NO Oxidation in the Gas Space between the Sieve Plates	45
	The Overall Model for Predicting NO_x Removal in a Multistage Column	47
IV.	EXPERIMENTAL APPARATUS AND PROCEDURE	49
V.	EXPERIMENTAL DATA AND QUANTITATIVE DESCRIPTION OF RESULTS	54
VI.	CORRELATION OF DATA AND DISCUSSION OF RESULTS	75
	Single-Plate Data	75
	Three-Stage Column Data	80
VII.	CONCLUSIONS AND RECOMMENDATIONS	90
	Conclusions	90
	Recommendations	90
LIST OF REFERENCES		91

PAGE

APPENDIXES 95

A. THE REACTION REGIME OF THE HYDROLYSIS OF N_2O_4 96

B. LOCATION OF THE RESISTANCE TO ABSORPTION OF N_2O_4 102

C. CALCULATION OF TUBULAR REACTOR VOLUME REQUIRED FOR OXIDATION OF NO IN THE GAS STREAM SUPPLYING THE INFRARED ANALYZER 105

D. TEMPERATURE RISE AT THE GAS-LIQUID INTERFACE DUE TO HEAT EFFECTS ASSOCIATED WITH THE SOLUTION AND HYDROLYSIS OF N_2O_4 112

E. DETERMINATION OF SIEVE-PLATE INTERFACIAL AREA USING THE ABSORPTION OF CO_2 FROM AIR INTO NaOH SOLUTIONS 115

F. DECOMPOSITION OF HNO_2 IN THE FROTH OF THE SIEVE PLATES . . . 123

G. COMPUTER PROGRAM 126

LIST OF TABLES

TABLE		PAGE
1.	Values of Terms in Equation (12) at the Various Temperatures Used in Studying the Absorption of N_2O_4 into Water	7
2.	Experimentally Determined Values of Constants k_3, k_{-3}, and $k_{p,3}$ at Various Temperatures Used in Studying the Reactions Involving Aqueous HNO_2	21
3.	Experimental Values for the Reaction Rate Constant for the Oxidation of NO	25
4.	Steady-State NO_x Scrubbing Data for Recirculating and Nonrecirculating Scrubber Liquid	55
5.	Steady-State NO_x Scrubbing Data	56
6.	Steady-State NO_x Scrubbing Data for Nonrecirculating Scrubber Liquid	57
7.	Data Showing the Approach to Steady State for NO_x Scrubbing with Recirculating Scrubber Liquid	58
8.	Steady-State NO_2^* Scrubbing Data for a Single Sieve Plate and a Nonrecirculating Scrubber Liquid	59
9.	A Comparison of NO_x Removal Efficiencies Calculated from Experimental Data versus NO_x Removal Predicted by Model for Experiment 53	81
10.	Calculated Partial Pressures of Gaseous Components for Stage, i, and Position, j, Where j = 1 Entering Froth and j = 2 Leaving Froth for Experiment 53	82
E-1.	Steady-State Data for the Absorption of CO_2 into NaOH Solutions in a Sieve-Plate Column	116
E-2.	Calculational Results of the Interfacial Area Determination in a Single-Stage Sieve-Plate Column	119

LIST OF FIGURES

FIGURE		PAGE
1.	Efficiency of NO_2^* Removal by Bubble-Cap Column versus NO_2^* Concentration Obtained by Peters, Ross, and Klein . . .	14
2.	Efficiency of NO_2^* Removal from Dilute Gas with Different Types of Equipment Obtained by Peters	16
3.	Efficiency of NO_2^{**} Removal by Sieve-Plate Column versus NO_2^{**} Concentration Obtained by Andrews and Hanson	19
4.	Effect of NO_2^* Concentration in Entering Gases on Plate Efficiency with a Three-Plate Bubble-Cap Column Obtained by Peters	28
5.	Flowsheet of Equipment Used in NO_x Scrubbing Experiment . .	50
6.	Typical Plate and Downcomer Arrangement for Sieve-Plate Column	51
7.	NO_x Conversion and Temperature Profiles for NO_x Removal in Three-Stage Sieve-Plate Column for Varied Scrubber-Liquid Flow Rates	61
8.	Overall NO_x Removal in Three-Stage Sieve-Plate Column for Varied Feed-Gas Flow Rates	62
9.	Overall NO_x Removal in Three-Stage Sieve-Plate Column for Varied Partial Pressure of NO_2 in Feed Gas	63
10.	Overall NO_x Removal in Three-Stage Sieve-Plate Column as a Function of Acid Molarity in Scrubber Liquid	65
11.	Overall NO_x Removal in Three-Stage Sieve-Plate Column for Varied Ratios of Steam to Air and NO_2^* in the Feed Gas	66
12.	Overall NO_x Conversion in Three-Stage Sieve-Plate Column and Concentration of HNO_2 in the Scrubber Liquid during the Approach to Steady-State Operation	67
13.	Overall NO_x Removal in Three-Stage Sieve-Plate Column for Varied Sparge Rates of the Liquid Holdup Tank	68

FIGURE PAGE

14. Overall NO_x Removal in Three-Stage Sieve-Plate Column for Varied Rates of Single-Pass Process Water Scrubber Liquid 70

15. Overall NO_x Removal in Three-Stage Sieve-Plate Column for a Single-Pass Process Water Scrubber Liquid and Varied Feed-Gas Flow Rates 71

16. Effect of Increasing Steam Flow Rates on NO_2^* Absorption in a Single-Plate Column 73

17. Effect of Increasing Liquid Flow Rates on NO_2^* Absorption When Steam Is Present in the Feed Gas in a Single-Plate Column 74

18. Experimental and Model-Predicted NO_2^* Absorption versus the Partial Pressure of NO_2^* Entering the Tray at a Total Gas Flow Rate of 1.4×10^{-4} m^3/sec in a Single-Plate Column 76

19. Experimental and Model-Predicted NO_2^* Absorption versus the Partial Pressure of NO_2^* Entering the Tray at a Total Gas Flow Rate of 1.86×10^{-4} m^3/sec in a Single-Plate Column 77

20. Experimental and Model-Predicted NO_2^* Absorption versus the Partial Pressure of NO_2^* Entering the Tray at a Total Gas Flow Rate of 2.33×10^{-4} m^3/sec in a Single-Plate Column 78

21. Experimental and Model-Predicted NO_2^* Absorption versus Liquid Flow Rate in a Single-Plate Column 79

22. Experimental NO_x Removal Efficiencies versus Those Predicted by the Model for Varying Gas Flow Rates with No Steam in Feed Gas at Otherwise Reference Conditions for Steady-State Three-Stage Sieve-Plate Column Operation . 83

23. Experimental NO_x Removal Efficiencies versus Those Predicted by the Model for Varying Scrubber Liquid Flow Rates at Otherwise Reference Conditions for Steady-State Three-Stage Column Operation 85

24. Experimental NO_x Removal Efficiencies versus Those Predicted by the Model for Varying Feed Gas Flow Rates at Otherwise Reference Conditions for Steady-State Three-Stage Column Operation 86

FIGURE PAGE

25. Experimental NO_x Removal Efficiencies versus Those Predicted by the Model for Varying Partial Pressure of NO_x in the Feed Gas at Otherwise Reference Conditions for Steady-State Three-Stage Column Operation 87

26. Experimental NO_x Removal Efficiencies versus Those Predicted by the Model for Varying Steam Flow Rates at Otherwise Reference Conditions for Steady-State Three-Stage Column Operation 88

27. Model-Predicted Removal Efficiency of NO_x for Varying Concentrations of HNO_2 in the Scrubber Liquid Stream to Column at Reference Conditions 89

E-1. Correlation of Experimental Results of the Absorption of CO_2 into NaOH Solutions in a Single-Stage Sieve-Plate Column 120

E-2. Correlation of Experimentally Determined Gas-Liquid Interfacial Area versus Gas Flow Rate for a Single-Stage Sieve-Plate Column 121

E-3. A Comparison of Experimentally Determined Interfacial Area in the Sieve Plate Having 0.6% Perforation with That Obtained by Other Experimenters Using Sieve Plates with Higher-Percent Perforation 122

LIST OF SYMBOLS

a	interfacial area per unit volume of froth, m^2/m^3
a_w	wetted surface per unit volume of packed bed, m^2/m^3
A	defined by Equation (68)
B	defined by Equation (69)
C	defined by Equation (70)
$C^*_{HNO_2}$	defined by Equation (99)
C_j	liquid-phase concentration of component j, kg·moles/m^3
C_p	heat capacity, W sec/(kg K)
d	diameter, m or derivative
D	defined by Equation (71)
$D_{j,k}$	diffusivity of component j, in phase k, m^2/sec
E	enhancement factor, dimensionless
E_z	axial dispersion coefficient, m^2/sec
f	function
f_1	property of Bromley and Wilkey equation[46]
F	defined by Equation (89)
g	gas-phase component
g	acceleration due to gravity, m/sec^2
G	superficial gas volumetric flow rate, m^3/sec
$\mathcal{G}$	defined by Equation (90)
h_L	heat transfer coefficient, kcal/(m^2 sec K)
H	defined by Equation (91)

H_R	heat of reaction, kcal/kg•mole
H_S	heat of absorption, kcal/kg•mole
He_j	Henry's law constant for component j, P_j/C_j, m^3atm/kg•mole
I	Ionic strength, kg•mole/m^3
k	thermal conductivity, W/(m K)
k_j	reaction rate constant for reaction j, dimension depends on order of reaction
k_G	gas-phase mass transfer coefficient, m/sec or kg•moles/(m^2sec atm)
k_L	liquid-phase mass transfer coefficient, m/sec or kg•moles/(m^2sec atm)
$K_{p,j}$	pressure equilibrium constant for reaction j
ℓ	liquid-phase component
log	base 10 logarithm
ℓn	base e logarithm
L	superficial liquid volumetric flow rate, m^3/sec
M	molecular weight
P	pressure, atm
P_j	partial pressure of gas component j, atm
q	defined by Equation (84)
r	radius, m
r_j	reaction rate for jth component, dimension depends on order of reaction
R	gas constant, m^3-atm/(kg•mole K)
R_b	radius of gas bubble, m
$\overline{R}_j$	local absorption or desorption rate per unit area for component j, kg•moles/(m^2 sec)

t_d	diffusion time, sec
t_r	reaction time, sec
T	absolute temperature, K
$T_{G,j}$	absolute temperature of gas phase at stage j, K
$T_{L,j}$	absolute temperature of liquid phase at stage j, K
v	superficial velocity, m/sec
$\bar{v}$	interstitial velocity, m/sec
V	volume, m^3
X	defined by Equation (72)
X_j	conversion or removal efficiency of component j, amount of material converted or removed per amount of material entering, $(1 - \psi)/(1 - \varepsilon_k'' \psi)$, dimensionless
$X_{j,k}$	conversion or removal efficiency of component j at stage k
Y	defined by Equation (73)
Y_i	mole fraction of component i
Y	defined by Equation (83)
Z	length, m or stoichiometric coefficient
Z_n	ionic charge of species n

Subscripts

numbers	pertaining to a numbered chemical reaction
b	bubble
B	bulk
c	critical
F	fluid or final
FR	froth
f	final

g	gas
gas space	gas space in column between sieve plates
G	gas
i	gas-liquid interface
in	in
j	stage number in column
k	position of gas in particular stage
l	liquid
L	liquid
m	mixture
o	initial
OA	overall
out	out
NO	nitrogen oxide (nitric oxide)
NO_2	nitrogen dioxide
NO_2^*	sum of the NO_2 concentration plus twice the concentration of N_2O_4
NO_2^{**}	a mixture of nitrogen oxides consisting of $NO_2 + 2N_2O_4 + NO + N_2O_3 + \frac{1}{2}HNO_2$
NO_x	mixture of nitrogen oxides consisting of $NO_2 + 2N_2O_4 + NO$
N_2O_4	nitrogen tetroxide
p	packing
perf	sieve-plate perforations
r	reduced
s	sparge
T	total

Dimensionless Groups

G_1	a group used in calculations involving gas bubbles, $g'\mu_F^4/\rho_F\sigma^3$
G_2	a group used in calculations involving gas bubbles, $g'R_b^4V_b^4\rho_F^3/\sigma^3$
Pe_p	packing Peclet number, $d_p\bar{v}/E_z$
Pe_z	Peclet number, Zv/E_z
Pr	Prandtl number, $C_p\mu/k$
Re_b	bubble Reynolds number, $2\rho_F v_b R_b/\mu_F$
Re_p	packing Reynolds number, $d_p v\rho/\mu$
Sc	Schmidt number, $\mu/\rho D_{AB}$

Greek Letters

α	degree of dissociation, dimensionless
β	defined by Equation (80)
γ	defined by Equation (81)
Δ	change
ε	defined by Equation (82)
ϕ	defined by Equation (96)
ε'	void fraction, dimensionless
ε_k''	fractional volume change due to bulk removal of gas components
$\frac{e_i}{K}, \frac{\varepsilon_{i,j}}{K}$	a group used in calculating the collision integral,[46] Ω_D, K
τ	residence time, sec
ψ	$P_{NO_x,j,k=2}/P_{NO_x,j,k=1}$

μ	viscosity, kg/(m-sec)
ρ	density, kg/m^3
σ	surface tension, kg/sec^2
σ_i, $\sigma_{i,j}$	collision diameter, Å
π	3.14159
Δ	range of variable
Ω_D	collision integral, dimensionless

CHAPTER I

INTRODUCTION AND SIGNIFICANCE

The scrubbing of nitrogen oxides from gaseous mixtures of air, steam, and nitrogen oxide is being investigated as part of a research and development effort in support of a proposed plant which would reprocess spent fuel from nuclear reactors. This work is being conducted in the Chemical Technology Division under the auspices of the Advanced Fuel Recycle Program of the Oak Ridge National Laboratory. Removal of nitrogen oxides from gas streams is important to the reprocessing of spent nuclear fuels; many of the off-gas streams in such a facility will contain these oxides in sufficient concentration to interfere with further gas cleanup operations or to exceed discharge limits. The absorption of gaseous NO_2^* (the sum of the NO_2 concentration and the product of two times its equilibrium polymer concentration, N_2O_4) into water and dilute HNO_3 and the gas-phase oxidation reaction of NO provide the basis for one method of nitrogen oxide removal. Such an absorption process is accompanied by the reactions of nitrogen oxides with water, resulting in the production of HNO_3. This scheme is attractive for the proposed application because the HNO_3 that is produced could be recycled for use in the plant.

Commercial nitrogen oxide scrubbing equipment, usually bubble-cap columns, was designed for the HNO_3 industry and typically utilizes a water input flowing in a single pass through the column. The absorption reactions are very exothermic; thus commercial scrubbers generally

have cooling coils in the froth of each column stage. Because the absorber under development is intended for operation in a radioactive environment, the design of the scrubber should minimize the need for additional incoming process streams and be as simple as possible to facilitate maintenance. The scrubber system under investigation meets those requirements. In this system, dilute HNO_3 is recirculated through the column; the water input is provided by the condensing steam. The column under development is designed for high liquid flow rates which provide cooling for the gas and liquid phases. The sieve-plate design should provide for easier maintenance than a traditional bubble-cap plate. Heat associated with the absorption reactions and condensing steam is removed from the scrubber liquid in heat exchangers located outside the column. The described system appears to meet process requirements; however, some research and development will be necessary to optimize the equipment design.

CHAPTER II

LITERATURE REVIEW

The nitrogen oxides of importance are NO_2, N_2O_4, NO, and N_2O_3. The essential chemical reactions are usually written as follows:

$$2NO_2(g) \rightleftarrows N_2O_4(g) \quad , \tag{1}$$

$$N_2O_4(g) + H_2O(\ell) \rightarrow HNO_3(\ell) + HNO_2(\ell) \quad , \tag{2}$$

$$3HNO_2(\ell) \rightleftarrows HNO_3(\ell) + 2NO(g) + H_2O(\ell) \quad , \tag{3}$$

$$2NO(g) + O_2(g) \rightarrow 2NO_2(g) \quad , \tag{4}$$

$$NO(g) + NO_2(g) \rightleftarrows N_2O_3(g) \quad , \tag{5}$$

$$N_2O_3(g) + H_2O(g) \rightleftarrows 2HNO_2(g) \quad , \tag{6a}$$

or

$$N_2O_3(g) + H_2O(\ell) \rightleftarrows 2HNO_2(\ell) \quad . \tag{6b}$$

Reactions (2) and (3) are sometimes combined as:

$$3/2\ N_2O_4(g) + H_2O(\ell) \rightarrow 2HNO_3(\ell) + NO(g) \quad . \tag{7}$$

Reactions (1) through (4) adequately describe the absorption process if the gaseous NO concentration is low or the gaseous NO_2^* concentration is moderately high. If neither of these conditions is satisfied, reactions (1) through (6) may be required to describe the

absorption process. The heats of reaction associated with these reactions make the absorption a highly exothermic process.

I. THE NO_2-N_2O_4 EQUILIBRIUM

Bodenstein[1] studied reaction (1) at temperatures from 282 to 404 K. Data are expressed in the following equation for the log of the pressure equilibrium constant:

$$\log K_{p,1} = -\frac{2692}{T} + 1.75 \log T + 0.00483T - 7.144 \times 10^{-6}T^2 + 3.062 , \tag{8}$$

where

$$K_{p,1} = \frac{P^2_{NO_2}}{P_{N_2O_4}} \text{ atm} . \tag{9}$$

Verhoek and Daniels[2] also investigated reaction (1) but varied the temperature from 298 to 318 K. The following equation expresses their data for the log of the pressure equilibrium constant:

$$\log K_{p,1} = 9.8698 - \frac{3198}{T} . \tag{10}$$

Hoftyzer and Kwanten[3] give the following correlation for $K_{p,1}$ without temperature restrictions, which was derived from considerations of the work of Verhoek and Daniels[2] and the *JANAF Thermochemical Tables:*[4]

$$K_{p,1} = 1.46 \times 10^9 \exp(-6866.0/T) . \tag{11}$$

II. THE ABSORPTION OF NO_2^* INTO WATER AND DILUTE HNO_3 ACCOMPANIED BY REACTION WITH H_2O

The hydrolysis of N_2O_4 is essentially irreversible if the absorbing fluid is water or dilute HNO_3. The equilibrium hydrolysis of N_2O_4 is not considered in this report, although the subject is well covered in the literature.[5,6]

Chambers and Sherwood[7] studied the absorption of NO_2^* from nitrogen into HNO_3 solutions at 298 K using both a wetted-wall column and a batch system. Acid strengths were varied up to 18.5 M, and the NO_2^* partial pressure was approximately 0.05 to 0.06 atm. Assuming that reaction (3) is rapid and the hydrolysis of N_2O_4 is accurately represented by reaction (7), they concluded that gas-phase resistance is the controlling mechanism since the rate of absorption is proportional to the approximate 0.8 power of the gas velocity. A gas-phase hydrolysis reaction of NO_2^* was assumed; analysis of gas samples was accomplished by using a chemical method.

The effects of system temperature, NO_2^* concentration, and acid molarity on the absorption rate of NO_2^* from NO_2^*-N_2 gas mixtures into HNO_3 were investigated by Denbigh and Prince,[8] using a wetted-wall column. Temperatures of 298 and 313 K were used; the NO_2^* partial pressure ranged from 0 to 0.27 atm; and the acid molarity was varied from 1.7 to 13.0 M. They assumed that reaction (7) describes the reaction of N_2O_4 and water. For acid strengths up to 5.7 M, the absorption rate of NO_2^* may be accurately expressed by the following

equation in accordance with the theory representing the process of absorption combined with chemical reaction:[9]

$$R_{NO_2^*} = 2\left[\frac{\sqrt{D_{N_2O_4,H_2O}k_2}}{He_{N_2O_4}}\right]P_{N_2O_4} \quad . \tag{12}$$

The experimental values for the terms in this equation are given in Table 1. These investigators concluded that chemical reaction (7) is the rate-controlling step. Analysis of the gas phase was accomplished by using a calibrated photocell.

A wetted-wall column was also used by Caudle and Denbigh[10] to experimentally measure the rate of NO_2^* absorption from nitrogen into water and dilute HNO_3. The variables examined were gas composition, temperature, and gas and liquid flow rates. The hydrolysis of N_2O_4 is said to occur essentially as reaction (7). No effect of liquid flow rate was observed over a range of liquid Reynolds numbers [Re(ℓ)] from 140 to 600; no effect of gas flow rate was found over a range of gaseous Reynolds numbers [Re(g)] from 3500 to 12,000 except for the local eddying and mixing effects in the liquid phase that appeared to be functions of the gas flow rate. The absorption rate of NO_2^* can be calculated as a linear function of the partial pressure of N_2O_4 and can be expressed by Equation (12). Values of $\sqrt{D_{N_2O_4,H_2O}k_2}/He_{N_2O_4}$ can be obtained from Table 1.

Caudle and Denbigh[10] suggested that the hydrolysis of N_2O_4 occurs at the gas-liquid interface because (a) the absorption rate is

Table 1. Values of terms in Equation (12) at the various temperatures used in studying the absorption of N_2O_4 into water

Term	Temperature (K) 293	298	303	308	313	318	Investigators
$\frac{\sqrt{D_{N_2O_4,H_2O}k_2}}{He_{N_2O_4}}$ $\left(\frac{kg \cdot mole}{atm\ m^2 sec}\right)$		0.9×10^{-3}			0.12×10^{-3}		Denbigh and Prince[a]
		1.1×10^{-3}				2.5×10^{-3}	Caudle and Denbigh[b]
		0.58×10^{-3}			0.54×10^{-3}		Wendel and Pigford[c]
		1.1×10^{-3}		1.0×10^{-3}			Dekker, Snoeck, and Kramers[d]
	0.77×10^{-3}		0.89×10^{-3}				Kramers, Blind, and Snoeck[e]
		0.903×10^{-3}					Hoftyzer and Kwanten[f]
k_2 (sec^{-1})		290.0			1340.0		Wendel and Pigford[c]
	250.0		330.0				Kramers, Blind, and Snoeck[e]
$He_{N_2O_4}$ $\left(\frac{atm\ m^3}{kg \cdot mole}\right)$		1.04			2.86		Wendel and Pigford[c]
	0.72		0.81				Kramers, Blind, and Snoeck[e]
$D_{N_2O_4,H_2O}$ $\left(\frac{m^2}{sec}\right)$	1.23×10^{-9}		1.59×10^{-9}				Kramers, Blind, and Snoeck[e]

[a] K. G. Denbigh and A. J. Prince, *J. Chem. Soc.* 53: 790-801 (1947).

[b] P. G. Caudle and K. G. Denbigh, *Trans. Faraday Soc.* 49: 39-52 (1953).

[c] M. M. Wendel and R. L. Pigford, *AIChE J.* 4: 249-56 (1958).

[d] W. A. Dekker, E. Snoeck, and H. Kramers, *Chem. Eng. Sci.* 11: 61-71 (1959).

[e] H. Kramers, M. P. P. Blind, and E. Snoeck, *Chem. Eng. Sci.* 14: 115-23 (1961).

[f] P. J. Hoftyzer and F. J. G. Kwanten, *Process for Air Pollution Control*, 2nd ed., pp. 164-87, Chemical Rubber Co., Cleveland (1972).

proportional to the interfacial area instead of the volume of bulk phases; and (b) NO is liberated primarily in the column, with a small amount being evolved from the exiting liquor, when N_2O_4 is absorbed in the column. The absorption rate was determined by photometric gas analysis.

Wendel and Pigford[11] studied the absorption of NO_2^* into water using a wetted-wall column and nitrogen as the diluent gas. The NO_2^* partial pressure was varied up to 0.20 atm. The range of gas rates covered Re(g) from 170 to 350; water rates were varied to allow contact times between gas and liquid from 0.03 to 0.3 sec; and temperatures of 298 and 313 K were used. No effects of gas or liquid flow rates or of contact time on the two reaction rates were observed. The indicated rate-controlling step was the hydrolysis of N_2O_4, expressed by reaction (7). The absorption rate data were correlated via Equation (12). Experimental values are given in Table 1.

The results were interpreted by using the penetration theory and assuming that reaction (7) occurs in the liquid film. Table 1 shows a pseudo-first-order rate constant for reaction (7) and a Henry's law constant for N_2O_4 in water, both of which were calculated from the experimental data.

Peters and Holman[12] used both nitrogen and air as the diluent gas in their wetted-wall column experiments on the absorption of NO_2^* into water and NaOH solutions, and found no significant differences in results. The NO_2^* partial pressure was maintained at 0.048 atm; all runs were made at atmospheric pressure and at temperatures ranging from 301

to 329 K. Reaction (7) was assumed to apply for the reaction of N_2O_4 and water. The removal efficiency decreased significantly with increased temperature for runs using water or NaOH solutions. The following equation describes the reaction of NO_2^* and NaOH:

$$2NaOH + N_2O_4 \rightarrow NaNO_2 + NaNO_3 + H_2O \ . \tag{13}$$

Both the gas and liquid phases were analyzed, and inlet and outlet NO_2^* and HNO_3 or NaOH concentrations were determined by chemical methods.

The presence of NO in the off-gas when an NaOH solution is the absorbent liquid may suggest a gas-phase reaction for the hydrolysis of NO_2^*. However, no proportionality of NO_2^* removal to the water vapor fugacity was found in runs in which the feed-gas stream contained water vapor. The nonproportionality of the NO_2^* removal rate to water vapor fugacity was interpreted as an indication of the presence of a liquid-phase reaction; both liquid- and gas-phase reactions may contribute to NO_2^* absorption.

In a literature review in 1959, Carberry[13] concluded that, in cases where N_2O_4 is dissolved in solvents of high dielectric strength, ionization occurs according to the reaction

$$N_2O_4(\ell) \rightarrow NO^+(\ell) + NO_3^-(\ell) \ , \tag{14}$$

and N_2O_4 exists in these solutions in the ionized form. In the light of this conclusion, the reaction of dissolved N_2O_4 and water may be written as:

$$N_2O_4(\ell) + H_2O(\ell) \rightarrow NO^+(\ell) + OH^-(\ell) + H^+(\ell) + NO_3^-(\ell) \tag{15}$$

or

$$N_2O_4(\ell) + H_2O(\ell) \rightarrow HNO_2(\ell) + H^+(\ell) + NO_3^-(\ell) \ . \tag{16}$$

The ionization of N_2O_4 not only supports the kinetic and chemical equilibrium data, but also provides significant corroboration for the argument that a purely gas-phase reaction between N_2O_4 and water vapor is an unlikely occurrence.

Dekker, Snoeck, and Kramers[14] investigated NO_2^* absorption in a wetted-wall column for contact times of 0.2 to 0.4 sec, inlet NO_2^* partial pressures of 0.03 to 0.15 atm, and operating temperatures of 298 to 308 K. The absorption rate data were correlated with an equation similar to Equation (12); contact time had little effect on absorption rate. The experimental results, presented in Table 1 (page 7), are fairly consistent with the following model:

1. In the gas phase, NO_2 and N_2O_4 are in continuous equilibrium with each other.
2. At the gas-liquid interface, only N_2O_4 is dissolved in water.
3. The diffusion of N_2O_4 into water is accompanied by a rapid pseudo-first-order chemical reaction between N_2O_4 and water.

Absorption of NO_2^* was measured by photometric analysis of the gas phase and titration of the liquid acid phase for both HNO_3 and HNO_2.

Koval and Peters[15] examined the absorption of NO_2^* from feed-gas mixtures of NO_2^*-NO-N_2 into water at 304 K in a long wetted-wall column at atmospheric pressure. The NO_2^* partial pressure was varied up to

0.04 atm. Chemical analysis of the gas and liquid phases revealed that the presence of NO had a marked effect on the HNO_3-HNO_2 split, greatly increasing the production of HNO_2 at the expense of HNO_3 production. The chemical stoichiometry is described by the following equation:

$$(2 + \beta'/4)N_2O_4(g) + (2 + \beta'/2)H_2O(\ell) \rightarrow 2HNO_3(\ell) + 2(1 + \beta'/2)HNO_2(\ell) - (\beta'/2)NO(g) \ , \tag{17}$$

where β refers to the molar excess of HNO_2 over HNO_3. The following rate equation takes into account a varied amount of HNO_2 and best describes the experimental data:

$$R^*_{NO_2} = k'(P_{N_2O_4})_i + k''(P_{NO})_i(P_{NO_2})_i - k'''C^2_{HNO_2} \ . \tag{18}$$

Equation (18) allows for a significant and varied amount of HNO_2, whereas Equation (12) does not.

Moll[16] investigated the rate of hydrolysis of N_2O_4 over the temperature range 300 to 318 K. He injected liquid N_2O_4 directly into a flowing water stream and measured the resulting temperature rise downstream of the injection point. From these temperature profiles, he determined k_2. His correlation of k_2 with the temperature from 300 to 318 K is:

$$\log k_2 = 7.12 - 1375/T \ . \tag{19}$$

His work is the first direct evidence that the hydrolysis of N_2O_4 occurs as Equation (12), a first-order reaction.

Hoftyzer and Kwanten[3] investigated the absorption of N_2O_4 by using laminar jets. In their works, the following variables were studied: the partial pressure of NO_2^*, 0.05 to 1.70 atm; temperature, 276 to 348 K; and acid molarity. Data were correlated using Equation (12). The experimentally determined value of $\sqrt{D_{N_2O_4,H_2O}k_2}/He_{N_2O_4}$ is given in Table 1 (page 7) for 298 K, and the following correlation represents their data for temperatures from 276 to 348 K:

$$\log \left[0.98 \frac{\sqrt{D_{N_2O_4,H_2O}k_2}}{He_{N_2O_4}} \right] = -0.53 - 760/T \ . \tag{20}$$

These investigators found that the value of $\sqrt{D_{N_2O_4,H_2O}k_2}/He_{N_2O_4}$ decreased with increasing acid molarity. This decrease was attributed to the increase in the Henry's law constant (He) with increasing ionic strength. They stated that the values of He could be corrected by using the factor exp(-0.075 I), where I is the ionic strength defined by:

$$I = 1/2 \sum_{i=1}^{n} (Z_i^2 C_i) \ . \tag{21}$$

Detournay and Jadot[17] proved the existence of a homogeneous gas-phase reaction between N_2O_4 and water vapor with a second-order reaction rate constant of 0.13 kg•mole m^{-3} sec^{-1} at 333 K. When this rate constant is compared with the rate constant for the liquid-phase hydrolysis of N_2O_4 estimated from the work of Wendel and Pigford,[11] 96.0 kg•mole m^{-3} sec^{-1}, the contribution of a gas-phase reaction of N_2O_4 and water vapor to NO_x removal appears to be negligible.

Peters, Ross, and Klein[18] studied NO_2^* absorption in a single-plate 0.19-m-ID bubble-cap column equipped with seven bubble caps. The experiment was conducted at acid concentrations of 0 and 2.6 M and NO_2^* partial pressures up to 0.10 atm. Runs were made at liquid flow rates of 5.0×10^{-6} and 10.0×10^{-6} m^3/sec and gas velocities of 0.36 and 0.72 m/sec in the slots. All runs were conducted at atmospheric pressure and at temperatures from 292 to 297 K. No significant difference in the results was noted from the use of nitrogen or air as the diluent gas. These investigators assumed that reaction (7) applied for the hydrolysis of N_2O_4 and that a model developed from chemical reaction rates was adequate. Their results showed that the rate of removal of NO_2^* was proportional to the concentration of N_2O_4 in the gas phase. Plate efficiencies are presented in Figure 1. The fraction of entering oxides converted to HNO_3 was found to decrease as the contact time between gas and liquid decreased. Neither the liquid flow rate nor the acid molarity of the scrubbing liquid had any effect on plate efficiency; however, increasing the humidity in the feed gas increased plate efficiency. Peters, Ross, and Klein[18] concluded that the absorption reactions occur at the gas-liquid interface.

Peters[19] compared the absorption of NO_2^* from air into water and dilute HNO_3 (<2.6 M) in the following devices: a single-plate bubble-cap column previously described;[18] a 0.025-m-ID column, packed with 1/4-in. glass raschig rings to a height of 1.17 m; a 0.14-m-ID single-plate fritted bubbler column consisting of 12 medium-frit glass rods sealed

ORNL DWG 77-289 R1

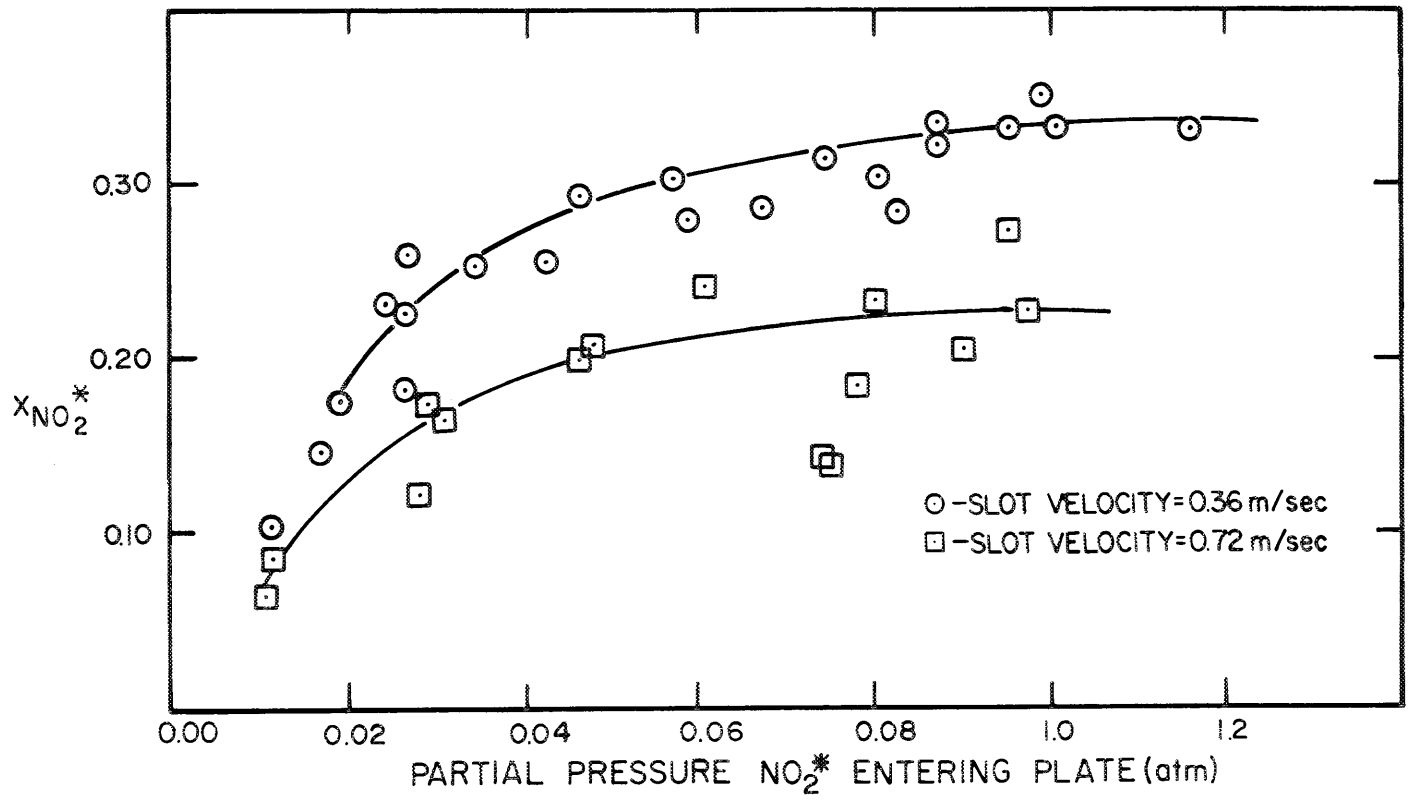

Figure 1. Efficiency of NO_2^* removal by bubble-cap column versus NO_2^* concentration obtained by Peters, Ross, and Klein.

Source: M. S. Peters, C. P. Ross, and J. E. Klein, *AIChE J.* 1: 105-11 (1955).

into the plate; a 0.025-m-ID, 1.32-m-high spray tower equipped with a single spray nozzle; and a 0.025-m-ID bed of silica gel packed to a height of 0.3 m. The partial pressure of NO_2^* was varied from 0.002 to 0.02 atm, but the total pressure was maintained at 1.0 atm. The temperature was maintained at 298 K. Efficiencies of the packed beds were reported in terms of 0.3 m of packing. Operating parameters were chosen to permit a fair comparison of the removal efficiencies of various types of contactors. The removal efficiency was found to be independent of the liquid rate in the bubble-cap and fritted bubbler columns as long as the HNO_3 concentration of the liquid did not increase above 2.8 M. The spray column was operated at a liquid flow rate that would yield a finely divided mist, and the packed column was operated at approximately 90% of flooding.

The experimental results are presented in Figure 2. The performance of the bubble-cap column improved with increasing NO_2^* concentration, and its removal efficiency is significantly surpassed only by that of the fritted bubbler column. The removal efficiency of the fritted bubbler column was higher than that of other devices except at NO_2^* concentrations of less than 0.004 atm. However, the pressure drop through the plate was about 30 times higher than that of the bubble-cap plate. Removal efficiencies with the packed column were lower than those found with the bubble-cap column or the fritted bubbler column. However, the decrease in efficiency with reduction in NO_2^* concentration is fairly gradual, and the performance at NO_2^* partial pressures of less than 0.002 atm becomes comparable to that of other

ORNL DWG. 77-291

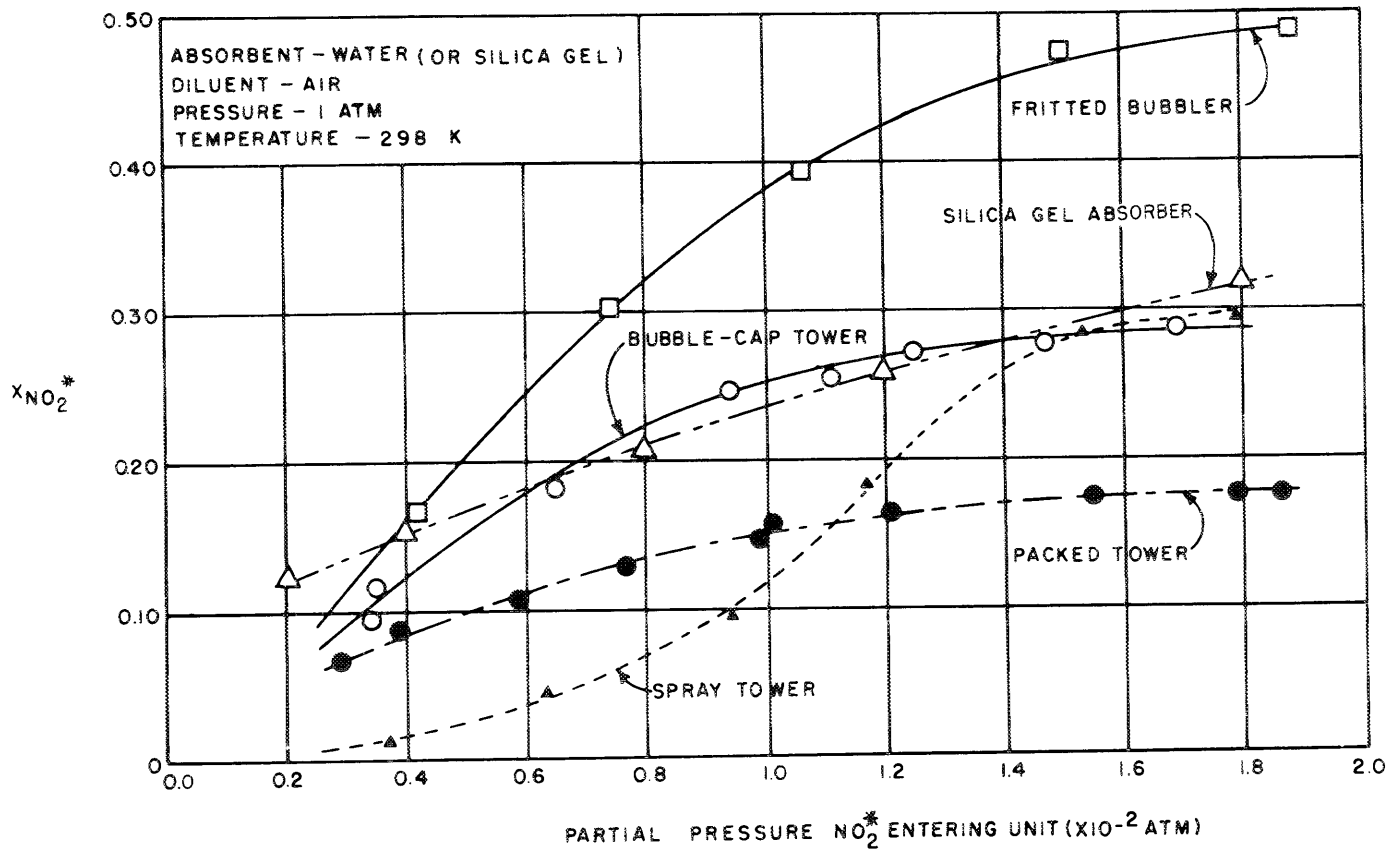

Figure 2. Efficiency of NO_2^* removal from dilute gas with different types of equipment obtained by Peters.

Source: M. S. Peters, *University of Illinois Engineering Experiment Report No. 14*, USAEC-COO-1015 (1955).

types of equipment. Results obtained with the spray column indicate that removal efficiencies at NO_2^* concentrations less than 0.001 atm are poor, but at higher concentrations are comparable to those obtained with other types of equipment. The silica gel absorber provides the best removal efficiency of the units tested at concentrations of less than 0.004 atm.

A stirred-tank reactor was used by Peters and Koval[20] to study the absorption of NO_2^* from NO_2^*-air mixtures into water. In their study, the partial pressure of NO_2^* was varied from 0.4 to 4.4 atm; both the gas and the liquid phases were analyzed to determine NO_2^* absorption. They found that removal efficiency improved with increased NO_2^* concentration and/or increased agitation. The agitator was designed to break up large gas bubbles into smaller ones. The data were correlated with the following rate equation:

$$R_{NO_2^*} = k_2 C_{N_2O_4,i} + \left[\frac{k_5 k_6 b C^2_{H_2O,i}}{k_{-5} + k_6 b C^2_{H_2O,i}} \right] (C_{NO,i} C_{NO_2,i}) \ . \qquad (22)$$

Equation (22), in contrast to Equation (12), adds a term to account for N_2O_3 reactions.

This experiment differs from the work with bubble-cap, sieve-plate, or wetted-wall columns in that the stirred tank provides for greater gas-liquid contact time and contact area. Under these conditions, the reaction of N_2O_3 with water cannot be ignored.

Andrews and Hanson[21] studied the absorption of NO_2^{**} from air-NO_2^{**} and air-NO_2^{**}-NO gaseous mixtures into dilute HNO_3 using a recirculating acid stream and a small single-sieve-tray column at 298 K. The concentration of NO_2^{**} in the gas mixture is defined as the sum of the NO_2^{*} and the N_2O_3 and (1/2)HNO_2 concentrations. The partial pressure of NO_2^{**} was varied up to 0.10 atm. For NO_2^{**} concentrations greater than 0.01 atm, the predominant absorption mechanism is the solution of N_2O_4 into the liquid followed by its rapid hydrolysis to HNO_3 and HNO_2. These investigators developed the following model for plate efficiency that correlates well with their experimental data:

$$\ell n(1 - X_{NO_2^{**}}) = \frac{-k^{*}a}{G} (P_{NO_2^{**},i}) \ , \tag{23}$$

where k* is a combination of equilibrium, kinetic, and transfer constants. The data are presented in Figure 3. Plate efficiencies increased slightly for NO_2^{**} absorption when NO was present at partial pressures of 0.05 atm and higher and when the NO_2^{**} partial pressure in the gas phase was less than 0.03 to 0.04 atm.

Kramers, Blind, and Snoeck[22] used a laminar water jet to study the absorption of NO_2^{*} from an inert carrier gas into water at 293 and 303 K. They determined the absorption rate by chemical analysis of the liquid phase for HNO_2 and HNO_3. The absorption rate data were correlated with Equation (12); experimental results are given in Table 1 (page 7).

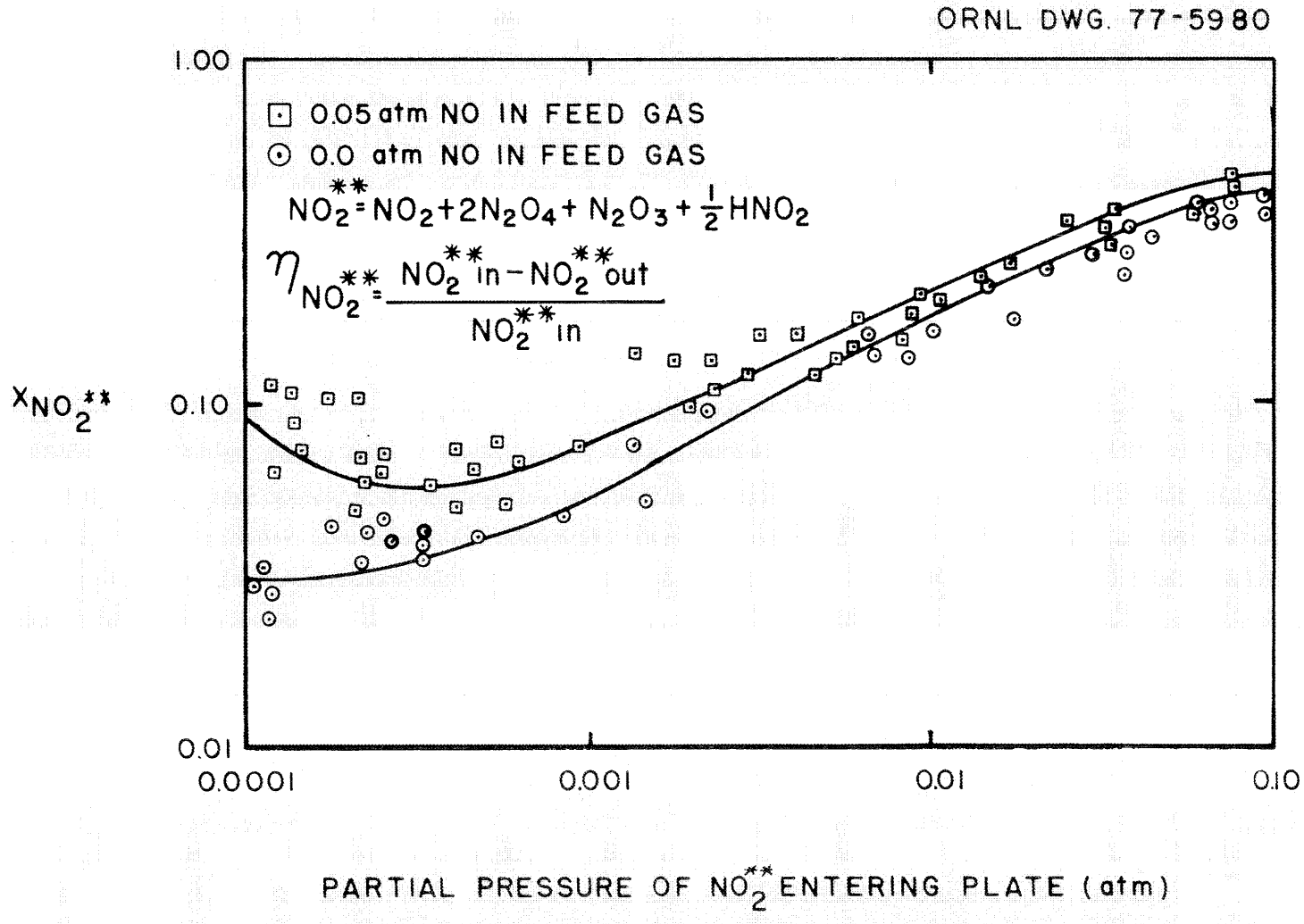

Figure 3. Efficiency of NO_2^{**} removal by sieve-plate column versus NO_2^{**} concentration obtained by Andrews and Hanson.

Source: S. P. Andrews and D. Hanson, *Chem. Eng. Sci.* 14: 105-13 (1961).

III. REACTIONS INVOLVING AQUEOUS HNO_2

Abel and others[23] performed several experiments to investigate the kinetics of the formation and decomposition of aqueous HNO_2. During the early stages of nitrous acid formation, the rate of reaction was found to be:

$$\frac{dC_{HNO_2}}{dt} = k_3(C_{HNO_2})(C_{H^+})(C_{NO_3^-}) \quad , \tag{24}$$

where the reaction was assumed to be:

$$HNO_3(\ell) + 2NO(g) + H_2O(\ell) \rightleftarrows 3HNO_2(\ell) \quad . \tag{25}$$

Equation (26) describes the disappearance of HNO_2 during the early stages of the decomposition:

$$-\frac{dC_{HNO_2}}{dt} = \frac{k_{-3}(C_{HNO_2})^4}{P_{NO}^2} \quad . \tag{26}$$

Abel suggests that the decomposition occurs as follows:

$$4HNO_2(\ell) \rightleftarrows N_2O_4(\ell) + 2NO(g) + 2H_2O(\ell) \quad . \tag{27}$$

At equilibrium,

$$K_{p,3} = \frac{k_{-3}}{k_3} = \frac{(C_{H^+})(C_{NO_3^-})(P_{NO})^2}{C_{HNO_2}^3} \quad .$$

The experimental values of k_3, k_{-3}, and $K_{p,3}$ are given in Table 2.

Table 2. Experimentally determined values of constants k_3, k_{-3}, and $k_{p,3}$ at various temperatures used in studying the reactions involving aqueous HNO_2

Reaction rate constant	Temperature (K)							
	272	285	285.5	288	298	303	313	333
k_{-3} $\left(\frac{m^9}{kg \cdot mole^3\ atm^2\ sec}\right)$	0.010	0.061			0.767		8.75	85.5
k_3 $\left(\frac{m^6}{kg \cdot mole^2\ sec}\right)$					0.027			
$k_{p,3}$ $\left(\frac{m^3}{kg \cdot mole\ atm^2}\right)$			13.3	14.1	28.7	39.6		

Source: E. Abel and H. Schmid, *Z. Physik. Chem.* 132: 56-77 (1928); 134: 279-300 (1928); 136: 135-45, 419-36 (1928).

The stoichiometry of Abel's chemical reaction equations seems to indicate a liquid-phase equilibrium of N_2O_4. However, using Carberry's[14] conclusions concerning the ionic nature of dissolved N_2O_4, it is possible to write Abel's equation representing the decomposition of HNO_2 in the liquid phase as follows:

$$4HNO_2(\ell) \rightleftarrows HNO_2(\ell) + H^+(\ell) + NO_3^-(\ell) + 2NO(g) + H_2O(\ell) \ . \tag{29}$$

If a molecule of HNO_2 is subtracted from both sides of the preceding equation, the stoichiometry becomes the same as that of Abel's chemical equation for the formation of HNO_2 in the liquid phase. Thus, the apparent discrepancy in Abel's use of two sets of stoichiometry for the formation and decomposition of HNO_2 in the liquid phase seems to be resolved.

Andrews and Hanson[21] calculated and verified the following equilibrium constant at 298 K:

$$\frac{(P_{NO_2})(P_{NO})}{C^2_{HNO_2}(\ell)} = 1.6 \times 10^{-2} \ \frac{\text{atm}^2 \ \text{m}^6}{\text{kg}\cdot\text{mole}^2} \ . \tag{30}$$

The decomposition of liquid HNO_2 at concentrations of 0.004 to 0.04 kg-mole/m^3 was studied at 273 to 295 K by Kobayashi, Takezawa, Hara, Nikki, and Kitano,[24] who used conditions that included both "agitation" and "nonagitation." They determined the stoichiometry to be the reverse of reaction (6a) or (6b) for the aqueous solution and a stoichiometry between the former two chemical equations and the forward reaction of Equation (3) for acid solutions.

The dissociation of liquid HNO_2 was determined to be diffusion-controlled for the nonagitated case and chemical rate-controlled for the agitated case. The results correlated with the following rate equations for the diffusion- and kinetics-controlled situations, respectively:

$$\overline{R} = k_L \, C_{HNO_2,B} \tag{31}$$

and

$$\overline{R} = k_3 \, C_{HNO_2,i} \; . \tag{32}$$

The dissociation reaction was found to be of first order with respect to the liquid HNO_2 concentration. The kinetic rate constants at 273, 287.5, and 294.5 K were 0.57×10^{-5}, 0.94×10^{-5}, and 1.7×10^{-5} m/sec. No effects of the partial pressures of gaseous NO and NO_2^* on the dissociation were found; in addition, no effect of the H^+ concentration was noted below 0.1 kg•mole/m^3. The authors are in agreement with Abel et al.[23] that the decomposition of liquid HNO_2 is chemical rate-controlled in agitated solutions. However, the nonequilibrium nature of this dissociation reaction is in disagreement with data obtained by Abel et al.[23] and by Andrews and Hanson.[21]

IV. THE OXIDATION OF NO

Bodenstein[25] studied the gas-phase oxidation of gaseous NO at 273, 303, 333, and 363 K; the partial pressure of NO was varied from 0.08 to 0.14 atm in excess oxygen. Bodenstein confirmed the third-order kinetics consistent with the following rate equation:

$$r_4 = k_4 P_{NO}^2 P_{O_2} \quad . \tag{33}$$

Rate constants are given in Table 3.

Under conditions comparable to those used by Bodenstein, Hasche and Patrick[26] examined the kinetics of the gas-phase reaction of NO and oxygen at 273 and 303 K and found that a third-order reaction occurs consistent with Equation (33). The reaction appears to be catalyzed by the presence of glass wool. Reaction rate constants are presented in Table 3.

Treacy and Daniels[27] also found a third-order reaction consistent with Equation (33) in their analysis of gas-phase reaction kinetics of NO and oxygen at 273, 298, and 338 K. The NO partial pressure was varied from 0.006 to 0.02 atm, and the oxygen partial pressure was varied from 0.026 to 0.006 atm. Reaction rate constants are listed in Table 3.

The reaction rate constant of Morrison, Rinker, and Corcoran,[28] who investigated the gas-phase oxidation of NO at 300 K, is also presented in Table 3. The NO concentration was varied from 2 to 75 ppm; the oxygen concentration ranged from 0.03 to 0.25 atm. The reaction appeared to proceed at third-order kinetics, consistent with Equation (33).

Greig and Hall[29] used similar parameters to investigate the gas-phase oxidation of NO. In their work, temperatures of 293, 322, 352, and 372 K were used; the partial pressure of NO varied from 0.05 to 0.11 atm, and the partial pressure of oxygen ranged from 0.01 to

Table 3. Experimental values for the reaction rate constant for the oxidation of NO

Reaction rate constant	Temperature (K)											Investigators
	273	293	298	300	303	322	333	338	352	363	372	
k_5 (atm^{-2} sec^{-1})	34.75				22.95		14.86			10.16		Bodenstein[a]
	43.24				26.19							Hasche and Patrick[b]
	25.9		13.4					9.75				Treacy and Daniels[c]
				21.47								Morrison, Rinker, and Corcoran[d]
		34.8				24.1			18.2		15.0	Greig and Hall[e]

[a] M. Bodenstein, *Z. Elektrochem.* 24: 183-201 (1918).

[b] R. L. Hasche and W. A. Patrick, *J. Am. Chem. Soc.* 46: 1207-14 (1925).

[c] J. C. Treacy and F. Daniels, *J. Am. Chem. Soc.* 77: 2033-36 (1955).

[d] M. E. Morrison, R. C. Rinker, and W. H. Corcoran, *Ind. Eng. Chem., Fundam.* 5: 175-81 (1966).

[e] J. D. Greig and P. G. Hall, *Trans. Faraday Soc.* 63: 655-61 (1967).

0.28 atm. These workers also confirmed third-order kinetics consistent with Equation (33). Rate constants are presented in Table 3.

V. REACTIONS INVOLVING N_2O_3

Verhoek and Daniels[2] studied the equilibrium reaction

$$N_2O_3(g) \rightleftarrows NO_2(g) + NO(g) \tag{5a}$$

and calculated values of 1.67, 2.83, and 4.53 for the equilibrium constant K_p (1/atm) at 298, 308, and 318 K, respectively. At temperatures of ambient and above, the equilibrium concentration of N_2O_3 is very low.

Wayne and Yost,[30] who studied reaction (6a) at 298 K, found that the forward reaction for the gas-phase hydrolysis of N_2O_3 is catalyzed by water and proceeds at third-order kinetics with a rate constant of 1.1×10^5 atm^{-2} sec^{-1}. The backward reaction is also catalyzed by water and proceeds as a third-order reaction with a rate constant of 6.6×10^{-4} atm^{-2} sec^{-1}. The dissociation rate of N_2O_3, reaction (5), proceeds with a first-order rate of 150 sec^{-1}.

VI. MULTIPLE-PLATE AND PACKED ABSORBERS

Currently, little published information exists on research involving the absorption of gaseous NO_x compounds into water or dilute HNO_3 in engineering-scale absorption columns. However, information is available concerning performances of engineering-scale and larger columns relative to the absorption of gaseous NO_x into nondilute HNO_3 solutions. This

literature usually originates in the HNO_3 production industry; however, some data presented in these reports are pertinent to the design of NO_x absorption equipment in which the hydrolysis reaction is considered essentially irreversible.

Peters[19] studied NO_2^* absorption from air into water and dilute HNO_3 (<2.6 M) in a three-stage bubble-cap column. A typical plate was described above. The distance between the plates was 0.3 m; the partial pressure of NO_2^* in the feed varied from 0.005 to 0.08 atm. Distilled water was fed into the top of the column at the rate of 5.0×10^{-6} m^3/sec. The gas flow rate was 5.9 m^3/sec. Other operating conditions were as described above. The efficiencies of the three plates are presented in Figure 4. The efficiency increases as the gas moves up the tower for any given NO_2^* partial pressure in the feed.

An industrial-scale bubble-cap column was used by Fauser[31] to measure the effects of temperature and pressure on NO_2^* absorption. He found that absorption rates increase with decreasing operating temperatures (288 to 259 K) and with increasing operating pressures (up to 5 atm).

Taylor, Chilton, and Handforth[32] studied the effects of temperature and pressure on NO_x absorption in a pilot-plant-scale bubble-cap column. They found that column efficiency could be increased by reducing the operating temperature or by increasing the operating pressure. The column performance was accurately predicted using Bodenstein's data for the oxidation of NO and existing equilibrium data for the NO_2-N_2O_4 equilibrium.

ORNL DWG 77-288 RI

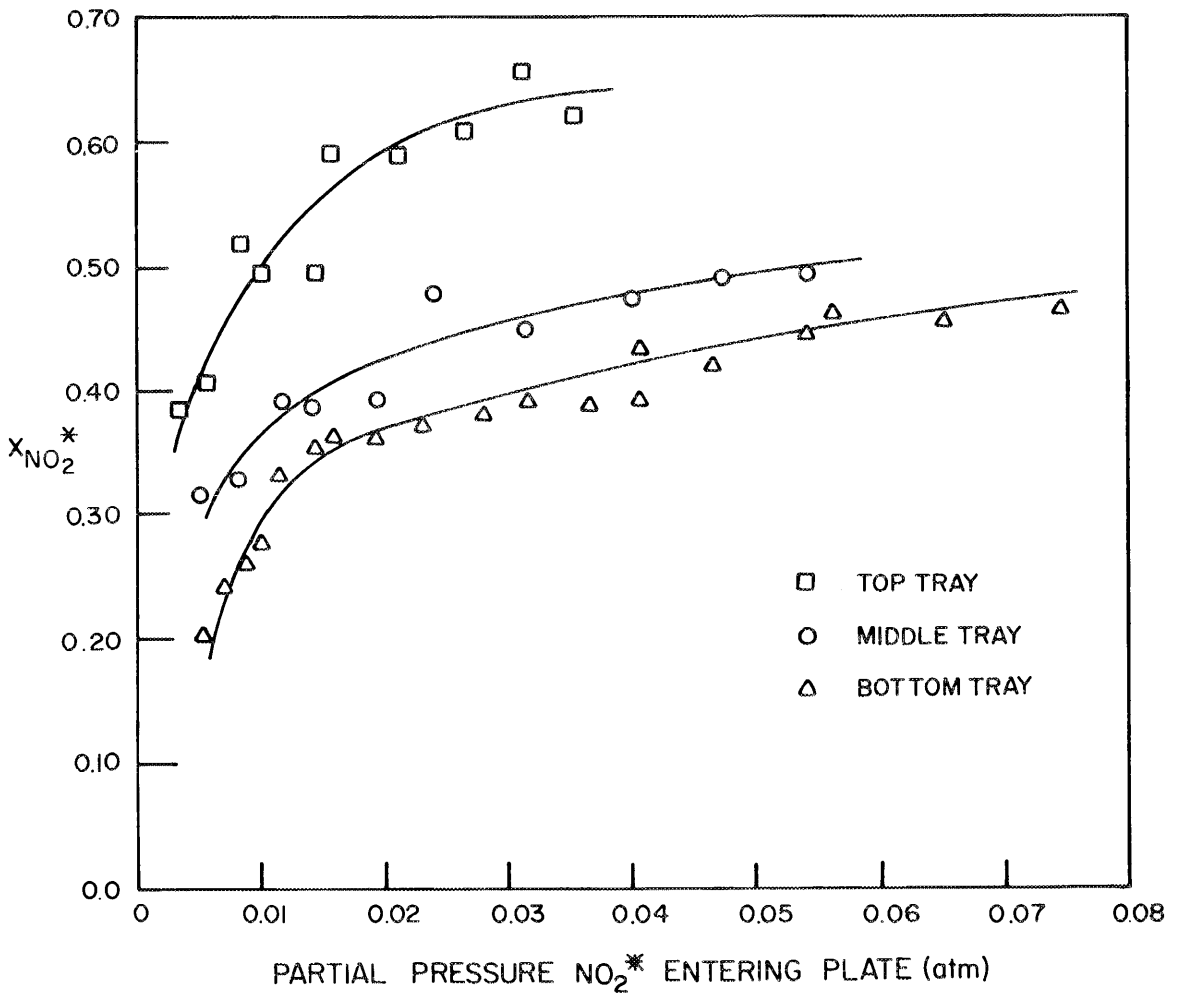

Figure 4. Effect of NO_2^* concentration in entering gases on plate efficiency with a three-plate bubble-cap column obtained by Peters.

Source: M. S. Peters, *University of Illinois Engineering Experiment Report No. 14*, USAEC-COO-1015 (1955).

Atroshchenko, Konvisar, and Kordysh[33] studied the absorption of NO_x compounds in a 0.03-m-ID bubble-cap column. Their results showed that Murphree plate efficiency generally increases with increasing NO_2^* partial pressures and with increasing interplate distance. Atroshchenko, Konvisar, and Ivakhnenko[34] later investigated the effects of plate hole size, the ratio of open area to total plate area, and the gas flow rate on gaseous NO_x absorption in a sieve-plate column. In general, they discovered that plate efficiencies increase with decreased plate open area and decreased gas flow rates.

Nitric acid production was examined by Hellmer,[35] who used a semi-industrial-scale sieve-plate column with cooling coils located in the bubble layer of the plates. The acid concentration was varied along with the NO_2^* concentration. According to Hellmer, it is possible to calculate the number of plates necessary for a given HNO_3 outlet concentration and entering NO_2^* concentration using literature rate constants for reactions (4) and (7). Murphree plate efficiencies ranged from 23 to 65% for acid concentrations varying from 0 to 15 M and from 23 to 67% for NO_2^* partial pressures varying from near zero to 0.25 atm.

Chilton[36] gives a fairly complete review of the Dupont Pressure Process of HNO_3 production.

Graham, Lyons, and Faucett[37] applied the Dupont Pressure Process in the construction of a bubble-cap HNO_3 production column. They give performance data of this design for a column rated at 50,000 kg of HNO_3 produced per day.

Bowman, Kulczak, and Shulman[38] tested a 0.76-m-ID scrubber packed to a height of 1.52 m. Removal efficiencies for NO_x varied from 18 to 37% for NO_2^* feed gas concentrations of 750 to 3750 ppm at 300 K. Other operating conditions were varied and, in general, NO_x removal efficiencies increased with decreasing temperature and decreasing gas flow rates.

VII. LITERATURE SUMMARY

The predominant mechanism for nitrogen oxide absorption at NO_2^* partial pressures greater than 0.01 atm appears to be the solution and hydrolysis of N_2O_4 to HNO_2 and HNO_3. However, if the gas-liquid contact time is extended, or if high concentrations of gaseous NO are present during gas-liquid contact, the solution and hydrolysis of N_2O_3 and/or the solution of HNO_2 tend to act as competitive absorption mechanisms. The dissociation of liquid HNO_2 cannot necessarily be assumed to occur rapidly. In a recirculating system, a steady-state HNO_2 concentration in equilibrium with the gas phase has been reported. The gas-phase oxidation of NO progresses rather slowly, requiring sufficient gas space and relatively cool temperatures to proceed. The absorption reactions are very exothermic, and absorption generally decreases with increasing temperature.

Currently, a void exists in the literature in the area of applying the available kinetic data for nitrogen oxide systems to the overall design of large-scale equipment for the absorption of gaseous NO_x into water or dilute HNO_3. The following characteristics are desirable for NO_x absorption equipment: (a) discrete and optimal gas-liquid contact

for N_2O_4 absorption, (b) intermittent and discrete gas spaces for NO oxidation, and (c) low operating temperatures.

Although HNO_3 manufacturers in the United States seem to prefer plate towers for NO_x absorption devices, packed towers continue to be used by some European manufacturers.[3] Both of these applications are valid for high-pressure (>5.0-atm) absorption, while the plate column appears to be the choice for scrubbing gaseous NO_x compounds at essentially atmospheric pressure. At sufficiently low gaseous concentrations of NO_x, the packed column is a reasonable alternative.

CHAPTER III

DEVELOPMENT OF THE MODEL

The overall chemical reactions involved in the steady-state absorption of NO_x compounds into water or dilute HNO_3 appear to be adequately represented as follows:

$$2NO_2(g) \rightleftharpoons N_2O_4(g) \tag{34}$$

$$N_2O_4(g) \rightleftharpoons N_2O_4(\ell) \tag{35}$$

$$N_2O_4(\ell) + H_2O(\ell) \rightarrow HNO_3(\ell) + HNO_2(\ell) \tag{36}$$

$$3HNO_2(\ell) \rightleftarrows H_2O(\ell) + HNO_3(\ell) + 2NO(g) \tag{37}$$

$$2NO(g) + O_2(g) \rightarrow 2NO_2(g) \tag{38}$$

A review of the literature indicates that the following generalizations about the overall reactions may be made:

1. The NO_2 and N_2O_4 are in continuous gas-phase equilibrium.[1,2,3,14,21]
2. Reaction of N_2O_4 with water proceeds by means of a pseudo-first-order liquid-phase reaction.[3,8,10-18]
3. The HNO_2 decomposes as described by Abel.[23]
4. Oxidation of NO occurs as a third-order gas-phase reaction.[25-29]

The following represents a mathematical simulation of the absorption of NO_x into dilute HNO_3. The NO_2-N_2O_4 equilibrium and the absorption

of gaseous N_2O_4 into water or dilute HNO_3 are simulated mathematically and combined into an equation for N_2O_4 absorption in the froth on the sieve plates. The dissociation of liquid HNO_2 is simulated, resulting in the production of gaseous NO. By using the gas-phase reaction rate for NO oxidation, a mathematical expression can be developed for the occurrence of this reaction in the gas space between the sieve plates. These three equations are combined into an overall mathematical model for NO_x removal in a multistage-plate column.

I. A MATHEMATICAL SIMULATION OF THE NO_2-N_2O_4 EQUILIBRIUM

The equilibrium between N_2O_4 and NO_2 can be defined by

$$K_{p,34} = \frac{P^2_{NO_2}}{P_{N_2O_4}} . \tag{39}$$

The quantity α represents the degree of dissociation of N_2O_4. Expressing the partial pressures of N_2O_4 and NO_2 in terms of NO_2^* and α yields:

$$P_{N_2O_4} = (1 - \alpha)P_{NO_2^*}/2 \tag{40}$$

and

$$P_{NO_2} = \alpha P_{NO_2^*} . \tag{41}$$

The equilibrium between N_2O_4 and NO_2 can now be expressed as:

$$K_{p,34} = \frac{\left[\alpha P_{NO_2}^*\right]^2}{(1 - \alpha)P_{NO_2}^*/2} = \frac{2\alpha^2 P_{NO_2}^*}{(1 - \alpha)} . \tag{42}$$

This equilibrium equation may be rearranged into

$$2P_{NO_2}^*\alpha^2 + K_{p,34}\alpha - K_{p,34} = 0 , \tag{43}$$

which is a second-order polynominal in α. The solution for α may be obtained by taking the positive root of the quadratic formula,

$$\alpha = \frac{-K_{p,34} + K_{p,34}\sqrt{1 + 8P_{NO_2}^*/K_{p,34}}}{4P_{NO_2}^*} . \tag{44}$$

II. THE LOCAL ABSORPTION RATE OF N_2O_4 INTO WATER

Using the two-film model for the transport of NO_2^* across both films in a steady-state process, the following equation can be written:

$$\overline{R}_{NO_2}^* = k_G(P_{NO_2}^* - P_{NO_2^*,i}) = Ek_L(C_{NO_2^*,i} - C_{NO_2^*,B}) . \tag{45}$$

Assuming Henry's law is obeyed,

$$P_{NO_2^*,i} = He_{NO_2^*}C_{NO_2^*,i} ; \tag{46}$$

and based on the sum of resistances approach,

$$\overline{R}_{NO_2}^* = \frac{P_{NO_2}^*/He_{NO_2}^* - C_{NO_2^*,B}}{\frac{1}{Ek_L} + \frac{1}{He_{NO_2^*}k_G}} . \tag{47}$$

Since N_2O_4 appears to be the major absorbing species of the NO_2^*-water system, the local absorption rate may be written as:

$$\overline{R}_{NO_2}^* = \frac{2P_{N_2O_4}/He_{N_2O_4} - 2C_{N_2O_4,B}}{\frac{1}{Ek_L} + \frac{1}{He_{NO_2}^* k_G}} . \tag{48}$$

The reaction of N_2O_4 and water is shown in Appendix A to fall in the "fast-reaction" regime.[9,39] The enhanced liquid-phase mass transfer coefficient, Ek_L, for the N_2O_4-water system is defined as:[9]

$$Ek_L = \frac{\sqrt{(D_{N_2O_4,H_2O})k_{36}}}{k_L} (k_L) = \sqrt{(D_{N_2O_4,H_2O})k_{36}} . \tag{49}$$

The local absorption rate may now be expressed as:

$$\overline{R}_{NO_2}^* = \frac{2P_{N_2O_4}/He_{N_2O_4} - 2C_{N_2O_4,B}}{\frac{1}{\sqrt{(D_{N_2O_4,H_2O})k_{36}}} + \frac{1}{He_{NO_2}^* k_G}} . \tag{50}$$

It is shown in Appendix B that

$$\sqrt{(D_{N_2O_4,H_2O})k_{36}} << He_{NO_2}^* k_G . \tag{51}$$

Thus the contribution of $1/He_{NO_2}^* k_G$, the gas-phase resistance group, to the local absorption rate of N_2O_4 is negligible. The absorption rate may now be expressed as:

$$\overline{R}_{NO_2}^* = 2\sqrt{(D_{N_2O_4,H_2O})k_{36}} \, (P_{N_2O_4}/He_{N_2O_4} - C_{N_2O_4,B}) . \tag{52}$$

It is shown in Appendix A that $C_{N_2O_4,B}$ is negligible. Elimination of this term reduces the local absorption rate equation for NO_2^* into water to:

$$\overline{R}_{NO_2^*} = 2\sqrt{(D_{N_2O_4,H_2O})k_{36}}\ (P_{N_2O_4}/He_{N_2O_4}) \ . \tag{53}$$

III. A MODEL FOR N_2O_4 ABSORPTION IN THE FROTH ON THE SIEVE PLATES

The mathematical expression for N_2O_4 absorption in the froth on the sieve plates utilizes the equilibrium relationship between N_2O_4 and NO_2 and the local absorption rate equation of NO_2^*, as shown in Equation (63). The assumptions used in developing the model include:

1. The froth on the sieve plates is well-mixed.
2. No backmixing occurs in the gas traveling through the sieve-plate froth.
3. The process is essentially isothermal (see Appendix D).
4. The change in the gas flow rate through the froth is negligible.
5. The gases behave as ideal gases.

The steady-state performance equation for NO_2^* removal by the absorption of N_2O_4 in an element of volume in the sieve-plate froth may be written as:

$$\text{Input} = \text{Output} + \text{Disappearance by absorption} \ . \tag{54}$$

The feed rate of NO_2^* may be represented by $GP_{NO_2^*}/RT$. If the plate is considered as a whole, the following equations may be derived:

$$\text{Input of } NO_2^* = GP_{NO_2^*}/RT \ , \tag{55}$$

$$\text{Output of } NO_2^* = G(P_{NO_2^*} + dP_{NO_2^*})/RT \ , \tag{56}$$

and

$$\text{Loss of } NO_2^* \text{ by reaction of } N_2O_4 = \overline{R}_{NO_2^*}adV \ . \tag{57}$$

Introduction of these terms in the performance equation for NO_2^* removal yields:

$$GP_{NO_2^*}/RT = G(P_{NO_2^*} + dP_{NO_2^*})/RT + (\overline{R}_{NO_2^*}adV) \ . \tag{58}$$

Note that

$$dP_{NO_2^*} = d[P_{NO_2^*,in}(1 - X_{NO_2^*})] = -P_{NO_2^*,in}dX_{NO_2^*} \ . \tag{59}$$

Substitution of Equation (59) into Equation (58) and subsequent rearrangement result in:

$$GP_{NO_2^*,in}dX_{NO_2^*} = \overline{R}_{NO_2^*}aRTdV \ . \tag{60}$$

Relating $P_{N_2O_4}$ to $P_{NO_2^*}$, it may be seen that

$$P_{N_2O_4} = P_{NO_2^*,in}(1 - \alpha)(1 - X_{NO_2^*})/2 \ . \tag{61}$$

Substitution of Equations (53) and (61) into Equation (60) yields:

$$GP_{NO_2^*,in}dX_{NO_2^*} = [\sqrt{(D_{N_2O_4,H_2O})k_{36}}\ (P_{NO_2^*,in})(1 - \alpha)(1 - X_{NO_2^*})/He_{N_2O_4}](aRTdV) \ . \tag{62}$$

Division by $P_{NO_2^*,in}$ and rearrangement of terms yield:

$$\frac{\sqrt{(D_{N_2O_4,H_2O})k_{36}}\ aRT}{GHe_{N_2O_4}} \int_0^{V_{FR}} dV = \int_0^{X_{NO_2}^*} \frac{dX_{NO_2}^*}{(1-\alpha)(1-X_{NO_2}^*)} . \tag{63}$$

Equation (44) for calculating α is substituted to produce

$$\frac{\sqrt{(D_{N_2O_4,H_2O})k_{36}}\ aRT}{GHe_{N_2O_4}} \int_0^{V_{FR}} dV$$

$$= \int_0^{X_{NO_2}^*} \frac{dX_{NO_2}^*}{[1+(K_{p,34}-K_{p,34}\sqrt{1+8P_{NO_2}^*/K_{p,34}})/(4P_{NO_2}^*)](1-X_{NO_2}^*)} . \tag{64}$$

Substituting the definition of $P_{NO_2}^*$ and combining terms in the denominator yield:

$$\frac{\sqrt{(D_{N_2O_4,H_2O})k_{36}}\ aRT}{GHe_{N_2O_4}} \int_0^{V_{FR}} dV$$

$$= \int_0^{X_{NO_2}^*} \frac{dX_{NO_2}^*}{1-X_{NO_2}^*+[(K_{p,34}-K_{p,34}\sqrt{1+8P_{NO_2,in}^*(1-X_{NO_2}^*)/K_{p,34}})/(4P_{NO_2,in}^*)]} . \tag{65}$$

Integration of the left-hand side of Equation (65), multiplication of both sides by $K_{p,34}/4P_{NO_2,in}^*$, and some rearrangement yield:

$$\frac{K_{p,1}\sqrt{(D_{N_2O_4,H_2O})k_{36}}\ aRTV_{FR}}{4P_{NO_2,in}^* GHe_{N_2O_4}}$$

$$= \int_0^{X_{NO_2}^*} \frac{dX_{NO_2}^*}{(1+4P_{NO_2,in}^*/K_{p,34})-\sqrt{(1+8P_{NO_2,in}^*/K_{p,34})-(8P_{NO_2,in}^*/K_{p,34})X}-4P_{NO_2,in}^*X/K_{p,34}} . \tag{66}$$

The right-hand side (R.H.S.) of Equation (66) is now in the form

$$\text{R.H.S.} = \int_0^{X_{NO_2^*}} \frac{dX}{A - \sqrt{B - CX} - DX} , \tag{67}$$

where

$$A = 1 + 4P_{NO_2^*,in}/K_{p,34} ; \tag{68}$$

$$B = 1 + 8P_{NO_2^*,in}/K_{p,34} ; \tag{69}$$

$$C = 8P_{NO_2^*,in}/K_{p,34} ; \tag{70}$$

$$D = 4P_{NO_2^*,in}/K_{p,34} ; \tag{71}$$

and

$$X = X_{NO_2^*} . \tag{72}$$

Utilizing the definition

$$Y^2 = B - CX \tag{73}$$

yields

$$X = \frac{B - Y^2}{C} \tag{74}$$

and

$$dX = -(2/C)YdY . \tag{75}$$

Upon substitution of these terms,

$$\text{R.H.S.} = \int_{Y_0}^{Y_F} \frac{-(2/C)YdY}{A - Y - D\left[\frac{B - Y^2}{C}\right]} \quad . \tag{76}$$

Multiplication of numerator and denominator by C and some rearrangement yield:

$$\text{R.H.S.} = -2 \int_{Y_0}^{Y_F} \frac{YdY}{(CA - DB) - CY + DY^2} \ , \tag{77}$$

which is integrable[40] in the form of

$$\text{R.H.S.} = -2 \int_{Y_0}^{Y_F} \frac{YdY}{\beta + \gamma Y + \varepsilon Y^2} \tag{78}$$

or

$$\text{R.H.S.} = -2 \int_{Y_0}^{Y_F} \frac{YdY}{\mathcal{Y}} \ , \tag{79}$$

where

$$\beta = CA - DB \ , \tag{80}$$

$$\gamma = -C \ , \tag{81}$$

$$\varepsilon = D \ , \tag{82}$$

and

$$\mathcal{Y} = \beta + \gamma Y + \varepsilon Y^2 \ . \tag{83}$$

The integration is dependent upon whether the quantity q, defined by[40]

$$q = 4\beta\varepsilon - \gamma^2 \ , \tag{84}$$

is positive, negative, or equal to zero. Substitution for β, ε, and γ yields:

$$q = 4(CA - DB)D - (-C)^2 = 4[2E(1 + E) - E(1 + 2E)]E - (-2E)^2 = 0 \ ; \tag{85}$$

for this situation, where q is equal to zero, the integration requires redefinition[40] as follows:

$$\mathcal{Y} = \varepsilon[Y + \frac{\gamma}{2\varepsilon}]^2 \tag{86}$$

and

$$\text{R.H.S.} = -2 \int_{Y_0}^{Y_F} \frac{YdY}{\varepsilon\left[Y + \frac{\gamma}{2\varepsilon}\right]^2} = -\frac{2}{\varepsilon} \int_{Y_0}^{Y_F} \frac{YdY}{\left[Y + \frac{\gamma}{2\varepsilon}\right]^2} \ , \tag{87}$$

which is in the form

$$\text{R.H.S.} = 2F \int_{Y_0}^{Y_F} \frac{YdY}{(\mathcal{G}Y + H)^2} \ , \tag{88}$$

where

$$F = -\frac{2}{\varepsilon} \ , \tag{89}$$

$$\mathcal{G} = 1 \ , \tag{90}$$

and

$$H = \frac{\gamma}{2\varepsilon} \ . \tag{91}$$

Equation (88) is integrated[40] as:

$$\text{R.H.S.} = -2\,\frac{F}{G}\left[\ell n(H + GY) + \frac{H}{H + GY}\right]\Bigg]_{Y_0}^{Y_F} . \tag{92}$$

or equation in terms of $X_{NO_2}^*$ is:

$$\text{R.H.S.} = -\frac{2}{D}\left[\ell n\left(\frac{-C}{2D} + \sqrt{B - CX}\right) + \left(\frac{-C}{2D}\right) \Big/ \left(\frac{-C}{2D} + \sqrt{B - CX}\right)\right]\Bigg]_{0}^{X_{NO_2}^*} . \tag{93}$$

An insertion of the limits gives:

$$\text{R.H.S.} = -\frac{2}{D}\left[\ell n\left(\frac{\sqrt{B - CX_{NO_2}^*} - \frac{C}{2D}}{\sqrt{B} - \frac{C}{2D}}\right) + \frac{\frac{C}{2D}\left[\sqrt{B - CX_{NO_2}^*} - \sqrt{B}\right]}{\left[\sqrt{B - CX_{NO_2}^*} - \frac{C}{2D}\right]\left[\sqrt{B} - \frac{C}{2D}\right]}\right] . \tag{94}$$

Completing the substitution of original variables yields:

$$\text{R.H.S.} = -\frac{2}{\phi}\left[\ell n\left(\frac{\sqrt{1 + 2\phi - 2\phi X_{NO_2}^*} - 1}{\sqrt{1 + 2\phi} - 1}\right) + \frac{\sqrt{1 + 2\phi - 2\phi X_{NO_2}^*} - \sqrt{1 + 2\phi}}{(\sqrt{1 + 2\phi - 2\phi X_{NO_2}^*} - 1)(\sqrt{1 + 2\phi} - 1)}\right] , \tag{95}$$

where

$$\phi = 4P_{NO_2^*,in}/K_{p,34} . \tag{96}$$

The equation for NO_2^* absorption in the sieve-plate froth is now:

$$\frac{\phi\sqrt{(D_{N_2O_4,H_2O})k_{36}}\ aRTV_{FR}}{GHe_{N_2O_4}} + \frac{2}{\phi}\left[\ln\left(\frac{\sqrt{1+2\phi-2\phi X_{NO_2}^*}-1}{\sqrt{1+2\phi}-1}\right)\right.$$

$$\left. + \frac{\sqrt{1+2\phi-2\phi X_{NO_2}^*}-\sqrt{1+2\phi}}{(\sqrt{1+2\phi-2\phi X_{NO_2}^*}-1)(\sqrt{1+2\phi}-1)}\right] = 0 \ . \tag{97}$$

Solution of this equation involves finding the positive and real root, $X_{NO_2}^*$, of a rather complex expression.

IV. A MODEL FOR THE DISSOCIATION OF LIQUID HNO_2 IN THE FROTH ON THE SIEVE PLATES

The model for the decomposition of HNO_2 in the froth on the sieve plates is based on Equation (37). The assumptions used in developing the model are: (1) the froth is well mixed, (2) changes in the liquid flow rate are minimal, (3) the concentration of HNO_3 is relatively constant, (4) the chemical equilibrium as expressed in Equation (37) has been attained (see Appendix F), and (5) The gases behave ideally.

The system is represented by the following relationships when the entire plate is taken into consideration:

$$\text{Input of } HNO_2 = LC^*_{HNO_2,in} \ , \tag{98}$$

where $C^*_{HNO_2,in}$ is the quantity of HNO_2 in the incoming liquid stream plus that produced by absorption of N_2O_4,

$$C^*_{HNO_2,in} = C_{HNO_2,in} + 1/2[GP_{NO_2}^*\ X_{NO_2}^*/(RTL)] \ ; \tag{99}$$

$$\text{Input of NO} = GP_{NO,in}/(\mathcal{R}T) \ ; \tag{100}$$

$$\text{Output of } HNO_2 = LC^*_{HNO_2,in}(1 - X_{HNO_2}) \ ; \tag{101}$$

$$\text{Output of NO} = G(P_{NO,in} + \Delta P_{NO})/\mathcal{R}T \ . \tag{102}$$

The NO produced on the sieve tray, ΔP_{NO}, may be related to the decomposition of liquid HNO_2 by

$$G\Delta P_{NO}/(\mathcal{R}T) = 2/3 \ LC^*_{HNO_2,in}X_{HNO_2} \ , \tag{103}$$

which upon further rearrangement yields:

$$\Delta P_{NO} = (2/3)(L/G)\mathcal{R}TC^*_{HNO_2,in}X_{HNO_2} \ . \tag{104}$$

Using the equilibrium constant for reaction (37) as expressed by Equation (28) and the indicated assumptions and taking into consideration that HNO_2 is a weak acid,

$$K_{p,37} = \frac{(C_{H^+})(C_{NO_3^-})[P_{NO,in} + (2/3)(L/G)\mathcal{R}TC^*_{HNO_2,in}X_{HNO_2}]^2}{[C^*_{HNO_2,in}(1 - X_{HNO_2})]^3} \ . \tag{105}$$

After rearrangement,

$$K_{p,37}[C^*_{HNO_2,in}(1 - X_{HNO_2})]^3 - (C_{H^+})(C_{NO_3^-})[P_{NO,in} + (2/3)(L/G)\mathcal{R}TC^*_{HNO_2,in}X_{HNO_2}]^2 = 0 \ . \tag{106}$$

The solution of this equation involves finding the positive and real root, X_{HNO_2}, of this third-degree polynomial.

V. A MODEL FOR NO OXIDATION IN THE GAS SPACE BETWEEN THE SIEVE PLATES

The model for NO oxidation in the free volume between the sieve plates is based on the third-order gas-space reaction of NO and oxygen.[25-29] The assumptions used in developing the model are:

1. The gas is well mixed in the free volume between the sieve plates.
2. The changes in the gas flow rate through the free volume are minimal.
3. The gases behave ideally.

The steady-state performance equation for NO oxidation in the free volume of the sieve plates may be written as:

$$\text{Input} = \text{Output} + \text{Disappearance by reaction} \ . \tag{107}$$

The system is represented by the following equations when the entire gas space is taken into consideration:

$$\text{Input of NO} = GP_{NO,in}/(\mathcal{R}T) \ , \tag{108}$$

$$\text{Input of } O_2 = GP_{O_2,in}/(\mathcal{R}T) \ , \tag{109}$$

$$\text{Output of NO} = GP_{NO,in}(1 - X_{NO})/(\mathcal{R}T) \ , \tag{110}$$

$$\text{Output of } O_2 = GP_{O_2,in}\left(1 - \left(\frac{P_{NO,in}}{2P_{O_2,in}}\right)X_{NO}\right)/(\mathcal{R}T) \ , \tag{111}$$

and

$$\text{Loss of NO by reaction} = Gr_{NO}\tau/(\mathcal{R}T) \ , \tag{112}$$

where

$$\tau = V_{gas\ space}/G \ . \tag{113}$$

The reaction rate is expressed as:[25-29]

$$r_{NO} = k_{38} P_{NO}^2 P_{O_2} \tag{114}$$

or

$$r_{NO} = k_{38}[P_{NO,in}(1 - X_{NO})]\ P_{O_2,in}\left(1 - \left(\frac{P_{NO,in}}{2P_{O_2,in}}\right)X_{NO}\right) \ . \tag{115}$$

These terms are introduced into the performance equation for NO oxidation:

$$P_{NO,in} = P_{NO,in}(1 - X_{NO}) + k_{38}[P_{NO,in}(1 - X_{NO})]^2 P_{O_2,in}\left(1 - \left(\frac{P_{NO,in}}{2P_{O_2,in}}\right)X_{NO}\right)\tau \ . \tag{116}$$

Combining terms and rearranging yield:

$$-P_{NO,in}X_{NO} + k_{38}P_{NO,in}^2 P_{O_2,in}(1 - X_{NO})^2\left(1 - \left(\frac{P_{NO,in}}{2P_{O_2,in}}\right)X_{NO}\right)\tau = 0 \ . \tag{117}$$

Division by $P_{NO,in}$ and combination of terms results in:

$$-X_{NO} + k_{38}P_{NO,in}P_{O_2,in}\left[1 - \left(\frac{P_{NO,in}}{P_{O_2,in}} + 2\right)X_{NO} + \left(\frac{P_{NO,in}}{P_{O_2,in}} + 1\right)X_{NO}^2 - \left(\frac{P_{NO,in}}{2P_{O_2,in}}\right)X_{NO}^3\right]\tau = 0 \ . \tag{118}$$

Solution of this equation involves finding the positive and real root, X_{NO}, of a third-degree polynomial.

VI. THE OVERALL MODEL FOR PREDICTING NO_x REMOVAL IN A MULTISTAGE COLUMN

The following model is based on the mathematical simulation developed earlier for the NO_2^* absorption and HNO_2 decomposition in the froth on a sieve plate and NO oxidation in the gas spaces between the sieve plates. The use of the column model requires input of the following steady-state experimental conditions: the feed gas and liquid flow rates, the partial pressure of NO_x in the feed gas, the steam flow rate, the column gas and liquid temperature profile, and the nitric acid molarity. The model-predicted steady-state HNO_2 molarity was calculated by repeated iterations of the model calculations. Reaching the model-predicted steady state was based on reaching nonchanging column gas and liquid conditions. The model shown here allows for adjustment of the gas density upon leaving the froth and again upon leaving the gas space. The subscripts j and k are used to indicate the stage number in a column and the position of the gas in a particular stage, respectively. For gas entering the froth of plate j, k = 1; for gas leaving the froth of plate j, k = 2. The partial pressures of NO_2^*, NO, nitrogen and oxygen of a gas stream entering the froth on stage j are indicated by $P_{NO_2^*,j,k=1}$, $P_{NO,j,k=1}$, $P_{N_2,j,k=1}$, and $P_{O_2,j,k=1}$, respectively. The partial pressures of the components leaving the froth are indicated by:

$$P_{NO_2^*,j,k=2} = P_{NO_2^*,j,k=1}(1 - X_{NO_2^*})/(1 - \varepsilon'_{k=1}X_{NO_x}) \ , \tag{119}$$

$$P_{NO,j,k=2} = [P_{NO,j,k=1} + \Delta P_{NO,j}]/(1 - \varepsilon'_{k=1}X_{NO_x}) \ , \tag{120}$$

$$P_{N_2,j,k=2} = P_{N_2,j,k=1}/(1 - \varepsilon''_{k=1}X_{NO_x}) \quad , \tag{121}$$

and

$$P_{O_2,j,k=2} = P_{O_2,j,k=1}/(1 - \varepsilon''_{k=1}X_{NO_x}) \quad ; \tag{122}$$

those leaving the gas space of stage j or entering stage j+1 are indicated by:

$$P_{NO_2^*,j+1,k=1} = [P_{NO_2^*,j,k=2} + P_{NO,j,k=2}X_{NO}]/(1 - \varepsilon''_{k=2}X_{NO}) \quad , \tag{123}$$

$$P_{NO,j+1,k=1} = P_{NO,j,k=2}(1 - X_{NO})/(1 - \varepsilon''_{k=2}X_{NO}) \quad , \tag{124}$$

$$(P_{N_2,j+1,k=1} = P_{N_2,j,k=2}/(1 - \varepsilon''_{k=2}X_{NO}) \quad , \tag{125}$$

and

$$P_{O_2,j+1,k=1} = P_{O_2,j,k=2}(1 - \frac{P_{NO,in}}{2P_{O_2,in}} X_{NO})/(1 - \varepsilon''_{k=2}X_{NO}) \quad . \tag{126}$$

The partial pressures of the gas components as well as the gas flow rates are corrected for bulk removal of the gas-phase components. This correction may be made by division or multiplication by $(1 - \varepsilon''_k)$, where ε''_k is the fractional volume change due to removal of the gas components (k = 1 for the froth and k = 2 for the gas space). The quantities $X_{NO_2^*}$, $\Delta P_{NO,j}$, and X_{NO} are found using Eqs. (97), (104), and (118). Solution of Eq. (104) requires prior solution of Eq. (106). A multistage column may be modeled by letting j assume values from one to the number of required stages, provided the basic removal mechanisms remain valid.

CHAPTER IV

EXPERIMENTAL APPARATUS AND PROCEDURE

The flowsheet of the experimental equipment is shown in Figure 5. The NO_x scrubber is a three-stage sieve-plate column constructed of 0.076-m-ID by 0.254-m-long sections of Pyrex glass pipe. The plates and downcomers, shown in Figure 6, are constructed of stainless steel. The pertinent plate dimensions are as follows:

1. Distance between plates, 0.254 m.
2. Plate diameter, 0.073 m.
3. Outlet weir height, 0.025 m.
4. Downcomer weir height, 0.025 m.
5. Total plate area, 0.00419 m^2.
6. Downcomer area, 0.00174 m^2.
7. Overflow area, 0.000871 m^2.
8. Active area, 0.00213 m^2.
9. Number of perforations per plate, 3.
10. Area per perforation, 7.92×10^{-6} m^2.
11. Percent free area per plate, 0.6.
12. Available heat transfer area (per downcomer), 0.0198 m^2.

The percent free area per plate is relatively low when compared with that of a typical sieve-plate column.[41] This is because the column was designed for high L/G ratios in an attempt to remove the heat generated from the absorption reactions and condensation of the steam with increased liquid flow rates.

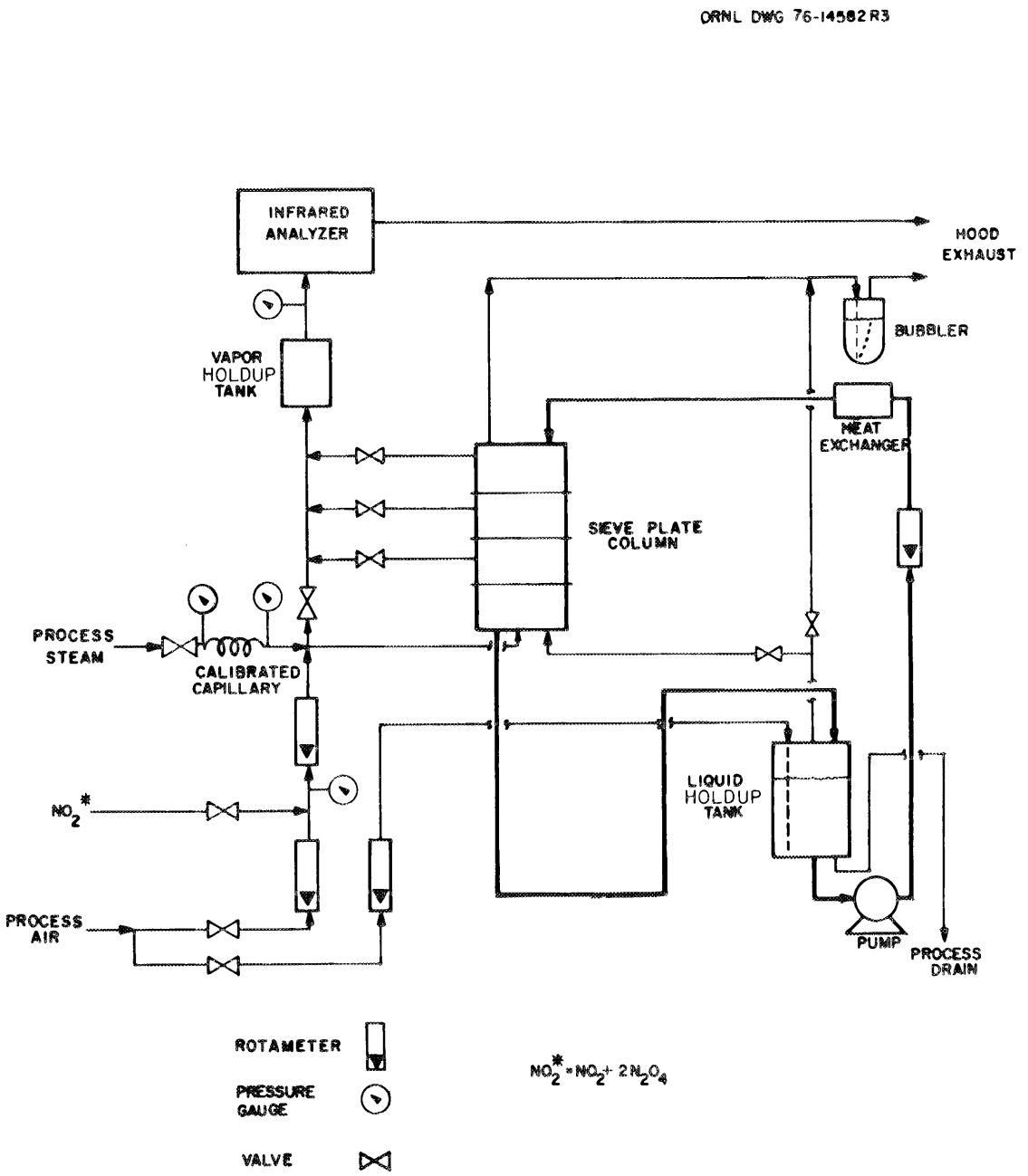

Figure 5. Flowsheet of equipment used in NO_x scrubbing experiment.

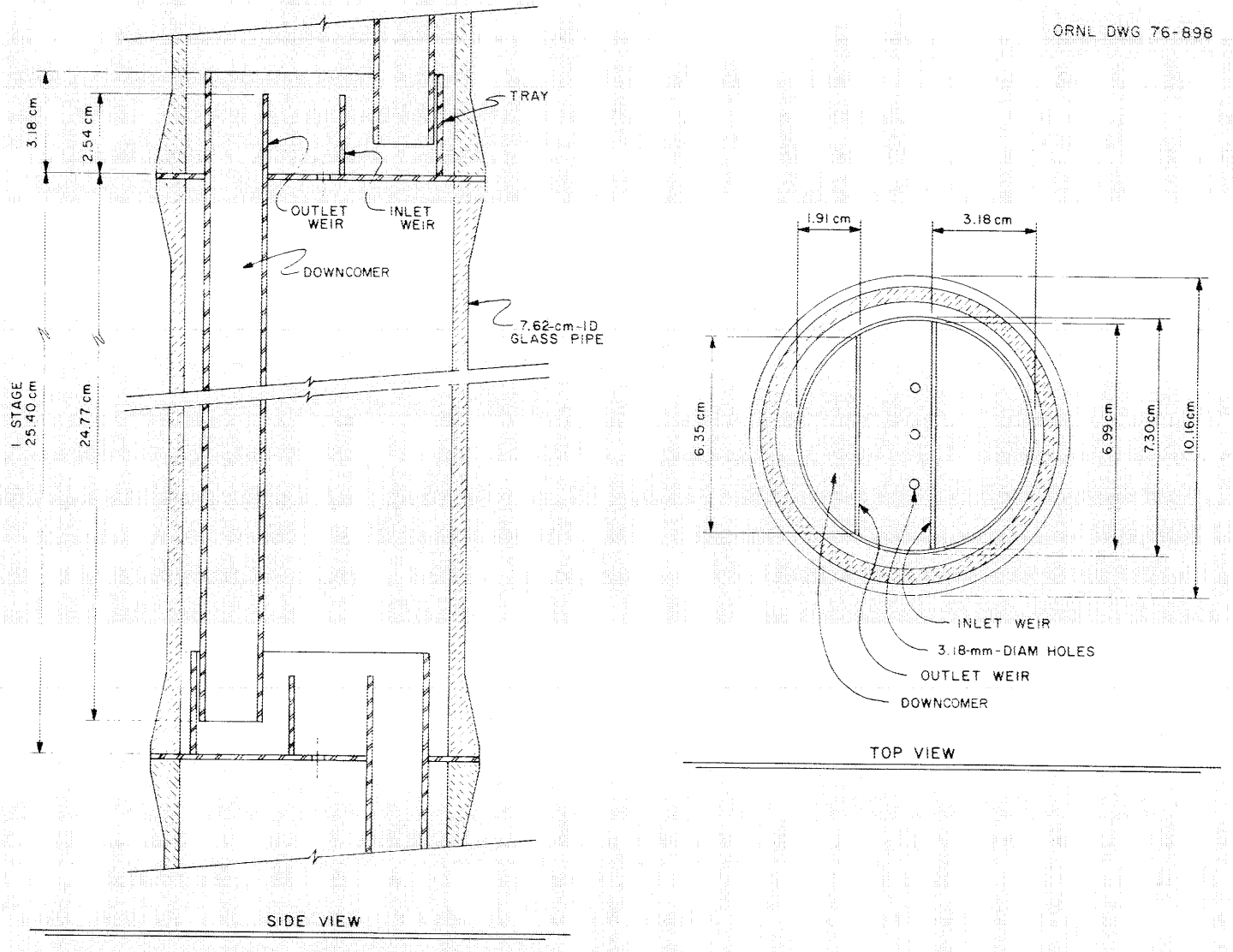

Figure 6. Typical plate and downcomer arrangement for sieve-plate column.

Other items of equipment used in the experiment include: a scrubber liquid holdup tank, pump, rotameter, and heat exchanger; a gaseous NO_2^* supply system; and process air, steam, and water supply systems. The gas-phase equipment includes a NO_2^*-air rotameter, an effluent gas holdup tank, an infrared analyzer to determine the concentrations of NO_x in the feed and effluent gas streams, a calibration gas supply system, and an exhaust gas system.

The system is normally operated by pumping the scrubber liquid from the scrubber liquid holdup tank and metering it through heat exchangers to the column. Upon leaving the column, the effluent liquid stream flows by gravity to the return tank. Gaseous NO_2^* is supplied to the system by vaporizing liquid NO_2^*, of commercial purity obtained from Matheson Gas Products, in a temperature-regulated water bath. Process air is metered along with the NO_2^* by a rotameter and blended with steam in a common feed stream to the column. Steam flows are controlled by maintaining a constant differential pressure across a calibrated capillary tube. The system is allowed to reach steady-state conditions before data are taken. The system is said to be at steady state when all gas and liquid flow rates, column temperatures, and NO_x concentrations in the feed and effluent streams have shown no change over a 30-min interval. The gas stream is sampled before and after leaving each stage. The streams, with the exception of the feed stream, are passed through a sample holdup tank to provide sufficient time for most of the NO_x gases to reach the NO_2^* state for analysis (see Appendix C). The sample streams are then metered to an infrared analyzer (Lira Model 202

purchased from Mine Safety Appliances). The analyzer is specific for NO_2^* and requires a gas with a known air-NO_2^* content for the purpose of calibration. Samples of the scrubber liquid may be taken entering and leaving the column. These liquid samples are normally analyzed for HNO_3 and HNO_2. Plate and column efficiencies are calculated from these concentration differences. The effluent gas stream is discharged through the hood exhaust. The liquid waste streams are sent to a liquid process waste system. The entire experiment is set up in a fume hood in which a constant airflow is maintained.

CHAPTER V

EXPERIMENTAL DATA AND QUANTITATIVE DESCRIPTION OF RESULTS

Experimental results using the apparatus previously described (stages are numbered from bottom to top) have been obtained for the following parameters and are given in Tables 4 and 5: (a) scrubber liquid flow rate, (b) feed gas flow rate, (c) partial pressure of NO_2^* in the feed gas, (d) HNO_3 concentration in the scrubber liquid, (e) amount of steam in the feed gas, and (f) effect of sparging of the liquid holdup tank. Some work involving a nonrecirculating liquid-phase system is shown in Tables 4 and 6. The period of time required to reach steady state has been investigated and is reported in Table 7. Some experiments using a single column plate and a nonrecirculating scrubber liquid have been performed; the results of these experiments are presented in Table 8.

The nominal run conditions were:

1. Scrubber liquid flow rate, 0.175×10^{-4} or 0.350×10^{-4} m^3/sec.
2. Combined air and NO_2^* flow rates, 2.0×10^{-4} m^3/sec.
3. Steam flow rate, 3.7 kg of steam per m^3 of air and NO_2^*.
4. Inlet scrubber temperature, 298 K.
5. Feed gas temperature, 363 K.
6. Scrubber molarity, $\sim$2.0.

Table 4. Steady-state NO_x scrubbing data for recirculating and nonrecirculating scrubber liquid

Run no.	NO_x partial pressure (atm)				Gas temperature (K)				Liquid temperature (K)		
	feed	stage 1	stage 2	stage 3	feed	stage 1	stage 2	stage 3	stage 1	stage 2	stage 3
Recirculating scrubber liquid											
9	0.308	0.106	0.067	0.051	352	314	306	305	310	298	297
10	0.312	0.114	0.068	0.053	353	312	305	303	310	297	297
11	0.299	0.114	0.073	0.058	353	312	304	304	310	297	297
12	0.295	0.110	0.068	0.053	351	309	305	304	310	297	297
13	0.273	0.012	0.073	0.062	353	312	305	303	310	297	297
15	0.341	0.128	0.073	0.051	353	313	305	304	312	297	297
16	0.310	0.141	0.084	0.070	298	302	303	305	297	297	297
17	0.293	0.100	0.057	0.040	352	312	304	303	310	297	297
18	0.332	0.103	0.057	0.042	351	312	304	303	309	297	297
19	0.0	0.0	0.0	0.0	351	303	299	299	310	297	297
20	0.310	0.117	0.066	0.042	351	316	305	303	309	297	297
31	0.341	0.125	0.079	0.057	353	312	305	304	310	297	297
32	0.352	0.117	0.070	0.051	353	313	305	304	310	297	297
42	0.306	0.141	0.088	0.062	364	320	307	305	320	298	297
44	0.295	0.136	0.095	0.066	365	320	308	306	320	298	297
45	0.301	0.150	0.097	0.084	299	303	306	299	298	297	297
46	0.301	0.125	0.088	0.070	357	311	306	305	310	298	297
47	0.301	0.143	0.097	0.068	368	322	308	305	331	299	298
48	0.350	0.141	0.090	0.068	363	315	307	305	313	299	297
49	0.301	0.107	0.069	0.051	363	317	305	304	309	298	297
50	0.312	0.171	0.112	0.075	367	333	310	305	337	299	297
51	0.145	0.066	0.048	0.040	362	317	304	303	318	298	297
52	0.215	0.127	0.110	0.105	298	300	300	301	298	297	297
53	0.317	0.183	0.123	0.103	299	303	307	309	298	297	297
54	0.321	0.132	0.101	0.079	365	317	306	305	318	296	295
60	0.293	0.129	0.079	0.057	366	317	306	303	310	298	297
61	0.400	0.174	0.101	0.070	366	315	305	303	311	297	296
62	0.308	0.114	0.068	0.050	357	336	313	300	310	297	297
Nonrecirculating scrubber liquid											
22	0.33	0.088	0.033	0.015	364	308	301	301	306	294	294
23	0.285	0.043	0.013	0.008	359	304	298	299	306	295	295
24	0.317	0.092	0.044	0.022	365	313	302	301	317	294	294
25	0.273	0.099	0.064	0.037	367	331	306	302	336	296	295
26	0.341	0.092	0.044	0.022	366	313	301	300	308	293	293
27	0.365	0.068	0.023	0.011	361	305	299	299	308	295	295

Table 5. Steady-state NO_x scrubbing data
(total pressure = 1.1 atm in all runs)

Run no.	Steam feed rate[a] (kg/sec × 10^3)	Air feed rate[a] (m^3/sec × 10^4)	Liquid feed rate[a] (m^3/sec × 10^4)	HNO_2 (M)	HNO_3 (M)	Recycle of gas from liquid holdup tank	Liquid holdup tank sparge rate (m^3/sec × 10^6)	Liquid holdup volume (m^3 × 10^2)
9	0.73	1.40	0.35	—	1.0	Yes	0.0	1.64
10	0.73	1.40	0.35	—	2.0	Yes	0.0	1.64
11	0.73	1.40	0.35	—	3.5	Yes	0.0	1.64
12	0.73	1.40	0.35	—	3.0	Yes	0.0	1.64
13	0.73	1.40	0.35	—	3.5	Yes	0.0	1.64
15	0.73	1.40	0.35	—	2.4	Yes	2.5	1.64
16	0.73	1.40	0.35	—	3.2	Yes	0.0	1.64
17	0.73	1.40	0.35	—	3.0	Yes	7.5	1.64
18	0.73	1.40	0.35	—	2.4	Yes	14.0	1.64
19	0.73	1.40	0.35	—	2.2	Yes	0.0	1.64
20	0.73	1.40	0.35	—	2.2	Yes	2.5	2.51
31	0.73	1.40	0.35	0.45	1.3	No	0.0	1.64
32	0.73	1.40	0.35	0.39	1.7	No	2.5	1.64
42	0.70	1.40	0.17	0.25	2.3	No	0.0	1.64
44	1.08	2.10	0.26	0.20	1.6	No	0.0	1.64
45	0.00	1.40	0.18	0.28	2.7	No	0.0	1.64
46	0.35	1.40	0.18	0.18	3.0	No	0.0	1.64
47	1.09	1.40	0.18	0.18	2.8	No	0.0	1.64
48	0.67	1.40	0.26	0.30	2.6	No	0.0	1.64
49	0.67	1.40	0.35	—	2.0	No	0.0	1.64
50	0.67	1.40	0.09	0.20	2.4	No	0.0	1.64
51	0.67	1.70	0.18	0.21	2.0	No	0.0	1.64
52	0.00	1.80	0.18	—	2.1	No	0.0	1.64
53	0.00	2.16	0.26	0.20	3.0	No	0.0	1.64
54	0.85	1.80	0.22	0.20	3.0	No	0.0	1.64
60	0.83	1.80	0.22	0.19	1.5	No	0.0	1.64
61	0.65	1.24	0.17	0.28	2.4	No	0.0	1.64
62	0.36	1.22	0.13	0.27	2.4	No	0.0	1.64

[a]The tabulated numbers in the columns have been multiplied by the indicated factor.

Table 6. Steady-state NO_x scrubbing data for nonrecirculating scrubber liquid (total pressure = 1.1 atm in all runs)

Run no.	Steam feed rate[a] (kg/sec × 10^3)	Air feed rate[a] (m^3/sec × 10^4)	Liquid feed rate[a] (m^3/sec × 10^4)	HNO_3 in (M)	HNO_3 out (M)	Recycle of gas from liquid holdup tank
22	0.68	1.40	0.35	—	—	No
23	0.33	0.70	0.18	—	—	No
24	0.68	1.40	0.18	—	—	No
25	0.70	1.40	0.09	<0.005	0.180	No
26	1.00	2.10	0.53	<0.005	0.040	No
27	0.38	0.70	0.18	<0.005	0.069	No

[a]The tabulated numbers in the columns have been multiplied by the indicated factor.

Table 7. Data showing the approach to steady state for NO_x scrubbing with recirculating scrubber liquid

Run no.	Time (sec)	Partial pressure of NO_x (atm)				HNO_2 (M)		HNO_3 (M)
		Feed	stage 1	stage 2	stage 3	Feed liquid	Effluent liquid	
9	1800	0.313	0.092	0.048	0.026	—	—	—
	7200	0.308	0.099	0.058	0.040	—	—	—
	19800	0.308	0.108	0.067	0.051	—	—	1.7
31	0	0.341	0.100	0.047	0.023	0.02	0.02	1.01
	1800	0.341	—	—	0.024	0.09	0.22	0.94
	3600	0.341	—	—	0.036	0.23	0.25	0.95
	5400	0.341	—	—	0.041	0.30	0.30	0.98
	7200	0.341	—	—	0.044	0.35	0.31	1.02
	9000	0.341	—	—	0.051	0.29	0.43	1.10
	10800	0.341	—	—	0.053	0.44	0.46	1.12
	12600	0.341	—	—	0.057	0.46	0.47	1.18
	14400	0.341	—	—	0.059	0.46	0.43	1.23
	16200	0.341	0.125	0.079	0.059	0.45	0.46	1.31
32	0	0.361	0.108	0.062	0.040	0.02	0.02	1.67
	3600	0.361	—	—	—	0.06	0.08	1.60
	5400	0.361	—	—	—	0.15	0.16	1.56
	7200	0.360	—	—	—	0.18	0.18	1.59
	9000	0.355	—	—	—	0.28	0.31	1.58
	10800	0.350	—	—	0.042	0.32	0.34	1.60
	12600	0.350	—	—	0.044	0.32	0.36	1.64
	14400	0.350	—	—	0.048	0.33	0.38	1.62
	16200	0.350	—	—	0.051	0.33	0.38	1.70
	18000	0.350	—	—	0.050	0.40	0.42	1.70
	19800	0.350	0.116	0.070	0.051	0.38	0.39	1.78

Table 8. Steady-state NO_2^* scrubbing data for a single sieve plate and a nonrecirculating scrubber liquid

Run No.	$P_{NO_2^*,in}$ (atm)	$P_{NO_2^*,out}$ (atm)	$T_{G,in}$ (K)	$T_{G,out}$ (K)	T_L (K)	G (std m^3/sec)	F_{STEAM} (kg/sec)	L (m^3/sec)	a (m^2/m^3)
55a	0.026	0.012	293	297	292	2.0×10^{-4}	0	1.75×10^{-5}	
55b	0.051	0.020	294	297	292	2.0×10^{-4}	0	1.75×10^{-5}	
55c	0.101	0.040	294	297	292	2.0×10^{-4}	0	1.75×10^{-5}	
55d	0.161	0.059	294	297	292	2.0×10^{-4}	0	1.75×10^{-5}	
55e	0.207	0.081	294	297	292	2.0×10^{-4}	0	1.75×10^{-5}	
55f	0.267	0.103	294	297	292	2.0×10^{-4}	0	1.75×10^{-5}	
55g	0.330	0.117	294	297	292	2.0×10^{-4}	0	1.75×10^{-5}	
56a	0.035	0.013	294	298	293	1.5×10^{-4}	0	1.75×10^{-5}	
56b	0.053	0.017	294	298	293	1.5×10^{-4}	0	1.75×10^{-5}	
56c	0.107	0.035	294	298	293	1.5×10^{-4}	0	1.75×10^{-5}	
56d	0.167	0.057	294	298	293	1.5×10^{-4}	0	1.75×10^{-5}	
56e	0.187	0.075	294	298	293	1.5×10^{-4}	0	1.75×10^{-5}	
56f	0.260	0.088	294	298	293	1.5×10^{-4}	0	1.75×10^{-5}	
56g	0.330	0.094	294	298	293	1.5×10^{-4}	0	1.75×10^{-5}	
57a	0.020	0.011	294	297	293	2.5×10^{-4}	0	1.75×10^{-5}	
57b	0.044	0.020	294	298	293	2.5×10^{-4}	0	1.75×10^{-5}	
57c	0.101	0.044	294	298	293	2.5×10^{-4}	0	1.75×10^{-5}	
57d	0.161	0.068	295	298	292	2.5×10^{-4}	0	1.75×10^{-5}	
57e	0.216	0.094	295	298	292	2.5×10^{-4}	0	1.75×10^{-5}	
57f	0.279	0.119	295	298	292	2.5×10^{-4}	0	1.75×10^{-5}	
57g	0.312	0.134	295	298	292	2.5×10^{-4}	0	1.75×10^{-5}	
58a	0.015	0.009	295	298	293	3.0×10^{-4}	0	1.75×10^{-5}	
58b	0.050	0.024	295	298	292	3.0×10^{-4}	0	1.75×10^{-5}	
58c	0.107	0.051	295	298	292	3.0×10^{-4}	0	1.75×10^{-5}	
58d	0.165	0.075	295	298	292	3.0×10^{-4}	0	1.75×10^{-5}	
58e	0.211	0.099	295	298	292	3.0×10^{-4}	0	1.75×10^{-5}	
58f	0.260	0.119	295	298	292	3.0×10^{-4}	0	1.75×10^{-5}	
59a	0.163	0.079	294	296	292	2.0×10^{-4}	0	0.44×10^{-5}	
59b	0.163	0.075	294	296	293	2.0×10^{-4}	0	0.88×10^{-5}	
59c	0.163	0.062	294	296	292	2.0×10^{-4}	0	2.60×10^{-5}	
59d	0.163	0.057	294	296	290	2.0×10^{-4}	0	3.50×10^{-5}	
63a	0.152	0.051	299	297	290	2.0×10^{-4}	0	1.75×10^{-5}	
63b	0.145	0.044	297	298	291	1.5×10^{-4}	0	1.31×10^{-5}	
63c	0.151	0.055	294	298	290	2.5×10^{-4}	0	2.19×10^{-5}	
63d	0.151	0.055	294	298	290	2.5×10^{-4}	0	2.19×10^{-5}	
64a	0.165	0.026	348	302	298	2.0×10^{-4}	1.67×10^{-4}	1.75×10^{-5}	622
64b	0.166	0.024	355	304	302	2.0×10^{-4}	3.67×10^{-4}	1.75×10^{-5}	724
64c	0.163	0.024	362	306	309	2.0×10^{-4}	7.83×10^{-4}	1.75×10^{-5}	850
64d	0.166	0.022	365	309	317	2.0×10^{-4}	11.83×10^{-4}	1.75×10^{-5}	1200
65a	0.141	0.031	368	316	337	2.0×10^{-4}	7.83×10^{-4}	0.44×10^{-5}	1650
65b	0.152	0.019	359	300	300	2.0×10^{-4}	7.83×10^{-4}	3.50×10^{-5}	781
65c	0.151	0.028	369	322	322	2.0×10^{-4}	7.83×10^{-4}	0.86×10^{-5}	1120

7. Feed gas partial pressure of NO_2^*, 0.31 atm.

8. Total pressure, 1.1 atm.

These conditions were subject to variation for the purpose of the study.

Increasing the flow rate of the scrubber liquid decreases the internal column temperatures. The decreased column temperatures result in a higher overall NO_x conversion, X_{NO_x}, as shown in Figure 7. The term X_{NO_x} is the partial pressure of the absorbed NO_x divided by the partial pressure of NO_x entering a stage or column corrected for any volume change. Within the column, the response to increased liquid flow rates is most apparent on the first plate, where the temperature decrease is most pronounced. The increased NO_x conversion on the first plate seems to be the major factor in greater overall NO_x conversion with increased liquid flow rates. This is consistent with the increase in absorption rates with decreased temperature reported in the literature.[3,8,10,11,12,14] Also, the oxidation of NO is increased at reduced temperatures.[25-29]

The effect of higher gas flow rates is a decrease in NO_x conversion throughout the column (see Figure 8). This effect is probably the result of higher column temperatures and a reduced gas residence time in the froth for absorption and in the gas spaces between the plates for NO oxidation.

The results of varied NO_2^* partial pressures in the gas feed stream are shown in Figure 9. The increased conversion of NO_x with higher NO_2^* partial pressures in the feed gas is consistent with increased absorption of NO_2^* and oxidation of NO due to higher driving force concentrations of NO_2^* and NO, respectively.

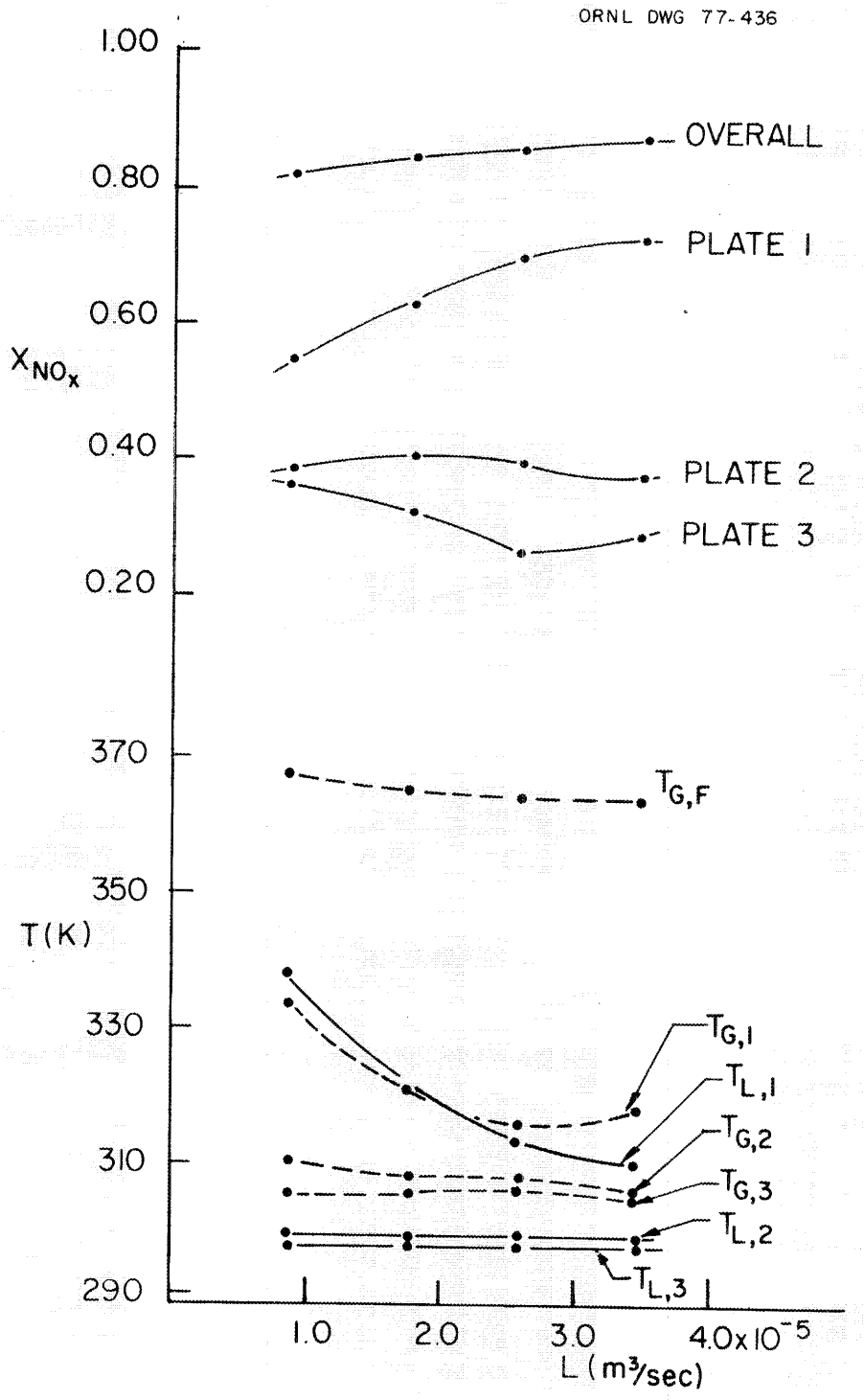

Figure 7. NO_x conversion and temperature profiles for NO_x removal in three-stage sieve-plate column for varied scrubber-liquid flow rates.

ORNL DWG. 77-442

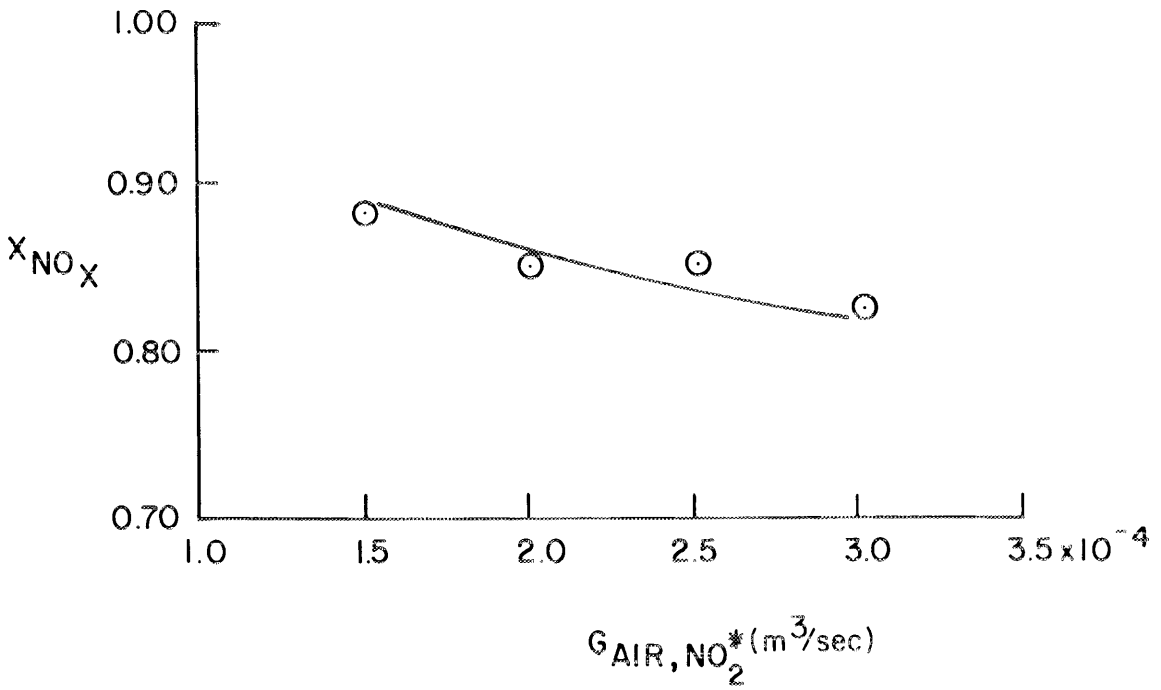

Figure 8. Overall NO_x removal in three-stage sieve-plate column for varied feed-gas flow rates.

ORNL DWG. 77-473 R1

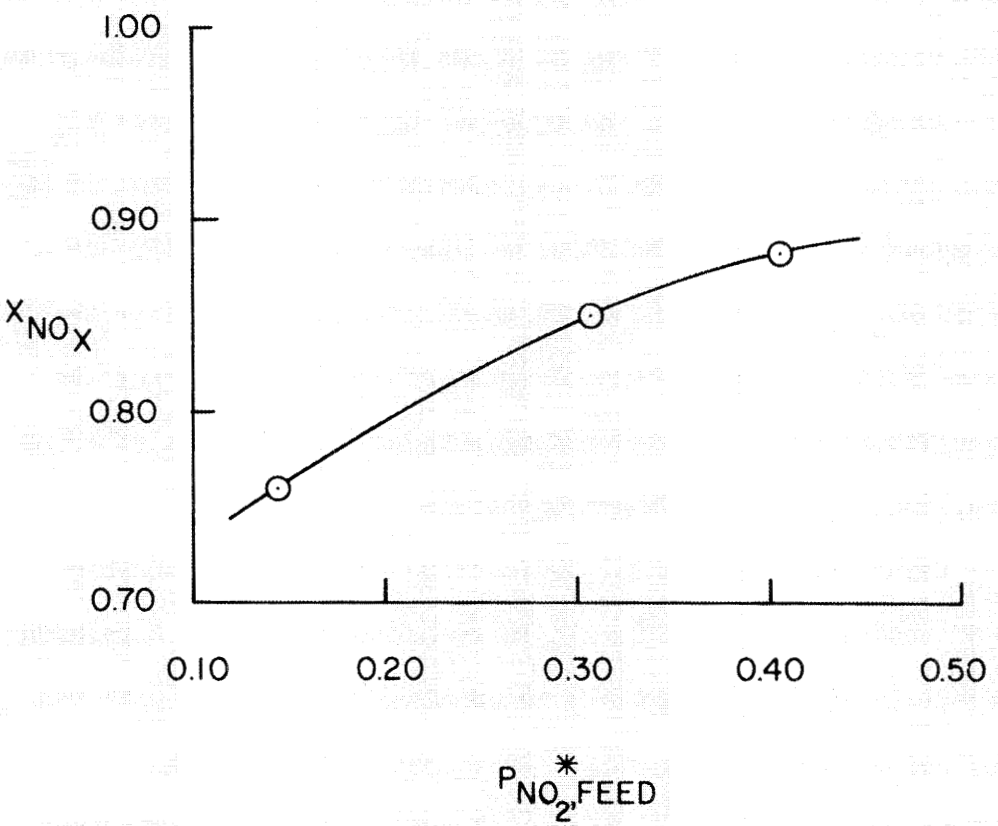

Figure 9. Overall NO_X removal in three-stage sieve-plate column for varied partial pressure of NO_2 in feed gas.

The equilibrium nature of NO_2^* absorption can be neglected at low HNO_3 concentrations. However, the Henry's law constant for N_2O_4 is a slight inverse function of the ionic strength. The decreased overall NO_x absorption with increased acid molarity (shown in Figure 10) is probably caused by a reduction in the respective solubilities of N_2O_4 with increased acid strengths.

The effect of varying the ratio of the steam flow rate to the air and NO_2^* flow rate in the feed gas is shown in Figure 11. An increase in the steam concentration in the feed gas appears to increase NO_x conversion up to approximately 3.5 kg of steam per cubic meter of NO_2^* and air; above this proportion, however, the effect appears to be a decrease in NO_x conversion. One explanation for this could be that the presence of steam enhances the absorption of NO_2^* by increasing the gas-liquid interfacial area and reducing the oxidation rate of NO by increasing the column operating temperature.

An interesting experimental observation was the relationship between NO_x conversion and HNO_2 liquid concentration. The attainment of steady-state operation appeared to be closely connected with the attainment of a steady-state HNO_2 liquid concentration. This relationship is illustrated in Figure 12, which summarizes the data for an experimental run from start-up to steady state. Increasing the air sparge rate of the liquid holdup tank resulted in a greater overall NO_x conversion, as shown in Figure 13. The air sparge of the liquid holdup tank probably drives the equilibrium reaction of HNO_2, Equation (37), to the dissociation of HNO_2. This insight seems

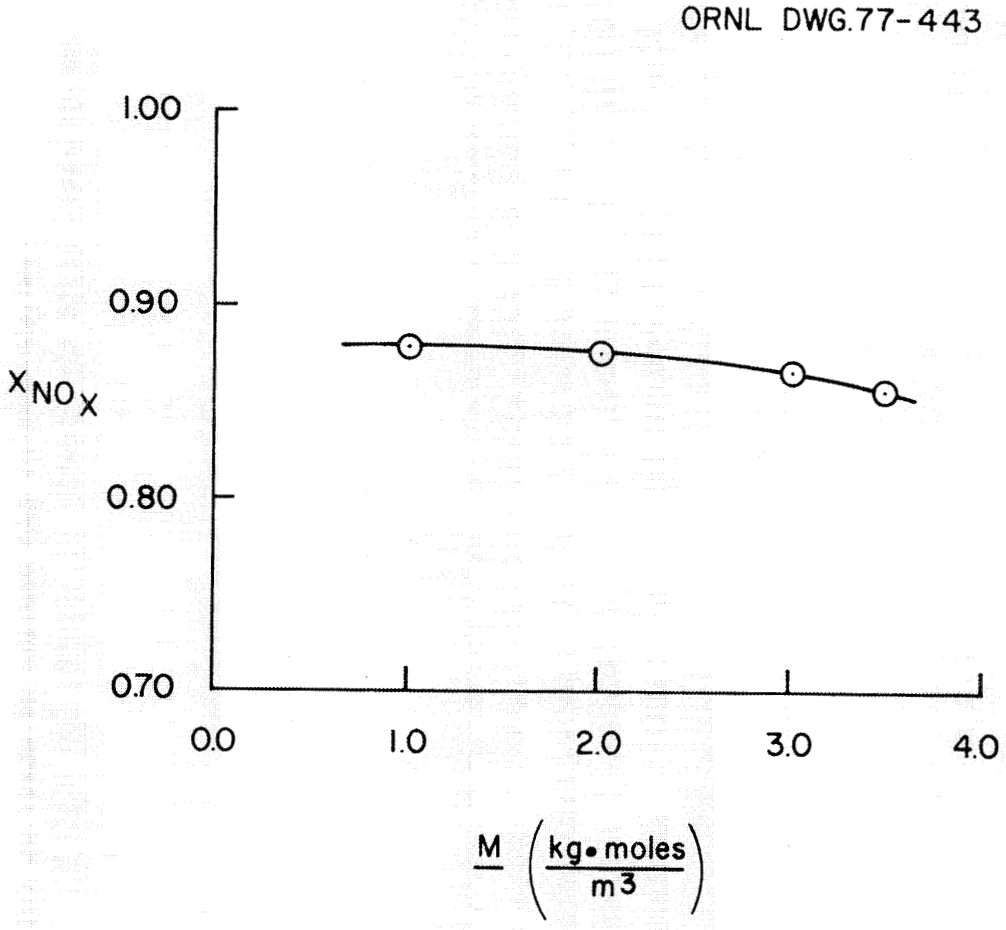

Figure 10. Overall NO_x removal in three-stage sieve-plate column as a function of acid molarity in scrubber liquid.

ORNL DWG.77-440

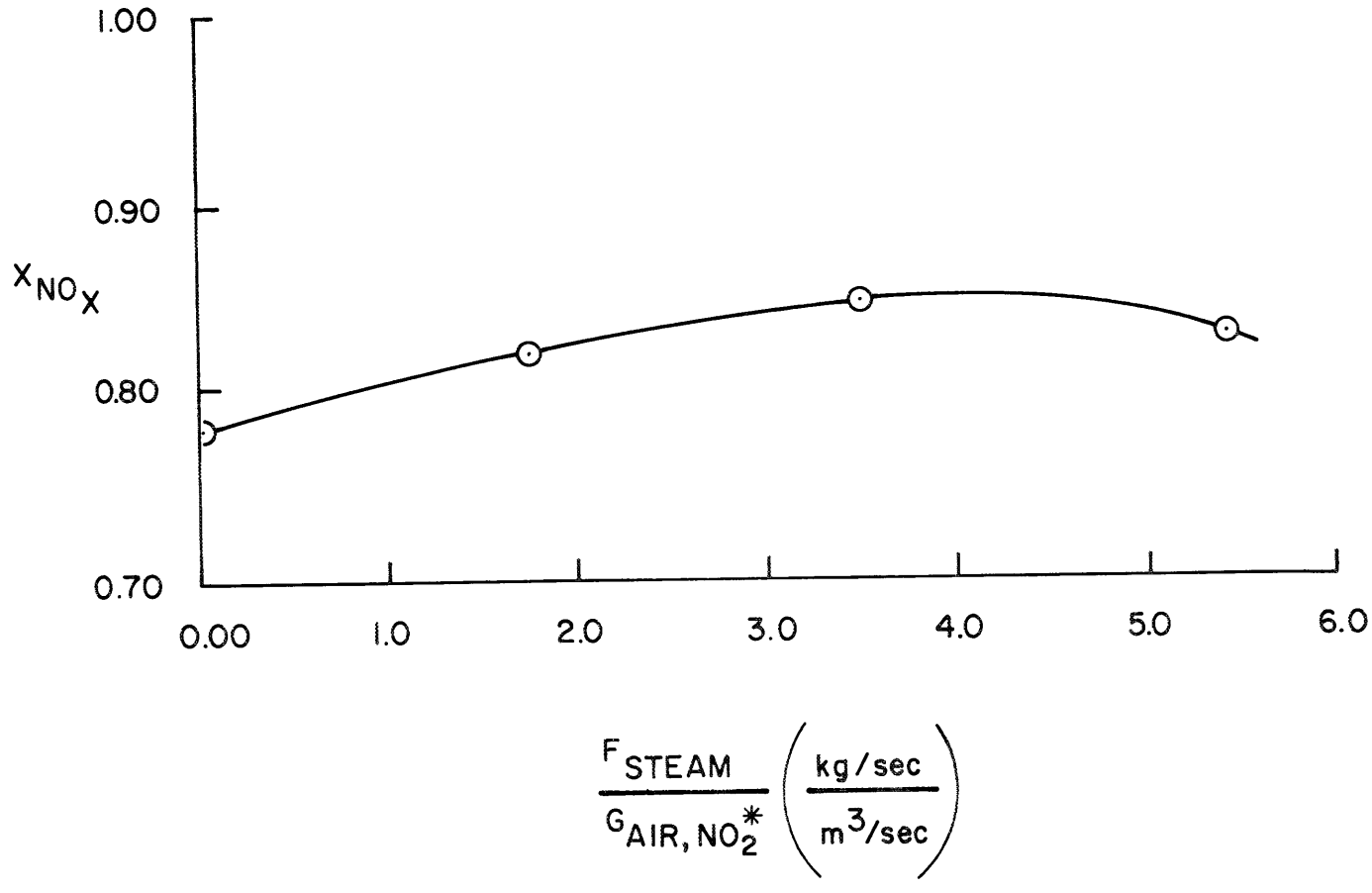

Figure 11. Overall NO_x removal in three-stage sieve-plate column for varied ratios of steam to air and NO_2^* in the feed gas.

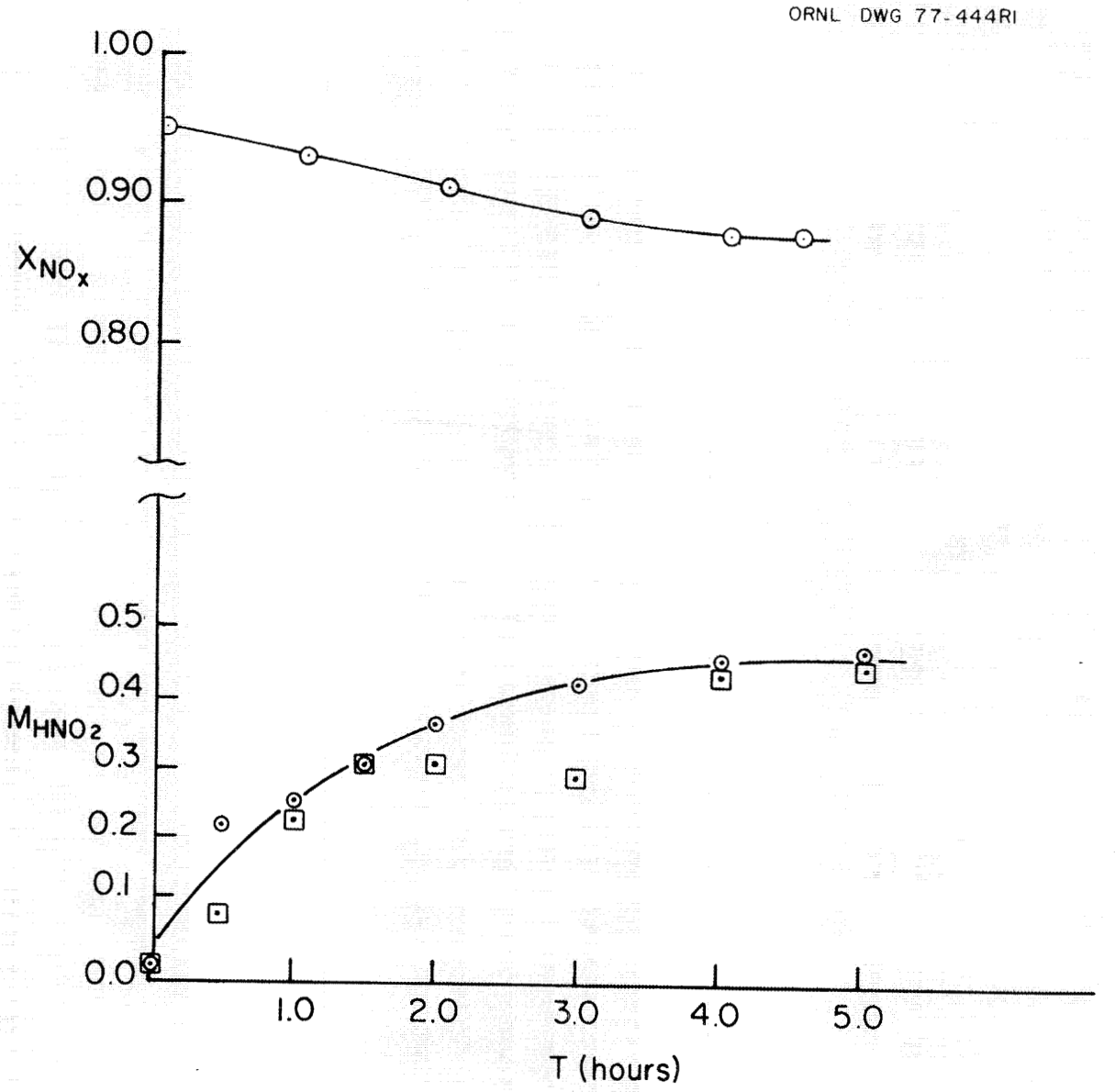

Figure 12. Overall NO_x conversion in three-stage sieve-plate column and concentration of HNO_2 in the scrubber liquid during the approach to steady-state operation.

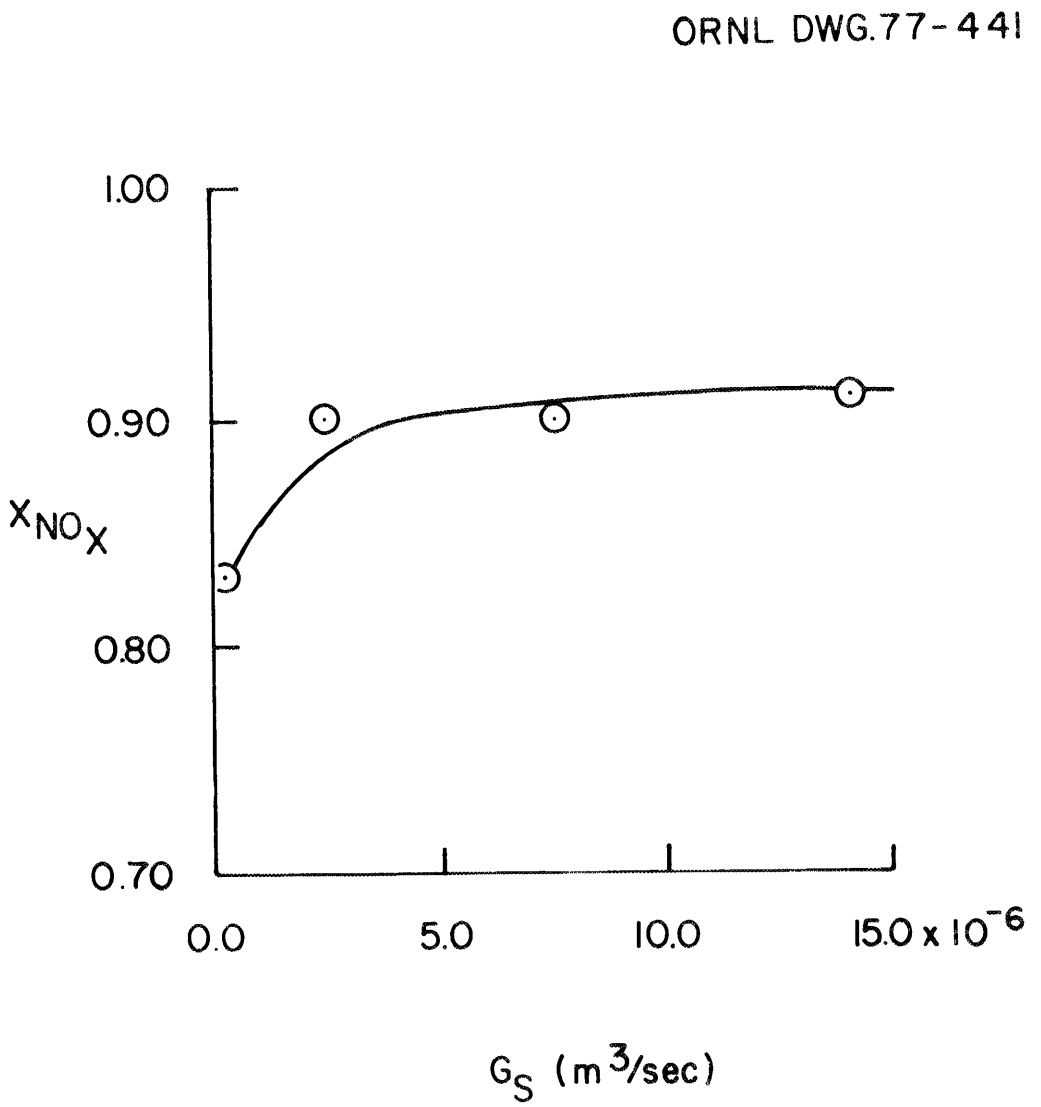

Figure 13. Overall NO_x removal in three-stage sieve-plate column for varied sparge rates of the liquid holdup tank.

to be confirmed by comparing the results obtained in experiment 31 with those for experiment 32 (see Table 4, page 55). The reduction of HNO_2 concentration in the liquid phase of experiment 32 versus that in experiment 31 coincides with the air sparge of the liquid holdup tank and greater NO_x conversion. The greater NO_x conversion probably results from the increased liquid capacity for holding NO in the liquid phase as HNO_2. The HNO_2 concentration entering the liquid holdup tank above the steady-state HNO_2 concentration in the liquid leaving the liquid holdup tank (determined by the air sparge rate) is released in the holdup tank as liquid HNO_3 and gaseous NO.

Some work involved the scrubbing of NO_x compounds using process water as the scrubber liquid (on a single-pass basis). The overall NO_x conversion was found to increase with increasing scrubber-liquid flow rates and decreasing feed-gas rates, as shown in Figures 14 and 15, respectively. The overall NO_x removal rates were considerably higher than in runs with recirculating scrubber liquid. The increase in NO_x conversion using process water is probably the result of the nondissociation of HNO_2 because of the non-steady-state concentrations of HNO_2 generated during a single pass through the apparatus.

Some data, summarized in Table 8 (page 59), were taken using a single stage of the column. Water served as the scrubber liquid, while nitrogen was used as the diluent gas so that the amount of NO_2^* absorbed could be accurately determined. The following parameters were varied: gas flow rate, liquid flow rate, partial pressure of NO_2^*, and the amount of steam entering with the feed gas. In general, NO_2^* absorption

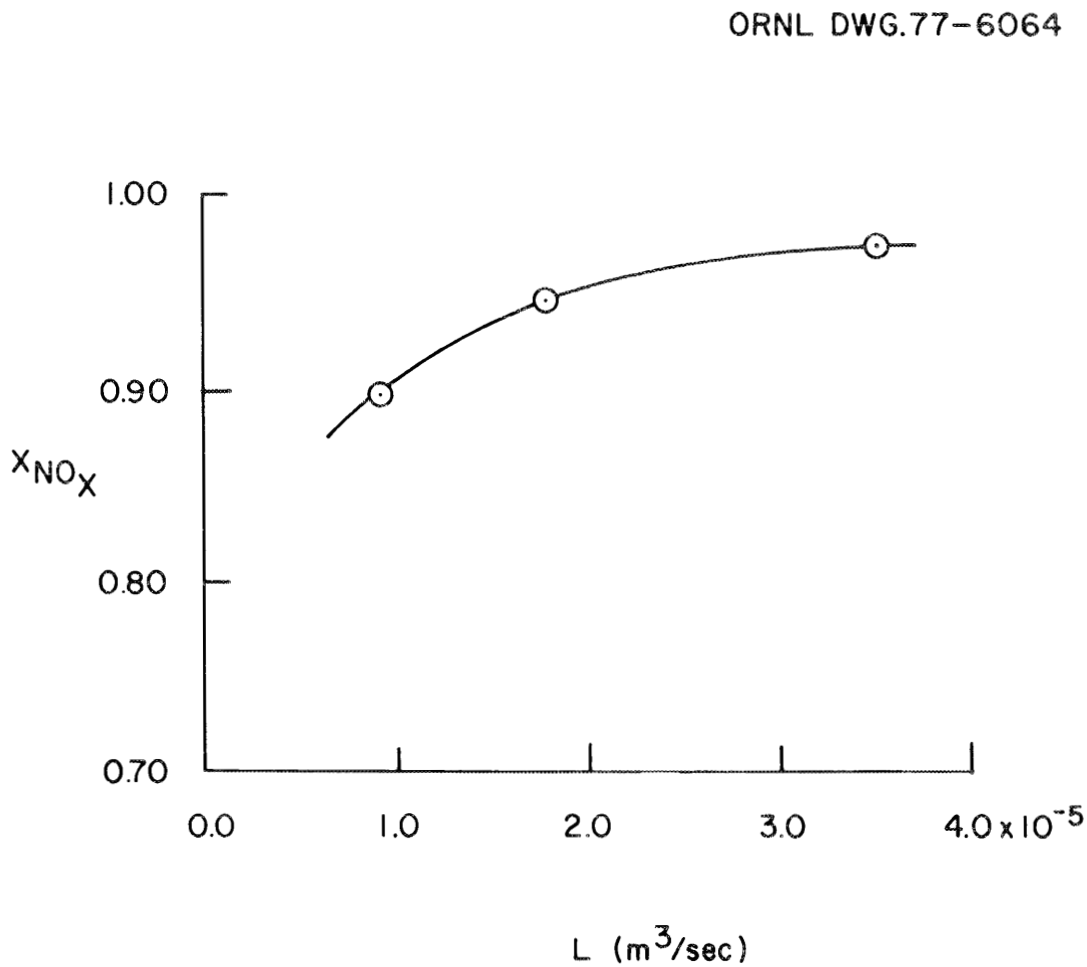

Figure 14. Overall NO_X removal in three-stage sieve-plate column for varied rates of single-pass process water scrubber liquid.

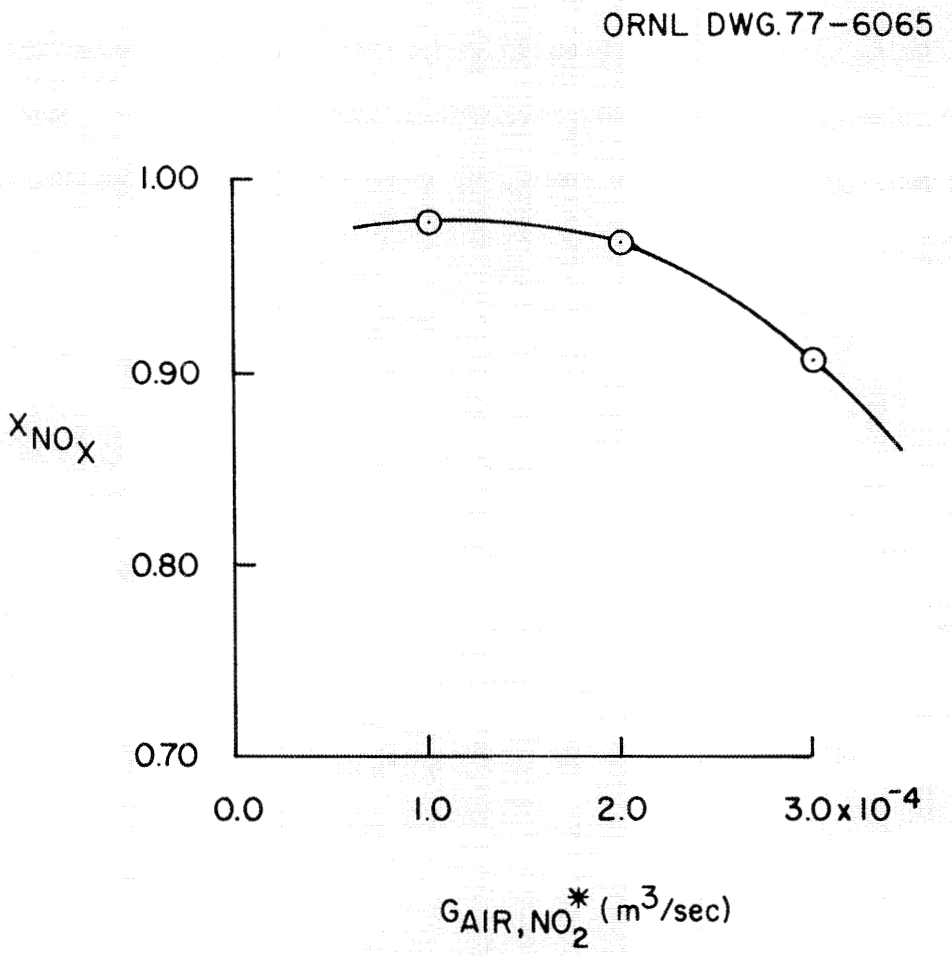

Figure 15. Overall NO_x removal in three-stage sieve-plate column for a single-pass process water scrubber liquid and varied feed-gas flow rates.

increased with increasing NO_2^* partial pressures, lower gas flow rates, higher liquid flow rates, and the presence of steam. The presence of steam in the gas feed stream increases the steady-state absorption of NO_x to an approximately constant conversion of 85% for this set of experimental conditions, as shown in Figure 16. An increase in the rate of liquid flow increases the NO_x absorption from air-steam-NO_x gas streams (see Figure 17). The remaining data are further examined in Chapter VI.

ORNL DWG 77-6084

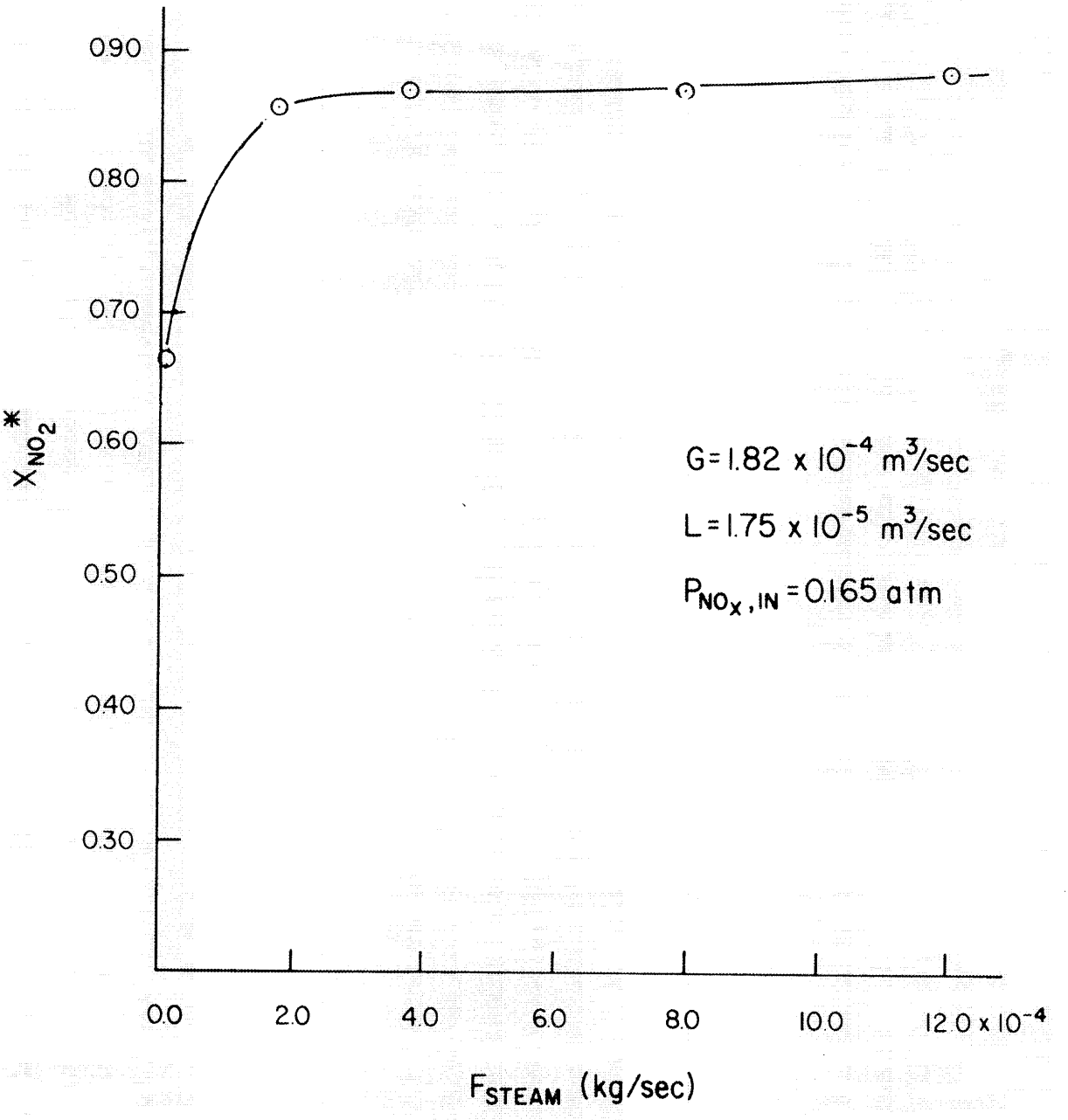

Figure 16. Effect of increasing steam flow rates on NO_2^* absorption in a single-plate column.

ORNL DWG 77-609C

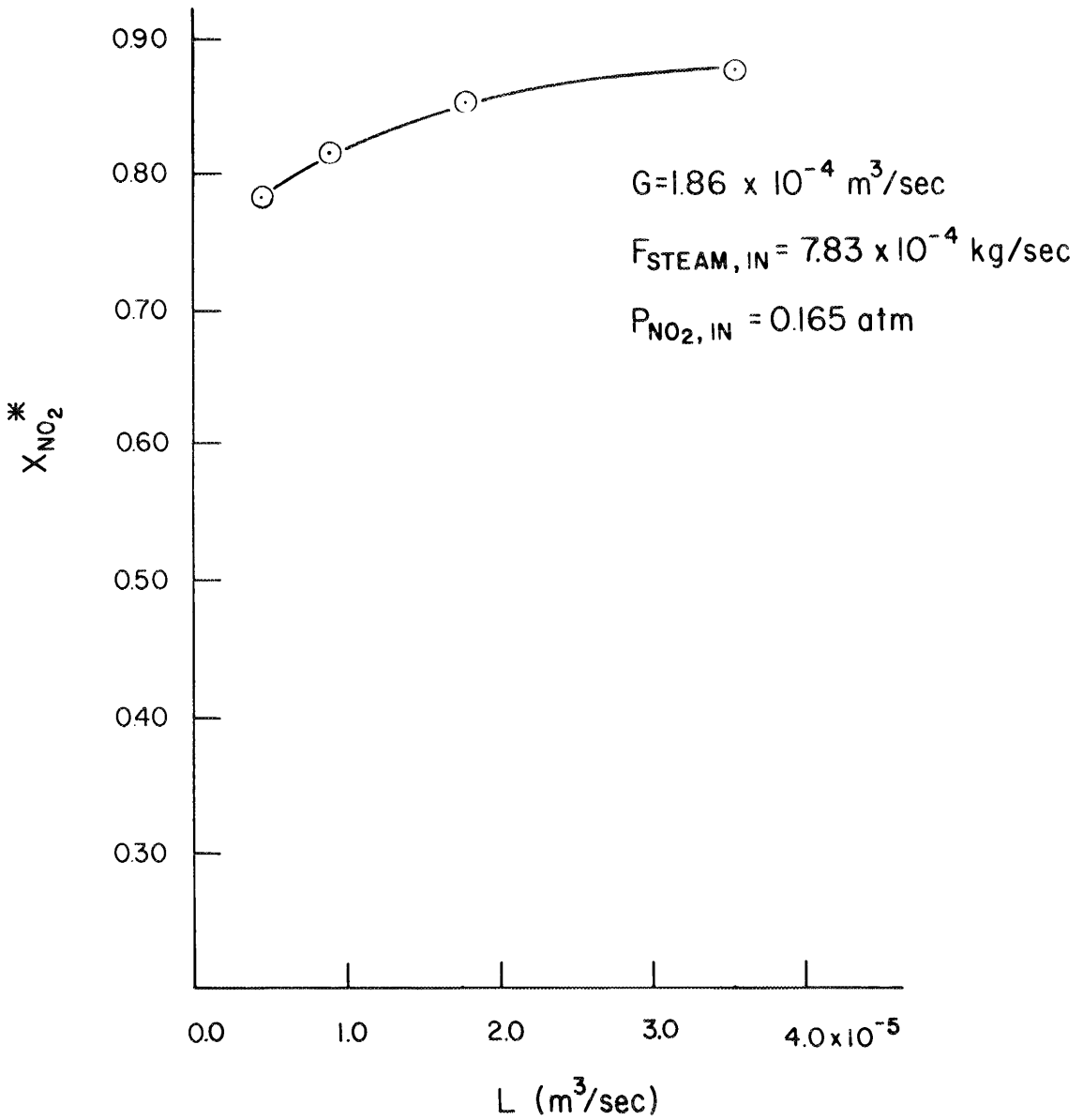

Figure 17. Effect of increasing liquid flow rates on NO_2^* absorption when steam is present in the feed gas in a single-plate column.

CHAPTER VI

CORRELATION OF DATA AND DISCUSSION OF RESULTS

The final evaluation of the mathematical model rests on a comparison of experimental data and model-predicted data. This discussion is given in the following sections. Two types of data that were taken during this experimental series yield themselves to modeling: (a) the steady-state single-plate NO_2^* scrubbing data, and (b) data from the steady-state three-stage column with no recycle of off-gas from the liquid holdup tank. In these cases, sufficient gas- and liquid-phase concentration data exist for a comparison with a model.

I. SINGLE-PLATE DATA

The model of NO_2^* absorption in the froth of the sieve plates was tested in a series of experiments involving the use of a single plate. The gas-liquid interfacial area was determined in experiments as described in Appendix E. The value of $\sqrt{D_{N_2O_4,H_2O}k_{36}}/He$ was that given by Nonhebel.[3] The NO_2^* absorption was determined experimentally for varying NO_2^* partial pressures at three different gas flow rates. The experimental NO_2^* absorption or conversion is plotted along with the model prediction for these cases in Figures 18-20. The effect of the liquid flow rate on the experimental and model-predicted conversion of NO_2^* is shown in Figure 21. In each case the agreement between experimental and model-predicted performance appears to be reasonable.

ORNL DWG 77-6088

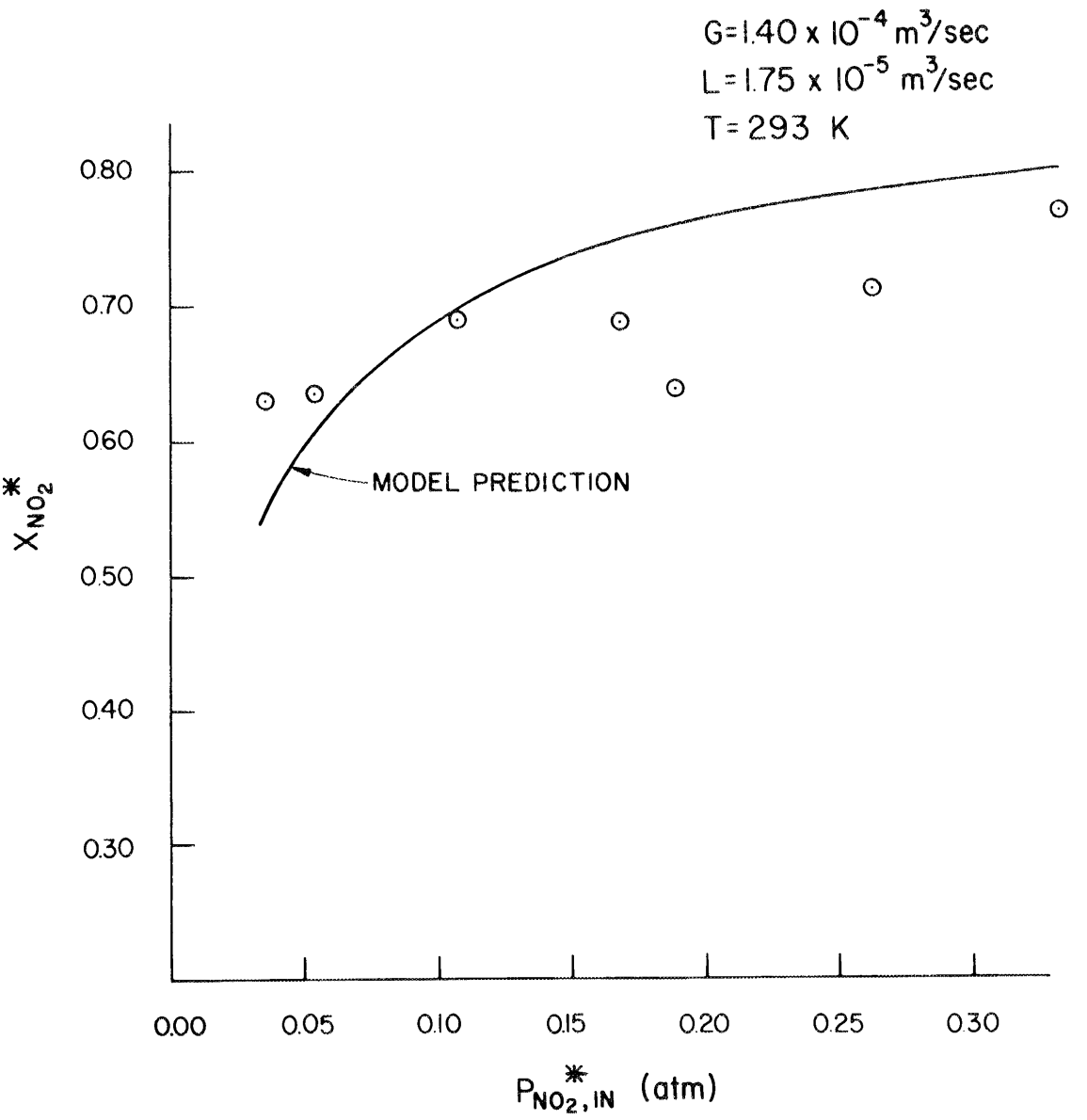

Figure 18. Experimental and model-predicted NO_2^* absorption versus the partial pressure of NO_2^* entering the tray at a total gas flow rate of 1.4×10^{-4} m^3/sec in a single-plate column.

ORNL DWG. 77-6086

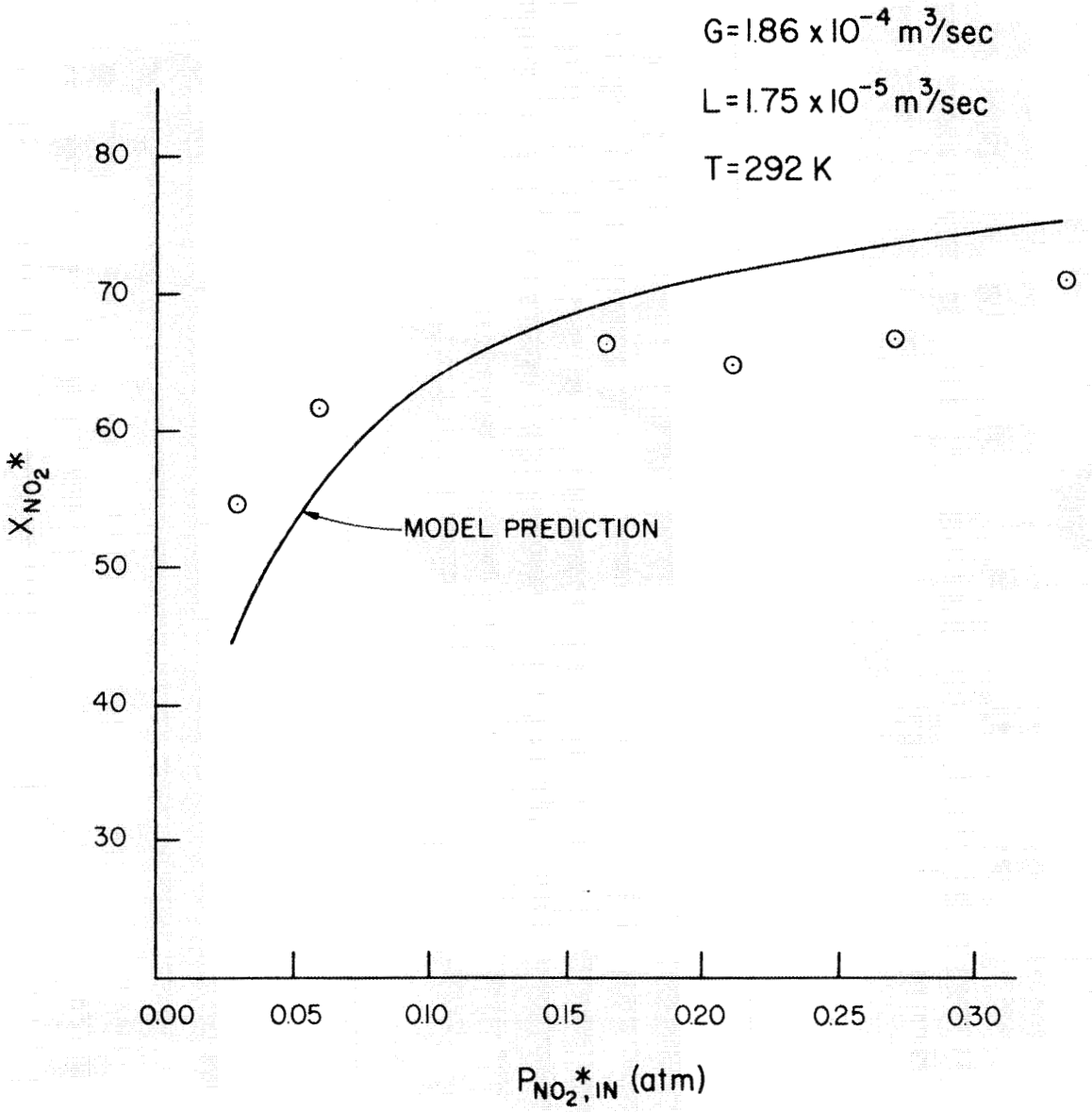

Figure 19. Experimental and model-predicted NO_2^* absorption versus the partial pressure of NO_2^* entering the tray at a total gas flow rate of 1.86×10^{-4} m^3/sec in a single-plate column.

ORNL DWG. 77-6085

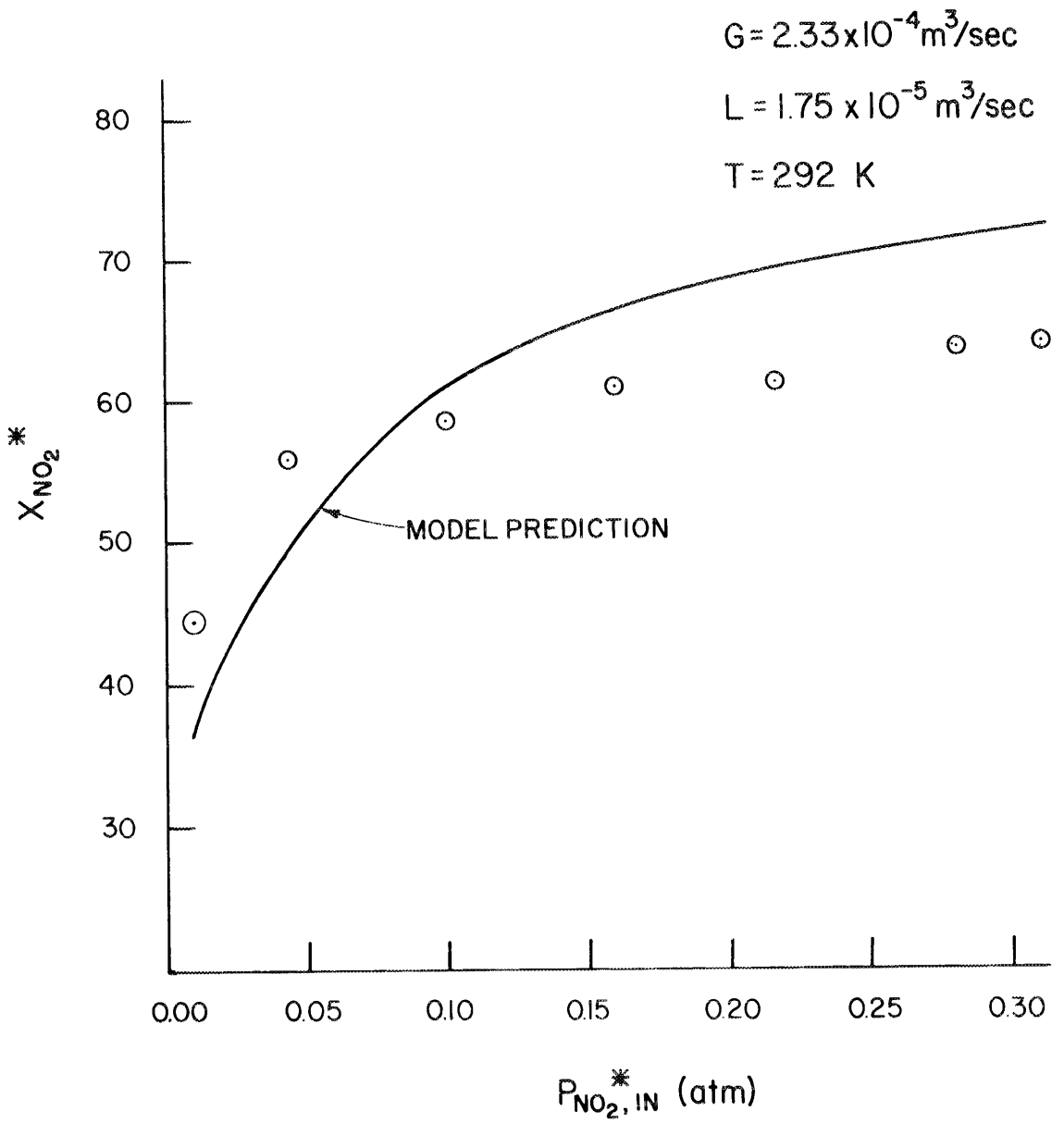

Figure 20. Experimental and model-predicted NO_2^* absorption versus the partial pressure of NO_2^* entering the tray at a total gas flow rate of 2.33×10^{-4} m^3/sec in a single-plate column.

ORNL DWG. 77-6082

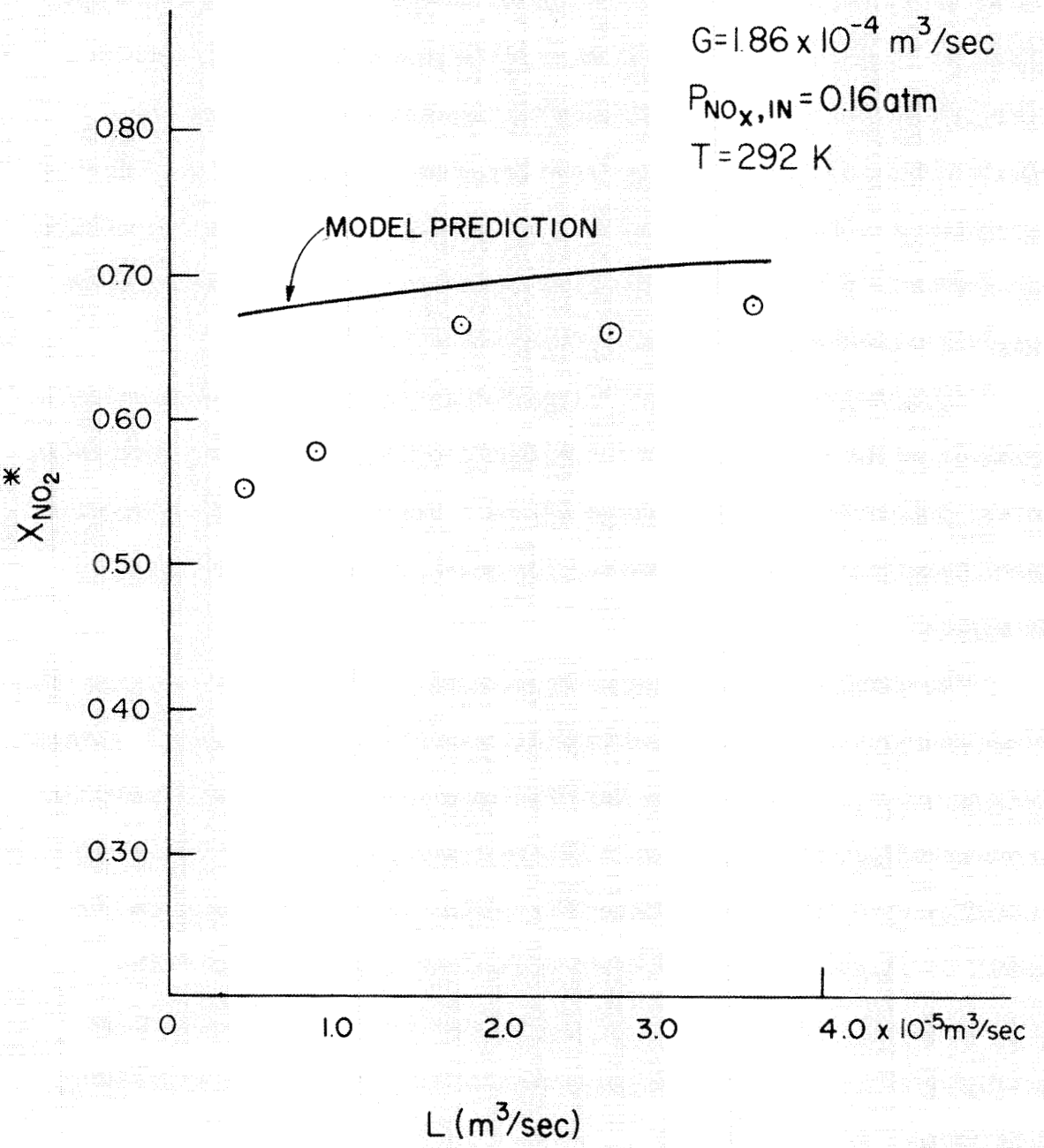

Figure 21. Experimental and model-predicted NO_2^* absorption versus liquid flow rate in a single-plate column.

II. THREE-STAGE COLUMN DATA

The purpose of the model is to predict total NO_x removal. The model performance versus NO_2^* absorption has been shown in the previous chapter. However, NO_x removal on a sieve plate depends not only on the absorption of NO_2^*, but also on the desorption of NO from the dissociation of liquid HNO_2 and the gas-phase oxidation of NO. Abel's equilibrium constants[23] were used to describe the decomposition of HNO_2 in the sieve plate froth. The rate constants for the oxidation of NO used in the model were those of Greig and Hall.[29]

The gas-liquid interfacial area for the first plate, when steam is present in the feed gas, was taken from a correlation of the interfacial areas presented in Table 8 (page 59) as a function of scrubber liquid and steam flow rates. Otherwise, the model is used as has been described.

The model-predicted gaseous NO_x removal efficiency is compared with that calculated from the experimental data of run 53 in Table 9. There was no steam in the feed gas for this experiment. The model-predicted removal efficiencies are very close to the experimentally determined efficiencies. The steady-state HNO_2 concentration calculated by the model is slightly lower than that determined experimentally. The calculated partial pressures of the gaseous component are given for each plate (i) and for positions entering the froth (j=1) and leaving the froth (j=2) in Table 10.

Experimentally determined NO_x removal efficiencies are compared with those predicted by the model in Figure 22 for two different feed

Table 9. A comparison of NO_x removal efficiencies calculated from experimental data versus NO_x removal predicted by model for experiment 53

Experiment 53 (no steam in feed gas)

$P_T = 1.1$ atm

$G_{feed} = 3.07 \times 10^{-4}$ m^3/sec

$L = 2.6 \times 10^{-5}$ m^3/sec

$\underline{M}_{HNO_3} = 3.0$

$\underline{M}_{HNO_2} = 0.20$ (experimental), 0.13 (calculated)

NO_x Profile in Column (atm)

	Experimental	Calculated
Feed	0.317	0.317
Stage 1	0.183	0.181
Stage 2	0.123	0.134
Stage 3	0.103	0.116

Table 5. Calculated partial pressures of gaseous components for stage, i, and position, j, where j = 1 entering froth and j = 2 leaving froth for experiment 53

Stage (i,j)	$P_{NO_2}^*$	P_{NO}	P_{O_2}	P_{N_2}
(1,1)	0.317	0.000	0.165	0.618
(1,2)	0.095	0.086	0.193	0.726
(2,1)	0.135	0.051	0.163	0.751
(2,2)	0.051	0.083	0.172	0.794
(3,1)	0.087	0.051	0.143	0.819
(3,2)	0.037	0.080	0.147	0.837

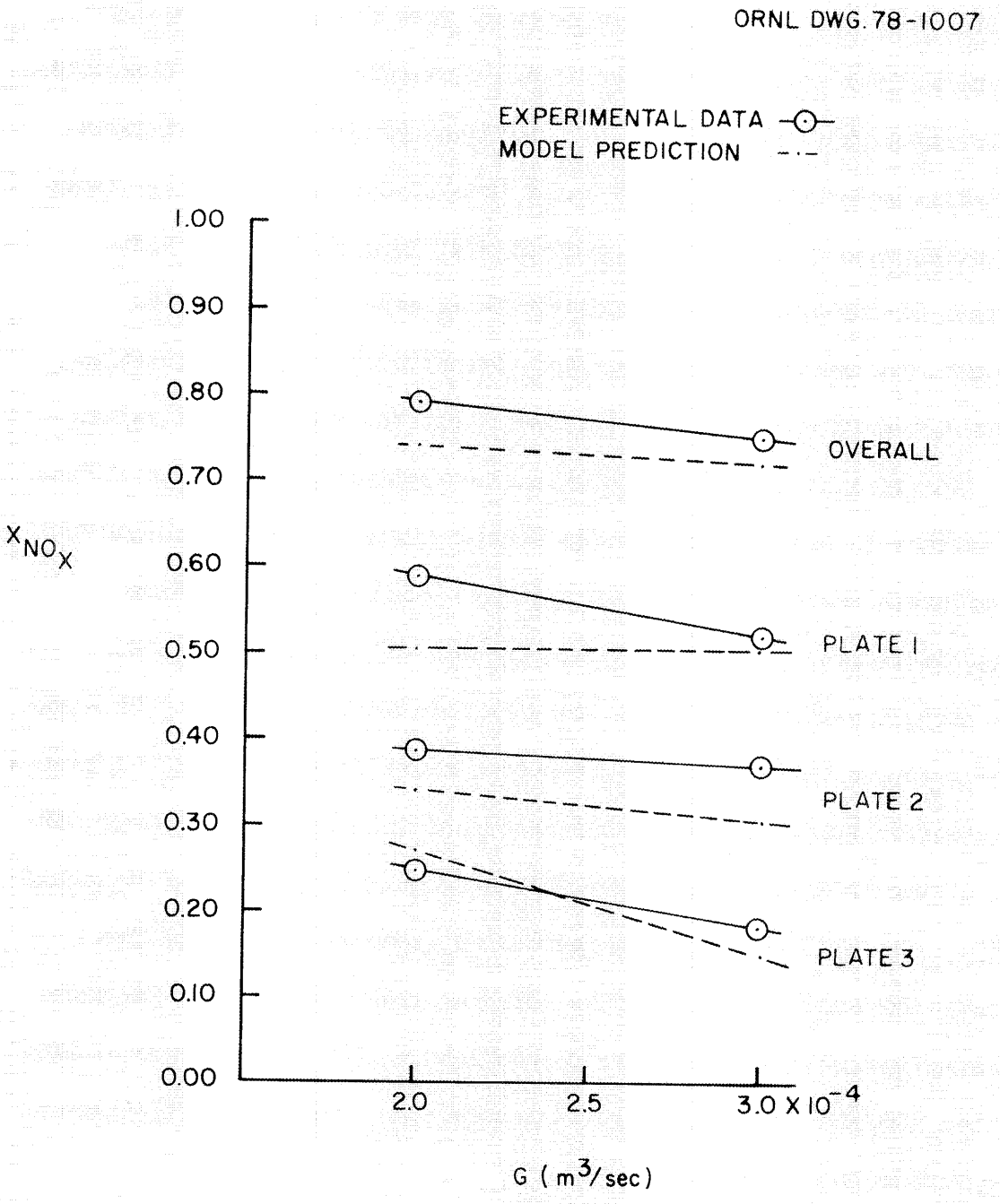

Figure 22. Experimental NO_x removal efficiencies versus those predicted by the model for varying gas flow rates with no steam in feed gas at otherwise reference conditions for steady-state three-stage sieve-plate column operation.

gas rates with no steam in feed gas. The NO_x removal efficiencies predicted by the model are then compared with those experimentally determined for varying scrubber liquid flow rates, feed gas flow rates, NO_x partial pressure in feed gas, and steam component in feed gas at otherwise reference conditions in Figures 23-26. In almost all cases, the model used to predict NO_x removal efficiencies in sieve plate columns is conservative with respect to absorption efficiencies. However, the steady-state predicted concentrations of HNO_2 (usually about 0.1 kg•mole/m^3) are always lower than the experimental values.

An exercise to vary the equilibrium constant for reaction (37) in an attempt to obtain a better fit between the model-predicted and the experimental data was of little success. Some researchers have consolidated the forward rates of Equation (37) and Equation (36), producing one-third mole of NO for one mole of NO_2^* absorbed. This was simulated and for the steady-state case there is no apparent difference in the revised model and the one described in this text. However, the use of such a stoichiometry does not account for the buildup of liquid HNO_2 in the system or for the reduced NO_x removal efficiency that results from its presence in the scrubber liquid as shown. The model clearly demonstrates the observed phenomenon that the presence of HNO_2 in the scrubber liquid impairs the overall NO_x scrubbing efficiency of the system (see Figure 27).

ORNL DWG. 78-1008

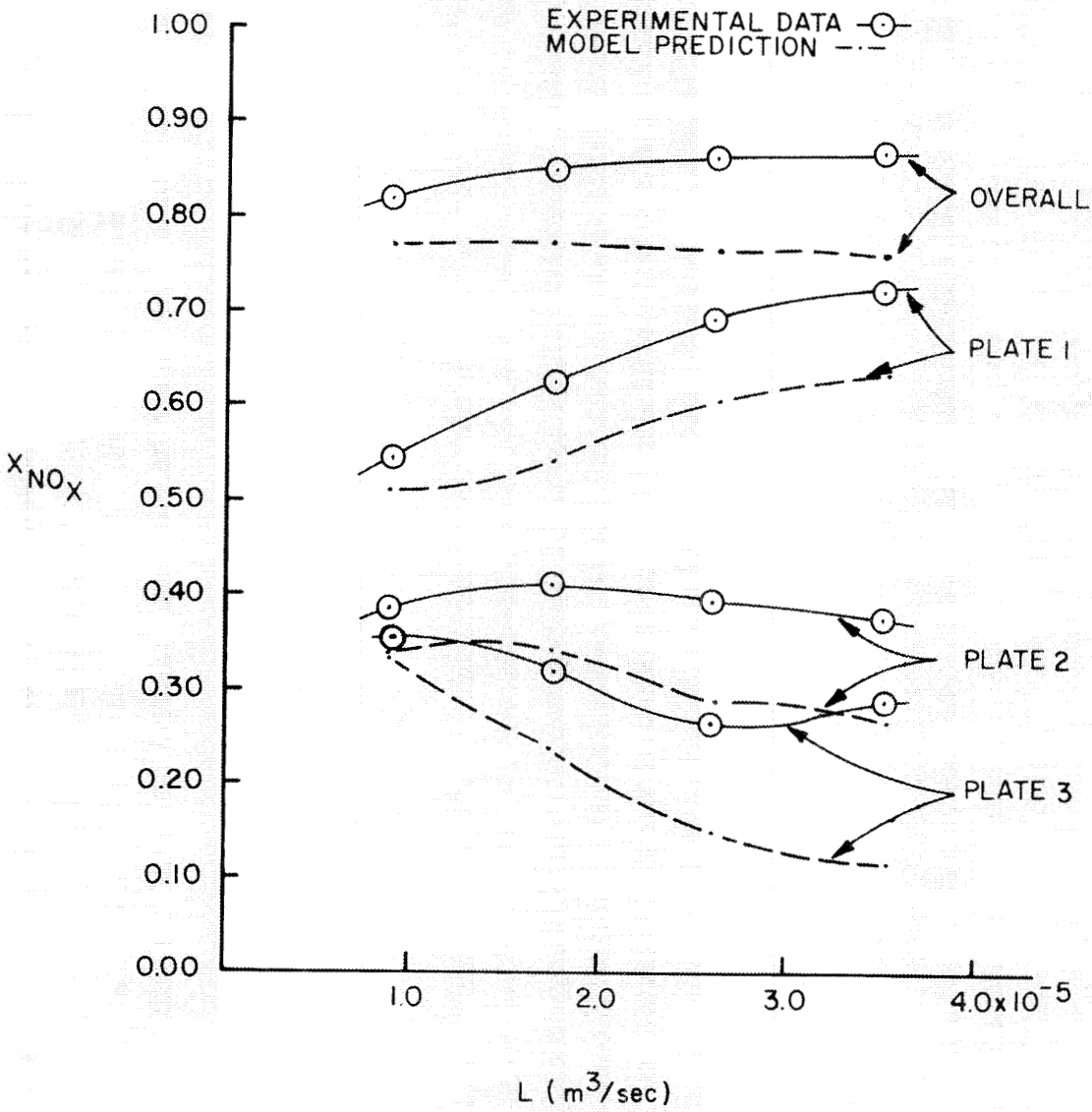

Figure 23. Experimental NO_X removal efficiencies versus those predicted by the model for varying scrubber liquid flow rates at otherwise reference conditions for steady-state three-stage column operation.

ORNL DWG.78-1009

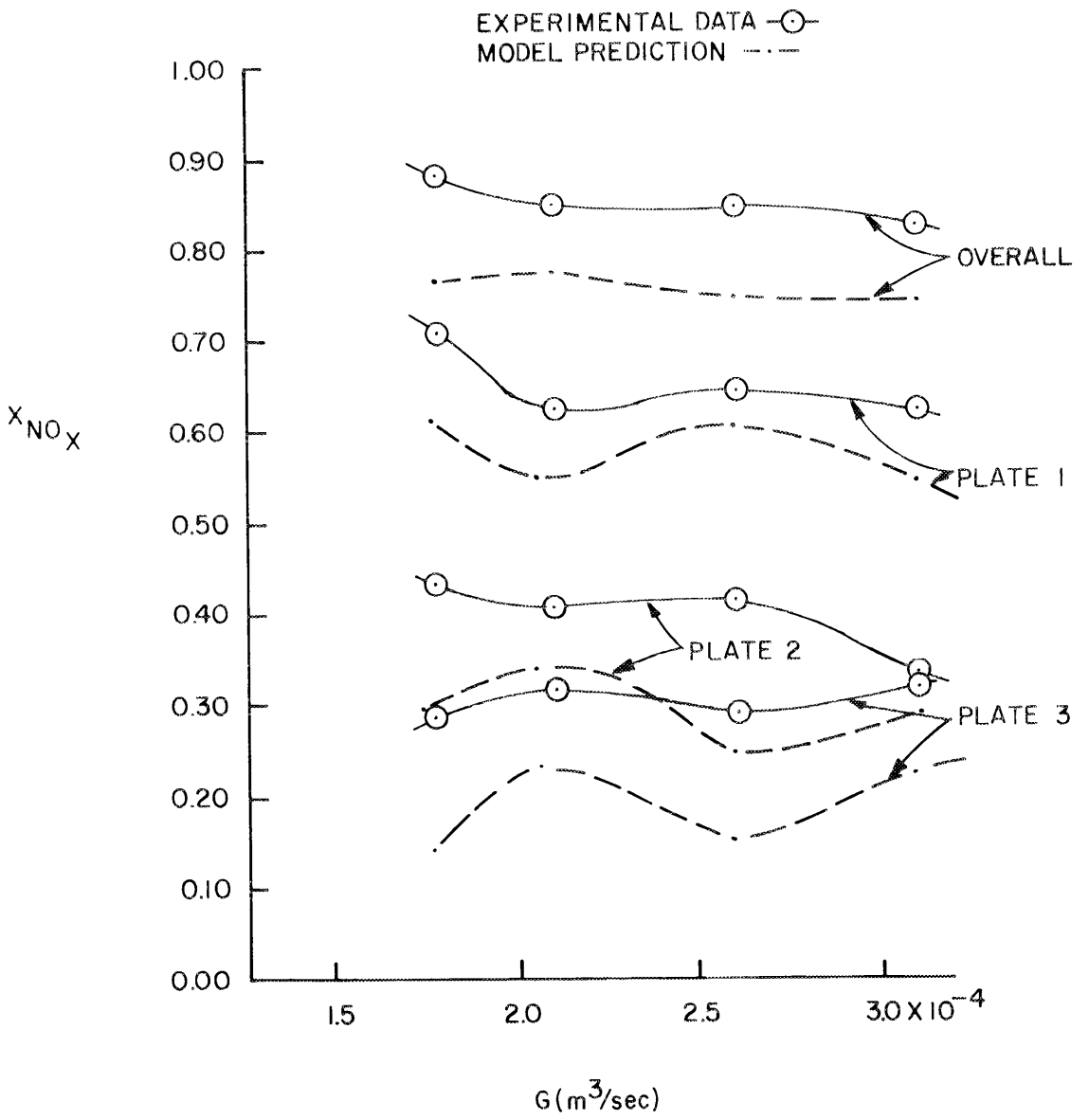

Figure 24. Experimental NO_x removal efficiencies versus those predicted by the model for varying feed gas flow rates at otherwise reference conditions for steady-state three-stage column operation.

ORNL DWG.78-1011

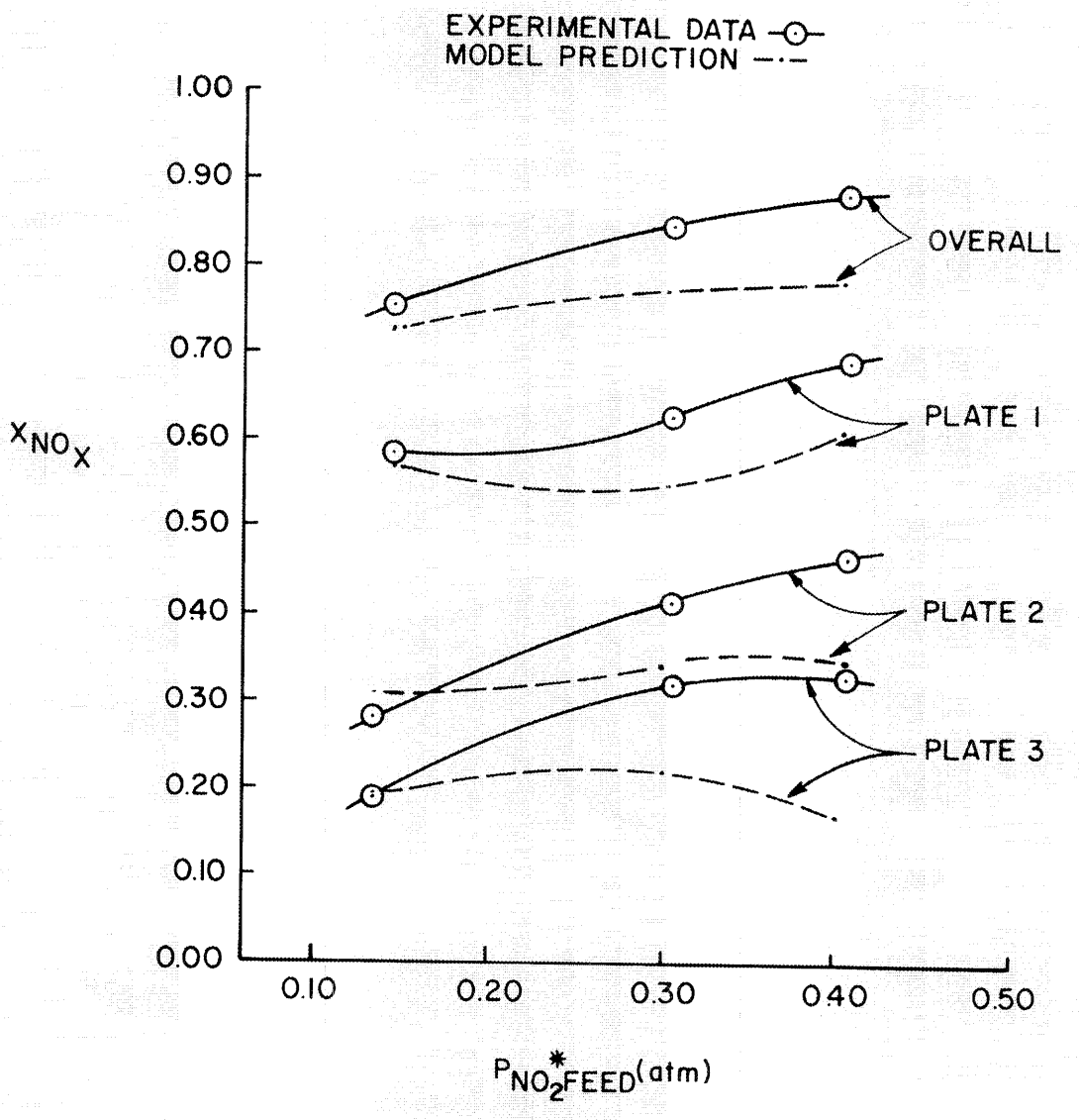

Figure 25. Experimental NO_x removal efficiencies versus those predicted by the model for varying partial pressure of NO_x in the feed gas at otherwise reference conditions for steady-state three-stage column operation.

ORNL DWG.78-1012

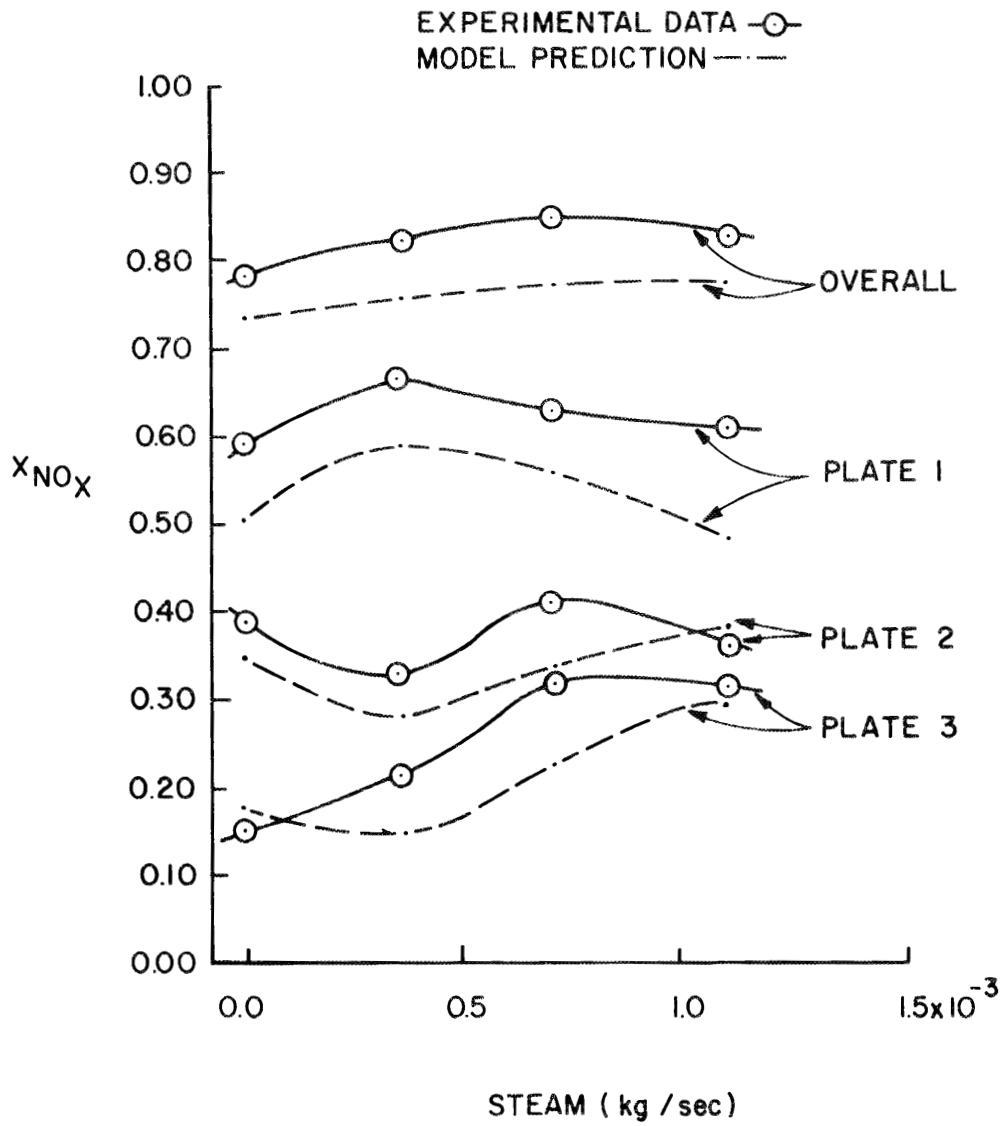

Figure 26. Experimental NO_x-removal efficiencies versus those predicted by the model for varying steam flow rates at otherwise reference conditions for steady-state three-stage column operation.

ORNL DWG. 78-1010

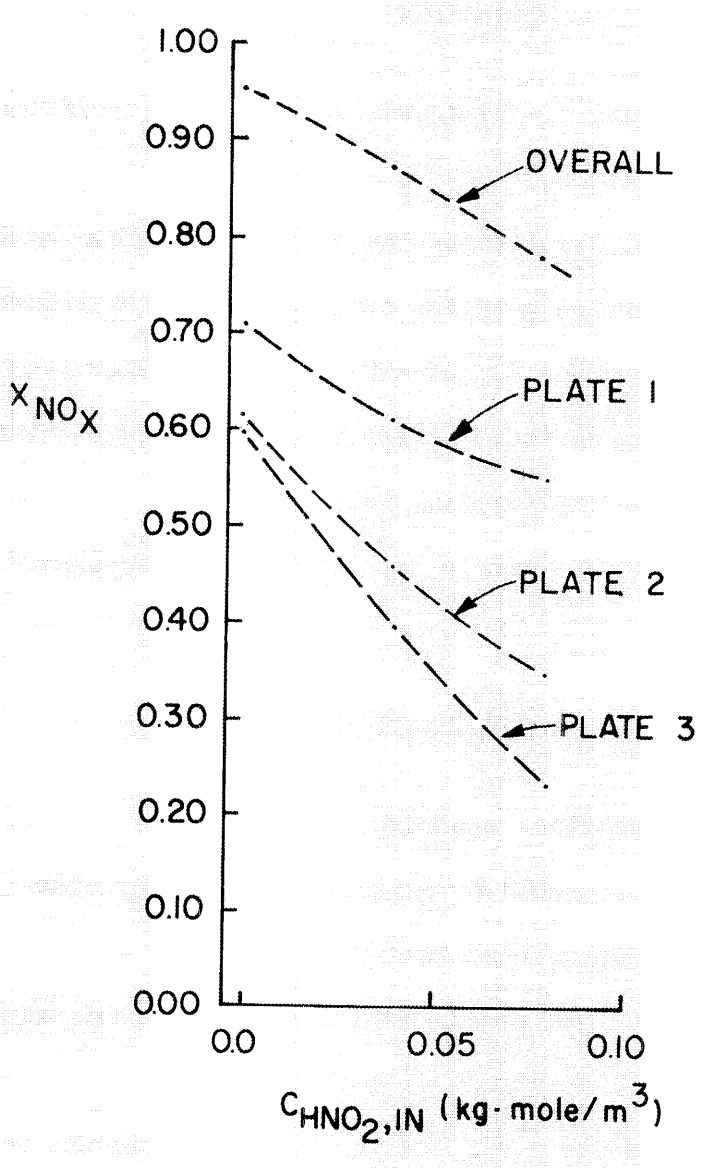

Figure 27. Model-predicted removal efficiency of NO_x for varying concentrations of HNO_2 in the scrubber liquid stream to column at reference conditions.

CHAPTER VII

CONCLUSIONS AND RECOMMENDATIONS

I. CONCLUSIONS

The following conclusions can be drawn from the results of this study:

1. The model adequately represents the experimental results for the experimental system over the range of variables studied.
2. The model predicts a buildup of HNO_2 in the scrubber liquid and a corresponding decrease in scrubbing efficiency. This was verified in the experimental work.
3. The proposed model can lead to the conservative design of NO_x scrubbers.

II. RECOMMENDATIONS

The following recommendations are made:

1. The described model should be expanded to consider other possible NO_x absorption reactions or mechanisms.
2. The study should be continued, with the objective of examining other absorption devices such as packed columns.
3. The mathematical model described in this report should be used for a conservative design of NO_x scrubbers.

LIST OF REFERENCES

LIST OF REFERENCES

1. M. Bodenstein, *Z. Elektrochem.* 100: 68-123 (1922).

2. F. H. Verhoek and F. J. Daniels, *J. Am. Chem. Soc.* 53: 1250-63 (1931).

3. P. J. Hoftyzer and F. J. G. Kwanten, *Process for Air Pollution Control,* 2nd ed., pp. 164-87, Chemical Rubber Co., Cleveland, 1972.

4. *JANAF Thermodynamic Tables,* The Dow Chemical Company, Midland, Michigan.

5. W. R. Forsythe and W. F. Guiaqul, *J. Am. Chem. Soc.* 64: 48-61 (1942); 65: 479-80 (1943).

6. L. Ya. Tereshchenko, V. P. Panov, and M. E. Pozin, *J. Appl. Chem. USSR* 41: 474-77 (1968).

7. F. S. Chambers and T. K. Sherwood, *Ind. Eng. Chem.* 29: 579-603 (1937).

8. K. G. Denbigh and A. J. Prince, *J. Chem. Soc.* 53: 790-801 (1947).

9. P. V. Danckwerts, *Gas-Liquid Reactions,* pp. 96-150, 117-118, 227, McGraw-Hill, New York, 1970.

10. P. G. Caudle and K. G. Denbigh, *Trans. Faraday Soc.* 49: 39-52 (1953).

11. M. M. Wendel and R. L. Pigford, *AIChE J.* 4: 249-56 (1958).

12. M. S. Peters and J. L. Holman, *Ind. Eng. Chem.* 47: 2536-39 (1955).

13. J. J. Carberry, *Chem. Eng. Sci.* 9: 189-94 (1959).

14. W. A. Dekker, E. Snoeck, and H. Kramers, *Chem. Eng. Sci.* 11: 61-71 (1959).

15. E. S. Koval and M. S. Peters, *Ind. Eng. Chem.* 52: 1011-14 (1960).

16. A. J. Moll, *The Rate of Hydrolysis of Nitrogen Tetroxide,* Ph.D. Dissertation, Univ. of Washington (1966).

17. J. P. Detournay and R. H. Jadot, *Chem. Eng. Sci.* 28: 2099-2102 (1973).

18. M. S. Peters, C. P. Ross, and J. E. Klein, *AIChE J.* 1: 105-11 (1955).

19. M. S. Peters, *University of Illinois Engineering Experiment Report No. 14*, USAEC-COO-1015 (1955).

20. M. S. Peters and E. J. Koval, *Ind. Eng. Chem.* 51: 577-80 (1959).

21. S. P. Andrews and D. Hanson, *Chem. Eng. Sci.* 14: 105-13 (1961).

22. H. Kramers, M. P. P. Blind, and E. Snoeck, *Chem. Eng. Sci.* 14: 115-23 (1961).

23. E. Abel and H. Schmid, *Z. Physik. Chem.* 132: 56-77 (1928); 134: 279-300 (1928); 136: 135-45, 419-36 (1928).

24. H. Kobayashi, N. Takezawa, K. Hara, T. Nikki, and K. Kitano, *Nippon Kagaku Kaishi* 3: 383-87 (1976); ORNL/tr-4405.

25. M. Bodenstein, *Z. Elektrochem.* 24: 183-201 (1918).

26. R. L. Hasche and W. A. Patrick, *J. Am. Chem. Soc.* 47: 1207-14 (1925).

27. J. C. Treacy and F. Daniels, *J. Am. Chem. Soc.* 77: 2033-36 (1955).

28. M. E. Morrison, R. C. Rinker, and W. H. Corcoran, *Ind. Eng. Chem., Fundam.* 5: 175-81 (1966).

29. J. D. Greig and P. G. Hall, *Trans. Faraday Soc.* 63: 655-61 (1967).

30. L. G. Wayne and D. M. Yost, *J. Chem. Phys.* 19: 41-47 (1951).

31. G. Fauser, *Chem. Metall. Eng.* 35: 474-78 (1928).

32. G. B. Taylor, T. H. Chilton, and S. L. Handforth, *Ind. Eng. Chem.* 23: 860-65 (1931).

33. V. I. Atroshchenko, V. I. Konvisar, and E. I. Kordysh, *J. Appl. Chem. USSR* 33: 288-94 (1960).

34. V. I. Atroshchenko, V. I. Konvisar, and M. T. Ivakhnenko, *J. Appl. Chem. USSR* 38: 2619-22 (1965).

35. L. Hellmer, *Chem. Eng. Technol.* 44: 420-24 (1972); ORNL/tr-4162.

36. T. H. Chilton, *Chem. Eng. Prog. Monogr. Ser. No. 3* 56: (1960).

37. H. G. Graham, V. E. Lyons, and H. L. Faucett, *Chem. Eng. Prog.* 60: 77-84 (1964).

38. D. H. Bowman, C. J. Kulczak, and J. J. Shulman, *Pollut. Control Eng.* 6: 38-39 (1974).

39. G. Astrarita, *Mass Transfer with Chemical Reaction*, pp. 5, 11-19, 35, 65, 90-92, Elsevier, New York, 1967.

40. R. C. Weast, *Handbook of Chemistry and Physics*, 55th ed., pp. A-112 to A-120, D-212, CRC Press, Cleveland, 1973.

41. R. H. Perry and C. H. Chilton, *Chemical Engineers' Handbook*, 5th ed., pp. 5-4, 18-8, McGraw-Hill, New York, 1973.

42. G. B. Wallis, *One Dimensional Two-Phase Flow*, pp. 248-51, McGraw-Hill, New York, 1969.

43. O. Levenspiel, *Chemical Reaction Engineering*, 2nd ed., pp. 113, 277, 307, Wiley, New York, 1973.

44. J. S. Ayala, B. W. Brian, and A. C. Sharon, *Flooding and Mass Transfer in Goodloe-Packed Columns, Part 2*, ORNL/MIT-253 (April 1977).

45. J. M. Begovich and J. S. Watson, *Flooding Characteristics of Goodloe Packing*, ORNL/TM-5212 (August 1976).

46. R. C. Reid and T. K. Sherwood, *The Properties of Gases and Liquids*, pp. 403, 423, McGraw-Hill, New York, 1966.

47. E. R. C. Eckert and R. M. Drake, Jr., *Analysis of Heat and Mass Transfer*, p. 781, McGraw-Hill, New York, 1972.

48. C. L. Yaws and J. R. Hopper, *Chem. Eng.* 81: 99-106 (1974).

49. Matheson Gas Products, *Matheson Gas Products Catalog No. 31*, p. 417.

50. R. Mann and H. Moyles, *Chem. Eng. J.* 23: 17-23 (1977).

51. R. B. Bird, W. E. Stewart and E. N. Lightfoot, *Transport Phenomena*, p. 409, Wiley, New York, 1960.

52. R. A. T. O. Nijsing, R. H. Hendriksz, and H. Kramers, *Chem. Eng. Sci.* 10: 88-104 (1959).

53. A. Laurent and J. C. Charpentier, *Chem. Eng. J.* 8: 85-101 (1974); ORNL-tr-4158.

54. C. D. Eben and R. L. Pigford, *Chem. Eng. Sci.* 20: 803-11 (1965).

APPENDIXES

APPENDIX A

THE REACTION REGIME OF THE HYDROLYSIS OF N_2O_4

From the literature it appears that the hydrolysis of N_2O_4 meets the criteria for a fast reaction. A fast reaction is said to occur in the surface elements of the fluid.[39] In order to meet the criteria for a fast first-order reaction, the absorption rates must be:

1. proportional to the gas-liquid interfacial area,
2. independent of liquid holdup,
3. independent of k_L,
4. proportional to the square root of the reaction rate expressed in terms of kg•moles/(m^3 sec), and
5. proportional to the first power of the driving force.

Mathematically, the conditions for a fast first-order reaction are that

$$1 \ll \sqrt{\frac{t_d}{t_r}} \ll \frac{C_{H_2O,B}}{C_{N_2O_4,i}} \ . \tag{A.1}$$

Since depletion of the bulk water concentration is negligible, Equation (A.1) reduces to

$$1 \ll \sqrt{\frac{t_d}{t_r}} \ . \tag{A.2}$$

Here, the diffusion time according to the penetration theory is

$$t_d = d_b/v_b \ , \tag{A.3}$$

and the reaction time for a pseudo-first-order reaction with a kinetic constant k_{36} is

$$t_r = 1/k_{36} \ . \tag{A.4}$$

In order to calculate t_d, it is first necessary to calculate the diameter and the velocity of a bubble through the froth of a sieve plate. The following calculation of bubble diameter and velocity are given by Wallis.[42] The following equation is for a gas bubble formed by an orifice submerged in an immiscible liquid:

$$V_b = 1.138 \frac{G^{6/5}}{g'^{3/5}} \ . \tag{A.5}$$

Assuming that the bubble is spherical, the following equation may be written for its volume:

$$V_b = \frac{4}{3} \pi R_b^3 \ . \tag{A.6}$$

Combining Equations (A.5) and (A.6), and solving for R_b yield:

$$R_b = 0.648 \left[\frac{G^{2/5}}{g'^{1/5}} \right] . \tag{A.7}$$

Since there are three sieve-plate perforations, G_{perf} may be expressed as one-third the typical total gas flow rate:

$$G_{perf} = \frac{1}{3} G = \frac{1}{3} (2.2 \times 10^{-4} \ m^3/sec) = 0.73 \times 10^{-4} \ m^3/sec \ . \tag{A.8}$$

With $g' = 9.81\ m/sec^2$, the radius of the bubble may be obtained as follows:

$$R_b = 0.648\ \frac{(0.73 \times 10^{-4})^{2/5}}{(9.81)^{1/5}} = 0.91 \times 10^{-2}\ m\ . \tag{A.9}$$

The equation

$$v_b = 1.18\left(\frac{g'\sigma}{\rho_F}\right)^{0.25} \tag{A.10}$$

is applicable if the following conditions are satisfied:

$$3.1G_1^{-0.25} < Re_b \tag{A.11}$$

and

$$5.75 < G_2\ , \tag{A.12}$$

where

$$Re_b = \frac{2\rho_F v_b R_b}{\mu_F}\ , \tag{A.13}$$

$$G_1 = \frac{g'\mu_F^4}{\rho_F\sigma^3}\ , \tag{A.14}$$

and

$$G_2 = \frac{g'R_b^4 v_b^4 \rho_F^3}{\sigma^3}\ . \tag{A.15}$$

The assumption is made that the surface tension of HNO_3 against air approximately equals that against a mixture of air, NO_2, N_2O_4, and NO. The variables are defined as:[40]

$$\rho_F = 1.1 \times 10^3 \text{ kg/m}^3 , \tag{A.16}$$

$$\mu_F = 1.1 \times 10^{-3} \text{ kg/(m-sec)} , \tag{A.17}$$

$$g' = 9.81 \text{ m/sec}^2 , \tag{A.18}$$

and

$$\sigma = 6.9 \times 10^{-2} \text{ kg/sec}^2 . \tag{A.19}$$

The rise velocity of the bubble is estimated from a graph given by Wallis[42] of bubble rise velocities versus bubble radius:

$$v_b = 0.3 \text{ m/sec} . \tag{A.20}$$

The following quantities may now be calculated:

$$G_1 = \frac{(9.81)(1.1 \times 10^{-3})^4}{(1.1 \times 10^3)(6.9 \times 10^{-2})^3} = 3.97 \times 10^{-11} \tag{A.21}$$

and

$$3.1\ G_1^{-0.25} = 1235 . \tag{A.22}$$

The following quantities can be estimated:

$$Re_b = \frac{2\rho_F v_b R_b}{\mu_F} = \frac{(2)(1.1 \times 10^3)(0.3)(0.91 \times 10^{-2})}{(1.1 \times 10^{-3})} = 5460 \tag{A.23}$$

and

$$G_2 = \frac{g' R_b^4 v_b^4 \rho_F^3}{\sigma^3} = \frac{(9.81)(0.91 \times 10^{-2})^4 (1.1 \times 10^3)^3 (0.3)^4}{(6.9 \times 10^{-2})^3} = 2208 . \tag{A.24}$$

The constraining equations are now estimated to be satisfied:

$$3.1\ G_1^{-0.25} = 1235 < Re_b = 5460 \tag{A.25}$$

and

$$5.75 < G_2 = 2208\ . \tag{A.26}$$

The rise velocity is now calculated:

$$v_b = 1.18\left(\frac{g'\sigma}{\rho_F}\right)^{0.25} = 1.18\left[\frac{(9.81)(6.9 \times 10^{-2})}{1.1 \times 10^3}\right]^{0.25} = 0.186\ \text{m/sec.} \tag{A.27}$$

Recalculating dimensionless bubble groups yields:

$$Re_b = \frac{2\rho_F v_b R_b}{\mu_F} = \frac{2(1.1 \times 10^3)(0.186)(0.91 \times 10^{-2})}{1.1 \times 10^{-3}} = 3385 \tag{A.28}$$

and

$$G_2 = \frac{g' R_b^4 V_b^4 \rho_F^3}{\sigma^3} = \frac{((9.81)(0.91 \times 10^{-2})^4 (0.186)^4 (1.1 \times 10^3)^3}{(6.9 \times 10^{-2})^3} = 326.0\ : \tag{A.29}$$

A check of the constraining equations

$$3.10G^{-0.25} = 1235 < Re_b = 3385 \tag{A.30}$$

and

$$5.75 < G_2 = 326 \tag{A.31}$$

shows that the calculated velocity,

$$v_b = 0.186\ \text{m/sec}\ , \tag{A.32}$$

is still valid. The diameter of the bubble is calculated by the following expression:

$$d_b = 2R_b = 2(0.91 \times 10^{-2}\ \text{m}) = 1.82 \times 10^{-2}\ \text{m} . \tag{A.33}$$

The quantity t_d may now be calculated

$$t_d = \frac{d_b}{v_b} = \frac{1.82 \times 10^{-2}\ \text{m}}{0.186\ \text{m/sec}} = 0.098\ \text{sec} . \tag{A.34}$$

The calculation of t_r will involve the use of k_{36}, which is estimated at 290 sec^{-1} at 298 K,[11]

$$t_r = 1/k_{36} = 1/(290\ \text{sec}^{-1}) = 0.0035\ \text{sec} . \tag{A.35}$$

The mathematical criterion for a fast first-order reaction is satisfied by:

$$1 \ll \sqrt{\frac{t_d}{t_r}} = \sqrt{\frac{0.098}{0.0035}} = 5.3 . \tag{A.36}$$

The hydrolysis of N_2O_4 at 298 K appears to be in the fast-reaction regime. Over the range of normal operating temperatures, 297 to 323 K, the quantity t_d/t_r will increase slightly because the value t_r decreases faster than the value t_d increases; therefore, the reaction regime appears to be valid for expected operating temperatures. By utilizing the assumption that the hydrolysis of N_2O_4 is a fast reaction and the penetration theory for gas absorption, we are assuming that this reaction occurs within the lifetime of the surface elements of the liquid. Thus, the concentration of N_2O_4 in the bulk liquid phase will be negligible.

APPENDIX B

LOCATION OF THE RESISTANCE TO ABSORPTION OF N_2O_4

From the literature[7-22] it appears that the resistance to mass transfer is located in the liquid phase. Therefore, it should be correct that

$$Ek_L << He_{NO_2^*}k_G \tag{B.1}$$

or

$$\sqrt{(D_{N_2O_4,H_2O})k_{36}} << He_{NO_2^*}k_G \ . \tag{B.2}$$

It is assumed that little accuracy will be lost by using a median operating temperature for the following calculation. At 303 K[22]

$$\sqrt{(D_{N_2O_4,H_2O})k_{36}}/He_{N_2O_4} = 0.89 \times 10^{-3} \ \frac{\text{kg}\cdot\text{mole}}{\text{m}^2 \text{ atm sec}} \tag{B.3}$$

and

$$He_{N_2O_4} = 0.81 \ \frac{\text{m}^3 \text{ atm}}{\text{kg}\cdot\text{mole}} \ , \tag{B.4}$$

so that

$$\sqrt{(D_{N_2O_4,H_2O})k_{36}} = \left[\frac{\sqrt{(D_{N_2O_4,H_2O})k_{36}}}{He_{N_2O_4}}\right] He_{N_2O_4} = (0.89 \times 10^{-3})(0.81)$$

$$= 0.72 \times 10^{-3} \text{ m/sec} \ . \tag{B.5}$$

The solubility of NO_2^* in dilute HNO_3 at normal operating temperatures is primarily the solubility of N_2O_4. Although scant information is available for a Henry's law constant for NO_2^*, it may be defined as:

$$He_{NO_2^*} = \frac{P_{NO_2^*}}{C_{NO_2^*}} \ . \tag{B.6}$$

By using the definitions

$$P_{N_2O_4} = (1 - \alpha)P_{NO_2^*}/2 \tag{B.7}$$

or

$$P_{NO_2^*} = 2P_{N_2O_4}/(1 - \alpha) \tag{B.8}$$

and

$$C_{NO_2^*} = 2C_{N_2O_4} \ , \tag{B.9}$$

the Henry's law constant for NO_2^* may be expressed as:

$$He_{NO_2^*} = \frac{2P_{N_2O_4}/(1 - \alpha)}{2C_{N_2O_4}} = \frac{P_{N_2O_4}}{C_{N_2O_4}(1 - \alpha)} = \frac{He_{N_2O_4}}{(1 - \alpha)} \ . \tag{B.10}$$

The dissociation of N_2O_4 may be calculated by:

$$\alpha = \frac{-K_{p,34} + K_{p,34}\sqrt{1 + 8P_{NO_2^*}/K_{p,34}}}{4P_{NO_2^*}} \ . \tag{B.11}$$

The NO_2-N_2O_4 pressure equilibrium constant is calculated by[3]

$$K_{p,34} = 10^{(-3198/T + 9.8698)} = 10^{(-3198/303 + 9.8698)} = 0.21 \ . \tag{B.12}$$

Assuming that the NO_2^* partial pressure is fairly low, 0.15 for example, α may be calculated as:

$$\alpha = \frac{-0.21 + 0.21\sqrt{1 + 8(0.015)/0.21}}{4(0.015)} = 0.89 \ . \tag{B.13}$$

Then, $He_{NO_2}^*$ may be calculated as:

$$He_{NO_2}^* = \frac{He_{N_2O_4}}{(1 - \alpha)} = \frac{(0.81)}{(1 - 0.89)} = 7.36 \frac{m^3 \text{ atm}}{kg \cdot mole} . \tag{B.14}$$

Sharma and Gupta[9] report gas-side mass transfer coefficients, k_G, ranging from 0.1 to 0.45 kg•mole/(m^2-sec-atm) for various designs of sieve plates and various froth depths. The gas-side mass transfer group may be calculated using the smaller k_G values as:

$$He_{NO_2}^* k_G = (7.36)(0.1) = 0.74 \text{ m/sec} . \tag{B.15}$$

The liquid-phase mass transfer group is calculated as:

$$\sqrt{(D_{N_2O_4,H_2O})k_{36}} = 0.72 \times 10^{-3} \text{ m/sec} . \tag{B.16}$$

It may now be shown that

$$\sqrt{(D_{N_2O_4,H_2O})k_{36}} = 0.72 \times 10^{-3} \text{ m/sec} << He_{NO_2}^* k_G = 0.74 \text{ m/sec} . \tag{B.17}$$

Thus, the contribution of the gas-side resistance to mass transfer may be neglected.

APPENDIX C

CALCULATION OF TUBULAR REACTOR VOLUME REQUIRED FOR OXIDATION OF NO IN THE GAS STREAM SUPPLYING THE INFRARED ANALYZER

A packed tubular reactor was desired for the oxidation of NO in the gas stream supplying the infrared analyzer. Goodloe packing was added to more accurately approximate plug flow conditions.[43] The gas streams (other than the feed stream) contain air, NO, and NO_2^* (NO_2 and N_2O_4). The analyzer is specific for NO_2^*. Any remaining NO would not be included in a total NO_x analysis; thus, it is necessary to convert NO to NO_2^* for analysis.

The following development of a design equation assumes negligible axial dispersion. This assumption must be verified after sizing the reactor.

The reactor is to be designed under the following conditions:

$$T = 323 \text{ K} , \tag{C.1}$$

$$P_T = 1.0 \text{ atm} , \tag{C.2}$$

$$d = 0.076 \text{ m} , \tag{C.3}$$

$$k_{3s} = 16.0 \text{ atm}^{-2} \text{ sec}^{-1} \text{ (ref. 25)} , \tag{C.4}$$

$$P_{NO,in} = 0.13 \text{ atm}, \; P_{O_2,in} = 0.19 \text{ atm} , \tag{C.5}$$

$$X_{NO} = 0.96 , \tag{C.6}$$

and

$$G = 2.84 \times 10^{-5} \text{ m}^3/\text{sec or } v = 6.26 \times 10^{-3} \text{ m/sec} . \tag{C.7}$$

The volume of a plug flow reactor is given by:[43]

$$V = GP_{NO,in} \int_0^{X_{NO}} \frac{dX_{NO}}{-r_{NO}} . \tag{C.8}$$

The reaction rate is defined as:[25]

$$-r_{NO} = k^{38}P_{NO}^2 P_{O_2} = k_{38}[P_{NO,in}(1 - X_{NO})]^2 P_{O_2,in}(1 - X_{NO}/2) , \tag{C.9}$$

and Equation (C.8) becomes:

$$V = \frac{G}{k_{38}P_{NO,in}P_{O_2,in}} \int_0^{X_{NO}} \frac{dX_{NO}}{(1 - X_{NO})^2 \; 1 - \frac{P_{NO,in}}{2P_{O_2,in}} X_{NO})} . \tag{C.10}$$

Integration of the above equation yields:

$$V = \frac{G}{k_{38}P_{NO,in}P_{O_2,in}} \left[2\left(\frac{1}{1 - X_{NO}} - \ell n \frac{1 - \frac{P_{NO,in}}{2P_{O_2,in}} X_{NO}}{1 - X_{NO}} - 1 \right) \right] . \tag{C.11}$$

Thus, for 96% conversion, the reactor volume is as follows:

$$V = \frac{2.84 \times 10^{-5}}{(16.0)(0.13)(0.19)} \left[2\left(\frac{1}{1 - 0.96} - \ell n \frac{L - \frac{0.13}{2(0.19)}(0.96)}{1 - 0.96} - 1 \right) \right]$$
$$= 3.05 \times 10^{-3} \text{ m}^3 . \tag{C.12}$$

The reactor length is calculated as:

$$Z = \frac{V/\varepsilon'}{\pi d^2/4} = \frac{(3.08 \times 10^{-3})/0.95}{\pi(0.076)^2/4} = 0.71 \text{ m} . \tag{C.13}$$

From residence-time-distribution curves for columns with Goodloe packing operating at conditions comparable with present design conditions, Ayala, Brian, and Sharon[44] concluded that the plug flow assumption was justified. Experimental data for axial dispersion have been correlated with the packing Reynolds number and the Schmidt number by Levenspiel.[43] The packing Reynolds number is defined as:[43]

$$Re_p = \frac{d_p v \rho}{\mu} , \tag{C.14}$$

and the radius of the packing is:

$$r_p = \frac{2(1 - \varepsilon')}{a_w} . \tag{C.15}$$

For the Goodloe packing used in the column, it is reported[45] that $a_w = 2.0 \times 10^3\ m^{-1}$ and $\varepsilon' = 0.95$. The packing radius may be calculated by:

$$r_p = \frac{2(1 - 0.95)}{2.0 \times 10^3} = 5.0 \times 10^{-5}\ m . \tag{C.16}$$

The packing diameter is calculated as:

$$d_p = 2r_p = 1.0 \times 10^{-5}\ m . \tag{C.17}$$

For a superficial gas velocity of 6.26×10^{-3} m/sec,

$$\bar{v} = \frac{v}{\varepsilon'} = \frac{6.26 \times 10^{-3}}{0.95} = 6.6 \times 10^{-3}\ m/sec . \tag{C.18}$$

The design gas concentration (an average concentration) is given below:

Component	Mole fraction
O_2	0.157
N_2	0.714
NO	0.065
NO_2	0.061
N_2O_4	0.002

The density of the above mixture at the design temperature is 1.74 kg/m^3. The average viscosity of the mixture of n components can be calculated by the Herning-Zipperer method:[46]

$$\mu_m = \frac{\sum_{i=1}^{i=n} Y_i \mu_i (M_i)^{0.5}}{\sum_{i=1}^{i=n} Y_i (M_i)^{0.5}} \quad . \tag{C.19}$$

The viscosities for oxygen, nitrogen, NO, and NO_2 at the design conditions are, respectively: 2.2×10^{-5}, 1.9×10^{-5}, 2.0×10^{-5}, and 1.7×10^{-5} kg/(m sec).[47,48] The viscosity of N_2O_4 can be calculated as follows by the Bromley and Wilkey equation:[46]

$$\mu = 0.00333(MT_c)^{0.5} f_1(1.33\ T_r)/V_c^{0.667} \quad . \tag{C.20}$$

For N_2O_4, M = 92, T_c = 432 K,[49] V_c = 164 cm^3/g•mole,[49] and $f_1(1.33\ T_r)$ = 0.99.[46] The viscosity of N_2O_4 is calculated as:

$$\mu_{N_2O_4} = 0.00333[(92)(432)]^{0.5}(0.99)/(164)^{0.667} = 2.19 \times 10^{-2}\ \text{cP},$$

$$\text{or } 2.19 \times 10^{-5}\ \text{kg/(m-sec)} \quad . \tag{C.21}$$

The molecular weights for oxygen, nitrogen, NO, NO_2, and N_2O_4 are, respectively: 32, 28, 30, 46, and 92. The viscosity of the

mixture may now be calculated:

$$\mu_m = 1.9 \times 10^{-5} \text{ kg/(m-sec)} \ . \tag{C.22}$$

The packing Reynolds number may now be calculated:

$$Re_p = \frac{(1.0 \times 10^{-4})(6.26 \times 10^{-3})(1.74)}{1.9 \times 10^{-5}} = 5.7 \times 10^{-2} \ . \tag{C.23}$$

The Schmidt number is defined as:

$$Sc = \frac{\mu}{\rho D_{NO,mix}} \ . \tag{C.24}$$

The diffusivity of NO in the design gas mixture can be approximated by calculating the diffusivity of NO in air. For the diffusion of binary gas mixtures at low to moderate pressures[46] the Chapman-Enskog equation will be used:

$$D_{NO,AIR} = \frac{(1.858 \times 10^{-3})T^{1.5}[(M_{NO} + M_{AIR})/M_{NO}M_{AIR}]^{0.5}}{P\sigma^2_{NO,AIR}\Omega_D} \ , \tag{C.25}$$

where

$$\sigma^2_{NO,AIR} = \left[\frac{\sigma_{NO} + \sigma_{AIR}}{2}\right]^2 = \left[\frac{3.492 + 3.711}{2}\right]^2 = 12.97 \text{ Å}^2 \ , \tag{C.26}$$

$$\Omega_D = f(\varepsilon_{NO,AIR}/K,T) \ , \tag{C.27}$$

$$\frac{\varepsilon_{NO,AIR}}{K} = \sqrt{\left[\frac{\varepsilon_{NO}}{K}\right]\left[\frac{\varepsilon_{AIR}}{K}\right]} = \sqrt{(116.7)(78.6)} = 95.77 \ , \tag{C.28}$$

$$\frac{KT}{\varepsilon_{NO,AIR}} = \left[\frac{K}{\varepsilon_{NO,AIR}}\right](T) = \frac{323.0}{95.77} = 3.37 \ , \tag{C.29}$$

and

$$\Omega_D = 1.009 \ . \tag{C.30}$$

The diffusivity of NO in air is calculated as:

$$D_{NO,AIR} = 0.214 \ cm^2/sec \text{ or } 2.14 \times 10^{-5} \ m^2/sec \ . \tag{C.31}$$

The Schmidt number is calculated as:

$$Sc = \frac{1.9 \times 10^{-5}}{(1.74)(2.14 \times 10^{-5})} = 0.51 \ . \tag{C.32}$$

For a packing Reynolds number of 0.057 and a Schmidt number of 0.51, a slight extrapolation of Levenspiel's plot[43] is required to yield:

$$Pe_p = 3.0 \ . \tag{C.33}$$

The Peclet number is defined as:

$$Pe_p = \frac{d_p \bar{v}}{E_z} \ . \tag{C.34}$$

Another Peclet number may be defined as

$$Pe_z = \frac{Zv}{E_z} \ , \tag{C.35}$$

which is obtained by modifying the packing Peclet number in the following manner:

$$Pe_z = Pe_p \left[\frac{1}{\varepsilon'}\right] \left[\frac{Z}{d_p}\right] \quad . \tag{C.36}$$

Therefore,

$$Pe_z = (3.0)\left[\frac{1}{0.95}\right] \left[\frac{0.71}{1.0 \times 10^{-4}}\right] = 2.24 \times 10^4 \tag{C.37}$$

and

$$\frac{1}{Pe_z} = 4.46 \times 10^{-5} \quad . \tag{C.38}$$

According to Levenspiel,[43] the dispersion effects may be considered to be negligible when the dispersion group (the inverse Peclet number) is <0.002. Hence, the assumption of plug flow seems to be justified.

APPENDIX D

TEMPERATURE RISE AT THE GAS-LIQUID INTERFACE DUE TO HEAT EFFECTS ASSOCIATED WITH THE SOLUTION AND HYDROLYSIS OF N_2O_4

The release of the heats of reaction and solution near a gas-liquid interface is an inevitable accompaniment to the processes of gas dissolution, mass transfer, and chemical reaction. This is important because, in cases where the heat effects result in a significant temperature increase at the interface, the absorption rate behavior is influenced by the tendency toward reduced solubility of the absorbing gas and an increase in the reaction rate constant. In the case of N_2O_4 absorption, it is necessary to consider the additional interfacial heat effect of reducing the gas-phase concentration of N_2O_4 by shifting the NO_2-N_2O_4 equilibrium toward the increased production of NO_2. For fast reaction conditions, these effects are represented by:[50]

$$h_L(T_i - T_{FR}) = (\Delta H_R + \Delta H_S)P_{N_2O_4}(T_i)\sqrt{(D_{N_2O_4,H_2O})k(T_i)}/He(T_i) \qquad (D.1)$$

or

$$T_i = T_{FR} + (\Delta H_R + \Delta H_S)P_{N_2O_4}(T_i)\sqrt{(D_{N_2O_4,H_2O})k(T_i)}/[He(T_i)k_L] \ , \qquad (D.2)$$

where the variables most strongly affected by temperature are written as functions of the interfacial temperature. Moll[16] gives the heat of reaction and the heat of solution as 5.2×10^3 and 2.5×10^3 kcal/kg•mole, respectively. The partial pressure of N_2O_4 may be calculated from

$$P_{N_2O_4} = P^*_{NO_2}(1 - \alpha)/2 \ , \qquad (D.3)$$

where

$$\alpha = (-K_{p,34} + K_{p,34}\sqrt{1 + 8P_{NO}^{*}/K_{p,34}})/4P_{NO_2}^{*} \quad . \tag{D.4}$$

The pressure equilibrium constant can be calculated by:

$$K_{p,34} = 10^{(-3198/T + 9.8698)} \quad . \tag{D.5}$$

At 298 K, $K_{p,34} = 0.137$, and at an assumed NO_2^* partial pressure of 0.2 atm, $\alpha = 0.439$ and $P_{N_2O_4} = 0.056$ atm. Assuming very little temperature rise, the absorption rate group may be calculated as:

$$\sqrt{(D_{N_2O_4,H_2O})k(T_i)}/He(T_i) = 10^{(-0.53 - 760/T)} = 8.3 \times 10^{-4} \frac{\text{kg}\cdot\text{mole}}{\text{m}^2\text{-sec-atm}} \quad . \tag{D.6}$$

The heat transfer coefficient from a spherical surface as a rising bubble of gas may be calculated from:[51]

$$\frac{h_L d_b}{k} = 2 + 0.60\ Re_b^{1/2} Pr^{1/3} \quad . \tag{D.7}$$

The bubble diameter and the bubble Reynolds number are calculated (see Appendix A) to be 1.82×10^{-2} m and 3.4×10^{3}, respectively. The Prandtl number and the thermal conductivity of water are given by Eckert and Drake[47] as 6.5 and 0.6 W/(mk). The heat transfer coefficient from a rising gas bubble in the sieve-plate froth may be estimated from Equation (D.7):

$$h_L = 0.6[2 + 0.6(3.4 \times 10^3)^{0.5}(6.5)^{0.33}]/(1.82 \times 10^{-2})$$

$$= 2218.4 \text{ W/(m}^2\text{K)} = 0.53 \text{ kcal/(m}^2\text{-sec-K)} \ . \qquad \text{(D.8)}$$

The interfacial temperature can now be calculated from Equation (D.2) as follows:

$$T_i = 298 + (5.2 \times 10^3 + 2.5 \times 10^3)(0.056)(8.3 \times 10^{-4})/0.53$$

$$= 298.7 \text{ K} \ . \qquad \text{(D.9)}$$

The small difference in interfacial and bulk liquid temperatures should have a negligible effect on the absorption rate based on bulk liquid conditions.

APPENDIX E

DETERMINATION OF SIEVE-PLATE INTERFACIAL AREA USING THE ABSORPTION OF CO_2 FROM AIR INTO NaOH SOLUTIONS

A sieve plate with a low percent of perforation was used in the experimental column in an attempt to maintain a high interfacial area for gas-liquid contact while using fairly low superficial gas velocities to accommodate the oxidation of NO between plates. This type of perforation precluded the use of existing correlations for predicting the interfacial area of the sieve plate. The gas-liquid interfacial area for the previously described sieve plate was determined experimentally. In order to evaluate the interfacial area of the sieve plate, it is necessary to use absorption accompanied by chemical reaction; for convenience, the absorption of dilute CO_2 into solutions of NaOH was chosen. The experimental equipment has been described earlier in Chapter IV. The procedure is very similar to that previously described. The scrubber liquid was a NaOH solution in concentrations up to 0.5 kg•mole/m^3. Feed gas of two compositions was used: air containing 7.5% CO_2, and air containing 6.9% CO_2. Each stream was metered for a single pass through the sieve plate. The CO_2 absorption was determined by measuring the total carbon content of the scrubber liquid before and after it passed through the sieve plate. The analyses were performed by the Analytical Chemistry Division of the Oak Ridge National Laboratory. The paragraphs below describe the results of the experiments included in this study. The data are presented in Table E-1.

Table E-1. Steady-state data for the absorption of CO_2 into NaOH solutions in a sieve-plate column

Run	G_{in} (m^3/sec) $\times 10^4$	P_T (atm)	$P_{CO_2,in}$ (atm) $\times 10^2$	$P_{CO_2,avg}$ (atm) $\times 10^2$	L (m^3/sec) $\times 10^5$	$C_{CO_3,in}$ (kg/m^3)	$C_{CO_3,out}$ (kg/m^3)	RaV (kg·mole/sec) $\times 10^7$	$(RaV)^2$ (kg·mole^2/sec^2) $\times 10^{14}$	$C_{OH^-,out}$ (kg·mole/m^3)	T (K)	$D_{CO_2,H_2O\text{-}OH^-}$ (m^3/sec) $\times 10^9$	V (m^3) $\times 10^4$	He_{CO_2} (m^3atm/kg·mole)	A^a (kg·mole^2/sec^2) $\times 10^{11}$	k_{E1} (m^3/[kg·mole sec]) $\times 10^{-3}$
19-1	1.40	1.16	8.00	7.24	1.75	0.118	0.424	0.89	0.80	0.248	296	1.72	0.88	26.9	2.15	6.96
19-2	1.86	1.16	8.00	7.39	1.75	0.127	0.475	1.02	1.03	0.249	296	1.72	0.95	26.9	2.20	6.96
19-3	2.32	1.16	8.00	7.36	1.75	0.125	0.523	1.16	1.35	0.243	296	1.72	1.01	26.9	2.19	6.96
20-1	1.40	1.16	8.64	7.42	1.75	0.135	0.524	1.13	1.29	0.323	296	1.70	0.88	26.7	2.95	6.96
20-2	1.86	1.16	8.64	7.50	1.75	0.143	0.582	1.28	1.64	0.325	296	1.70	0.95	26.7	3.03	6.96
20-3	2.32	1.16	8.64	7.57	1.75	0.157	0.665	1.48	2.20	0.318	296	1.70	1.01	26.7	3.03	6.96
21-1	1.40	1.16	8.64	7.24	1.75	0.159	0.623	1.35	1.83	0.396	296	1.68	0.88	26.6	3.45	6.96
21-2	1.86	1.16	8.64	7.35	1.75	0.152	0.666	1.50	2.25	0.421	296	1.67	0.95	26.5	3.76	6.96
21-3	2.32	1.16	8.64	7.41	1.75	0.154	0.760	1.77	3.12	0.417	296	1.67	1.01	26.5	3.79	6.96
22-1	1.40	1.16	8.64	7.76	1.75	0.126	0.378	0.74	0.54	0.106	296	1.77	0.88	27.1	1.06	6.96
22-2	1.86	1.16	8.64	7.88	1.75	0.121	0.373	0.74	0.54	0.105	296	1.77	0.95	27.2	1.09	6.96
22-3	2.32	1.16	8.64	7.89	1.75	0.121	0.433	0.91	0.83	0.103	296	1.77	1.01	27.2	1.07	6.96
23-1	1.40	1.16	8.64	7.68	1.75	0.138	0.476	0.84	0.71	0.168	296	1.75	0.88	27.0	1.61	6.96
23-2	1.86	1.16	8.64	7.74	1.75	0.143	0.457	0.93	0.87	0.170	296	1.75	0.95	27.0	1.66	6.96
23-3	2.32	1.16	8.64	7.80	1.75	0.140	0.503	1.07	1.15	0.163	296	1.75	1.01	27.0	1.61	6.96

$^a A = (P_{CO_2,avg}/He_{CO_2})^2 D_{CO_2,H_2O\text{-}OH^-} C_{OH^-,out}$

The NaOH concentration was varied from 0.103 to 0.421 kg•mole/m^3. The partial pressure of CO_2 in air was 0.080 or 0.086 atm at a system pressure of 1.16 atm. The reaction between dissolved CO_2 and NaOH can be represented by:

$$CO_2(\ell) + 2NaOH(\ell) \rightarrow Na_2CO_3(\ell) + H_2O(\ell) \ . \tag{E.1}$$

The absorption of CO_2 may be represented by:[52]

$$RaV = P_{CO_2,avg} aV\sqrt{k_{E1}(D_{CO_2,H_2O-OH^-})C_{OH^-}} \Big/ He_{CO_2} \ , \tag{E.2}$$

provided the following conditions are met:

$$1 < \frac{\sqrt{(D_{CO_2,H_2O-OH^-})k_{E1}}C_{OH^-}}{k_L} < \frac{1}{2}\left[1 + \frac{(D_{OH^-,H_2O})(C_{OH^-})He_{CO_2}}{ZD_{CO_2,H_2O}P_{CO_2}}\right] \ . \tag{E.3}$$

In effect, it is assumed that the absorption of CO_2 occurs as a fast pseudo-first-order reaction. Further assumptions are that the gas-phase resistance to the absorption process is negligible, the gas passes through the froth in plug flow, and the froth is well-mixed.

The solubility of CO_2 in NaOH solutions is given by:[52]

$$\log\ (He_{CO_2,H_2O-OH^-}/He_{CO_2,H_2O}) = -\ k_s C_{OH^-} \ , \tag{E.4}$$

where

$$k_s = 0.149\ m^3/kg\cdot ion \ . \tag{E.5}$$

The reaction rate constant, k_{E1}, in dilute NaOH solutions is given by:[52]

$$\log k_{E1} = 13.635 - 2895/T \ . \tag{E.6}$$

This rate constant essentially described the above equation at hydroxyl ion concentrations of less than 0.5 kg•ion/m^3.[52] The diffusivity of CO_2 in hydroxide solutions is given by:[52]

$$D_{CO_2,H_2O\text{-}OH^-} = D_{CO_2,H_2O}\left[\frac{\eta_{H_2O}}{\eta_{H_2O\text{-}OH^-}}\right]^{0.85} \ . \tag{E.7}$$

The constraining equation, Equation (A.3), will be checked based on the following parameters, which are either calculated, referenced, or taken from Table E-1 (page 116) at experimental conditions at low and high concentrations of NaOH:

$$D_{CO_2,H_2O\text{-}OH^-} = 1.77 \times 10^{-9} \text{ m}^2/\text{sec (low NaOH)} \ , \tag{E.8}$$

$$= 1.67 \times 10^{-9} \text{ m}^2/\text{sec (high NaOH)} \ , \tag{E.9}$$

$$k_{E1} = 6.97 \times 10^3 \text{ m}^3/(\text{kg•mole sec}) \ , \tag{E.10}$$

$$C_{OH^-} = 0.103 \text{ kg•ion/m}^3 \text{ (low NaOH)} \ , \tag{E.11}$$

$$= 0.421 \text{ kg•ion/m}^3 \text{ (high NaOH)} \ , \tag{E.12}$$

$$\frac{D_{OH^-,H_2O}}{D_{CO_2,H_2O}} = 1.67 \text{ (ref. 52)} \ , \tag{E.13}$$

$$k_L = 1.5 \times 10^{-4} \text{ m/sec (ref. 9)} \ , \tag{E.14}$$

$$He_{CO_2,H_2O\text{-}OH} = 27.15 \text{ atm m}^3/\text{kg•mole (low NaOH)} \ , \tag{E.15}$$

$$= 26.52 \text{ atm m}^3/\text{kg•mole (high NaOH)} \ . \tag{E.16}$$

The constraining equations are satisfied by

$$3 < 7.5 < 15.6 \tag{E.17}$$

at the low NaOH concentrations, and by

$$3 < 15.9 < 63.9 \tag{E.18}$$

and at the highest NaOH concentration used. The interfacial area is determined graphically (see Figure E-1) by plotting $(RaV)^2$ versus $P^2_{CO_2,avg} k_{E1} (D_{CO_2H_2O-OH^-}) C_{OH^-} / He^2_{CO_2,H_2O-OH^-}$. The resulting slope is $(aV)^2$. The interfacial area per volume of froth is determined by taking the square root of the slope and dividing by the froth volume. Table E-2 and Figure E-2 give these results. The results are compared with other experimental values of interfacial area for various percentages of sieve-plate perforation[53] in Figure E-3.

Table E-2. Calculational results of the interfacial area determination in a single-stage sieve-plate column

G (m^3/sec)	$(aV)^2$ (m^4)	V^2 (m^6)	a (m^2/m^3)
1.40×10^{-4}	5.187×10^{-4}	7.74×10^{-9}	259
1.86×10^{-4}	6.316×10^{-4}	9.03×10^{-9}	265
2.32×10^{-4}	8.349×10^{-4}	10.20×10^{-9}	286

ORNL DWG. 77-6094

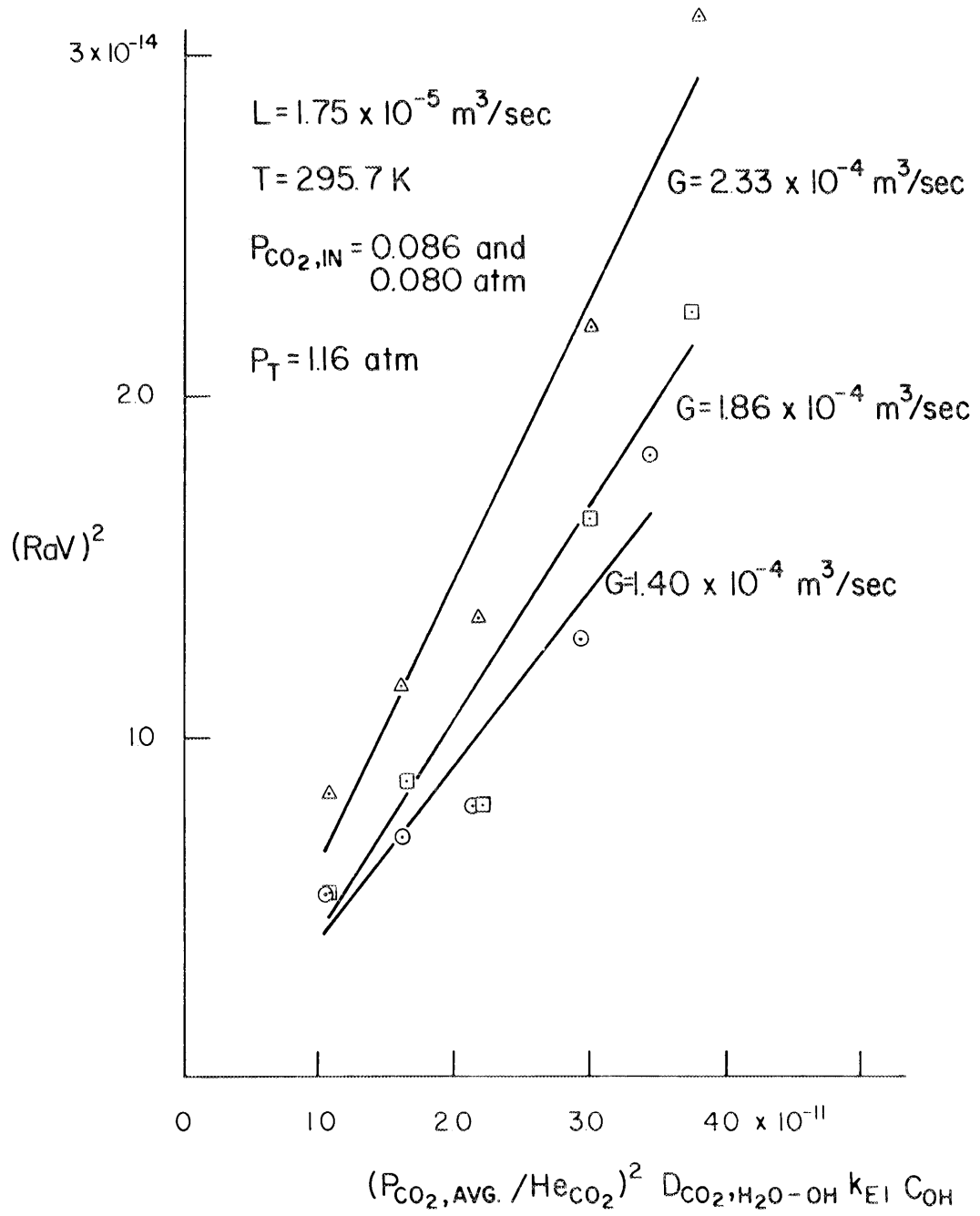

Figure E-1. Correlation of experimental results of the absorption of CO_2 into NaOH solutions in a single-stage sieve-plate column.

ORNL DWG-77-6091

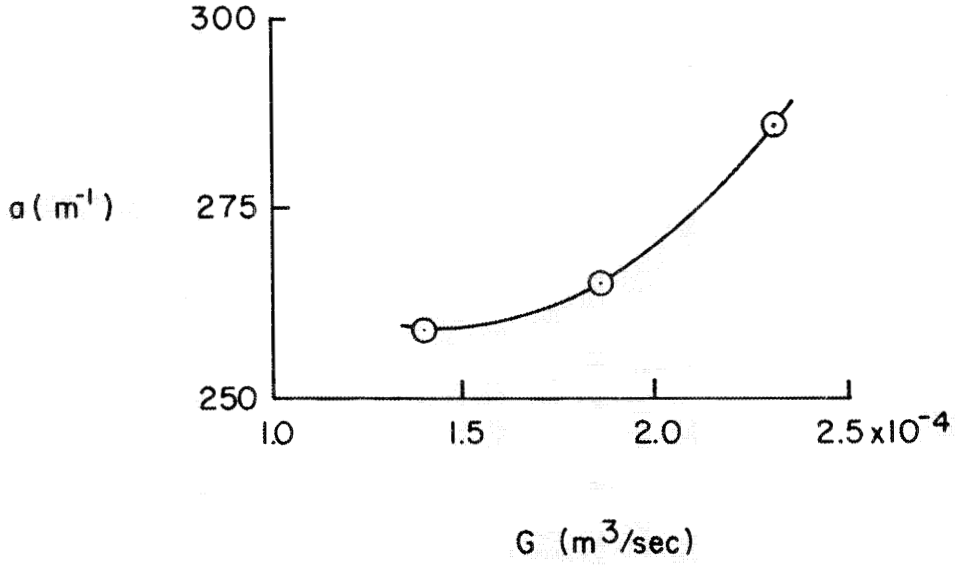

Figure E-2. Correlation of experimentally determined gas-liquid interfacial area versus gas flow rate for a single-stage sieve-plate column.

ORNL DWG. 77-6089

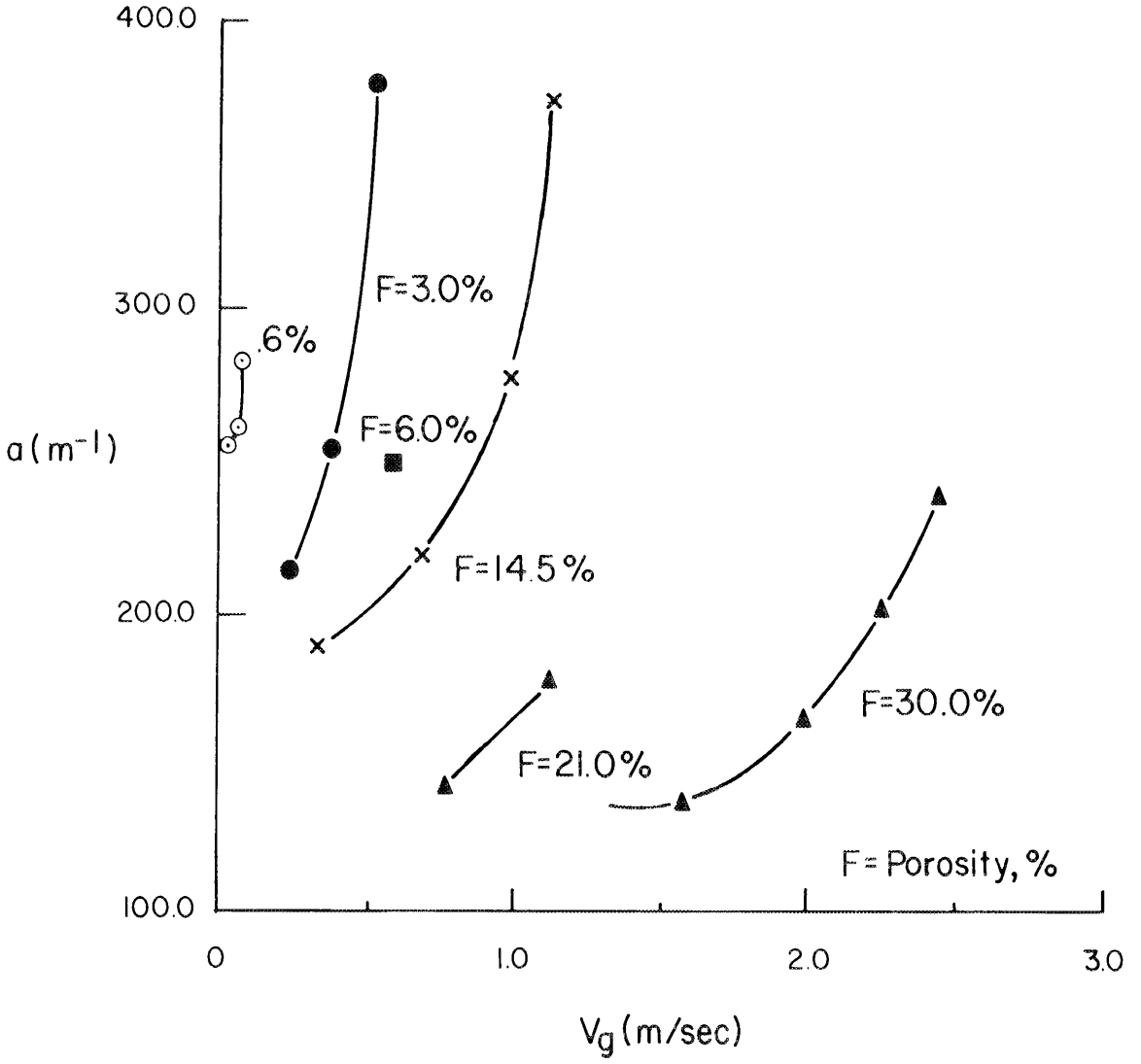

Figure E-3. A comparison of experimentally determined interfacial area in the sieve plate having 0.6% perforation with that obtained by other experimenters using sieve plates with higher-percent perforation.

APPENDIX F

DECOMPOSITION OF HNO_2 IN THE FROTH OF THE SIEVE PLATES

Decomposition of liquid HNO_2 has been described by Abel[23] to proceed by the reaction

$$-r_{HNO_2} = \frac{k_{37}(C_{HNO_2})^4}{P_{NO}^2} . \tag{F.1}$$

Assuming that the froth is well mixed,

$$-r_{HNO_2} = \frac{k_{37}(C_{HNO_2,out})^4}{P_{NO,out}^2} . \tag{F.2}$$

The steady-state decomposition of liquid HNO_2 on the first plate is calculated by using information from experiment 53:

$$\text{Froth temperature} = 298°K , \tag{F.3}$$

$$X_{HNO_2} = 0.29 , \tag{F.4}$$

$$P_{NO,out} = 0.095 \text{ atm} , \tag{F.5}$$

$$C^*_{HNO_2,in} = 0.182 \text{ kg•mole/m}^3 , \tag{F.6}$$

$$C_{HNO_2,out} = 0.129 \text{ kg•mole/m}^3 . \tag{F.7}$$

Abel's rate constant, k_{37}, at this temperature is -0.767 $m^9 atm^2/(kg \cdot mole^3\ sec)$. The quantity $C^*_{HNO_2,in}$ includes the HNO_2 produced on the tray. For a stirred system, the time required for the reaction is given by:

$$\tau = \frac{C^*_{HNO_2,in} X_{HNO_2}}{-r} . \tag{F.8}$$

Inserting numerical values yields:

$$\tau = \frac{(0.182)(0.29)}{(0.767)(0.129)^4/(0.095)^2} \tag{F.9}$$

and

$$\tau = 2.2 \text{ sec} . \tag{F.10}$$

The volume of froth at the experimental conditions is approximately $1.0 \times 10^{-4}\ m^3$; the scrubber liquid flow rate is $2.2 \times 10^{-5}\ m^3/sec$. Assuming a 25% void fraction,[54] the residence time for the liquid on a tray given by:

$$\tau = \frac{V_{FR}(1 - \varepsilon')}{L} \tag{F.11}$$

and

$$\tau = (1.0 \times 10^{-4})(1.0 - 0.25)/(2.2 \times 10^{-5}) = 3.4 \text{ sec} . \tag{F.12}$$

There appears to be time for the reaction to go to completion and the results in experiment 53 indicate that this is the case. The residence time of the liquid in the sieve plate froth is very close to the time

required for the decomposition of HNO_2. The assumption that equilibrium as expressed in Equations (3) and (37) has been attained means that the maximum HNO_2 decomposition and NO production are calculated. Thus, the overall model should be conservative in predicting NO_x removal.

APPENDIX G

COMPUTER PROGRAM

The computer code, which was written in FORTRAN, consisted of a main program and a number of subroutines which are given below.

```
                                                          PAGE  1
C       ***************************************************************
C       *                                                             *
C       *     THE MAIN PROGRAM IS FOR READING IN ANY DATA,CALLING     *
C       *     THE PROCESS MODEL OR THE OPTIMIZATION ROUTINE AND       *
C       *     PROVIDING OUTPUT OF THE RESULTS                         *
C       *                                                             *
C       ***************************************************************
C-----X IS CALCULATED CONVERSION OF NO2*
C-----XEXP IS THE EXPERMENTIAL CONVERSION NOX
C-----XNOX IS THE CALCULATED CONVERSION OF NOX
C-----TFROTH AND TGAS IS THE TEMP OF FROTH AND GAS IN DEGREES KELVIN
C-----CA, AND MTHREE ARE CONCENTRATIONS OF HNO3 IN KGMOLE/M3
C-----CB, AND MTWO ARE CONCENTRATIONS OF HNO2 IN KGMOLES/M3
C-----CBEQ IS THE EQULIBERIUM CONCENTRATION  OF HNO2 IN KGMOLES/M3
C-----MSUM IS THE TOTAL NO OF KGMOLES IN GAS PHASE ON BASIS OF 1 SEC
C-----M(I,J,K) IS KGMOLES OF COMPONENT K,STAGE I,POSITION J
C-----PREXP(I,J,K) IS THE EXPERIMENTAL PARTIAL PRESSURE OF COMPONENT I IN ATM
C-----PRCAL(I,J,K) IS THE CALCULATED PARTIAL PRESSURE OF COMPONENT K IN ATM
C-----PRNOX IS PRCAL(I,J,5)
C-----G(I,J) IS THE GAS FLOW RATE IN M3/SEC
C-----TGAS AND TFROTH ARE THE TEMPERATURES OF THE GAS AND LIQUID PHASES
C-----POSITION J = 1 ENTERING A STAGE AND J = 2 LEAVING THE BUBBLE LAYER
C-----NO2* IS COMPONENT 1
C-----NO  IS COMPONENT 2
C-----N2  IS COMPONENT 3
C-----O2  IS COMPONENT 4
C-----NOX IS COMPONENT 5
C-----L IS THE LIQUID FLOW RATE IN M3/SEC
C-----K IS A CHEMICAL REACTION RATE CONSTANT
C------TAW IS RESIDENCE TIME
C-----HFROTH,AFROTH,AND VFROTH ARE THE HEIGHT ,AREA AND THE VOLUME OF FROTH
C-----KLLOW AND KLHIGH ARE HIGH AND LOW LIQUID MASS TRANS. COEFF.
      DIMENSION P (6), STEP (6),DNO(6),RATIO(4)
      REAL KONE,KTHREE,KP,MU,PRCAL,PREXP,S,L,MACID,MTWO,MTHREE,KPCB,KKOB
     *,KVIS,KLHIGH,KLLOW
     #,KPABEL
      COMMON TFROTH(10),PRCAL(10,2,10),XEXP(10),G(10,2),NPLAT,X(10)
     *,TGAS(10),PREXP(10,2,10),MACID,XNO(10),XNOX(10),Y(10),CA,L
     *,CB(10),GAIR,KPCB(10),CBEQ(10),KPABEL(10),MTWO,KKOB(6),FSTEAM
     *,XCB(10)
      READ (14,1)NSET
  1   FORMAT (I10)
      DO 4 IN = 1,NSET
      READ (14,3) RUN,Y(1),Y(2),Y(3),Y(4),TGASF,TGAS(1),TGAS(2),TGAS(3),
     *TFROTH(1),TFROTH(2),TFROTH(3),FSTEAM,GAIR,L,MTWO,MTHREE,SPARGE,
     *FSPARG,RESLHT
  3   FORMAT (20F4.3)
C     CONVERSION OF DEGREES CENTIGRADE TO DEGREES KELVIN
      NPLAT=3
      TGASF=TGASF+273.
      NDATA=NPLAT+1
      DO 11 I = 1,NDATA
      TGAS(I)=TGAS(I)+273.
      TFROTH(I)=TFROTH(I)+273.
 11   CONTINUE
      DO 90 I = 1,NPLAT
```

```
C-----CALCULATION OF VISCOSITY IN CP
      MU=1.002*EXP(2.303*(1.327*(273.-TEROTH(I))-.001053*(TEROTH
     *(I)-273.)**2.)/(TEROTH(I)+105.))
C-----CALCULATION OF DIFFUSIVITY OF NO IN LIQUID PHASE
      DHNO2(I)=8.52E-8*TEROTH(I)/MU

C-----CALCULATION OF NITRIC ACID DENSITY
      ROH=(1.-2.83E-2*CA)-3.76E-4*(TEROTH(I)-293.)
C-----CALCULATION OF KINEMATIC VISCOSITY
      KVIS=MU/ROH
C-----CALCULATION OF LOW LIQUID MASS TRANS. COEFF.(CALDERBANK)
C-----CALCULATION OF HIGH LIQUID MASS TRANS. COEFF. (MOO-YOUNG)
 444  FORMAT (7F13.4)
      IF (MTWO .LE. 0.0) MTWO =.2
      CB(I)=0.0
      PRCAL(I,2,2)=.1-.03*FLOAT(I)
      CBEQ(I)=.1
C-----CALCULATION OF ABLE'S EQUILIBRIUM CONSTANT FOR HNO2
        TT=TEROTH(I)
C       KPABEL(I)=4.43*EXP(6648.52*(TT-273.2)/(TT*273.2))
        KPABEL(I)=13.3*EXP(5393.3*(TT-285.5)/(TT*285.5))
C       KPABEL(I)=1543.55-11.222*TEROTH(I)+.02054*TEROTH(I)**2.
      KPCB(I)=EXP((-2460.)/(1.987*TEROTH(I)))/600.
      R=82.05
      KPCB(I)=KPCB(I)*(R*TEROTH(I))**2.*1.E-6
  90  CONTINUE
      FSTEAM=.001*FSTEAM
      GAIR=.0001*GAIR
      GAIR=273./294.*GAIR
      L=.0001*L
      FSPARG=.000001*FSPARG
      CA=MTHREE
      MACID=MTWO+MTHREE
      TYPE 12,RUN,Y(1),Y(2),Y(3),Y(4),TGASF,TGAS(1),TGAS(2),TGAS(3),
     *TEROTH(1),TEROTH(2),TEROTH(3)
 12   FORMAT(5X,F2.0,11F11.3/)
      TYPE 13,FSTEAM,GAIR,L,MTWO,MTHREE,SPARGE,FSPARG,RESLHT
 13   FORMAT(7X,8E11.3)
C     CONVERSION OF MOLE FRACTION TO PARTIAL PRESSURE
      PREXP(1,1,1)=1.1*Y(1)
      PREXP(2,1,5)=1.1*Y(2)
      PREXP(3,1,5)=1.1*Y(3)
      PREXP(4,1,5)=1.1*Y(4)
      PREXP(1,1,2)=0.0
      PREXP(1,1,3)=.79*(1.1-PREXP(1,1,1))
      PREXP(1,1,4)=.21*(1.1-PREXP(1,1,1))
      PREXP(1,1,5)=PREXP(1,1,1)+PREXP(1,1,2)
      P(1)=0.0
        STEP(1)=.1
      DO 40 I = 1,NPLAT
        BB=PREXP(I+1,1,5)/PREXP(I,1,5)
        XEXP(I)=(1.-BB)/(1.-PREXP(I,1,5)*BB)
 40     CONTINUE
        CALL PROC (P,COST)
C       CALL PATERN(1,P,STEP,1,2,COST)
 344  CONTINUE
```

```
      TYPE 10
10    FORMAT(///)
      TYPE 15
15    FORMAT ('------------ PART. PRESSURE NOX IN COLUMN ------------'/)
      TYPE 16
16    FORMAT ('  RUN NO. ','   FEED   ','  STAGE 1 ','  STAGE 2 ','  STA
     *GE 3  '/)
      TYPE 20,RUN,PREXP(1,1,5),PREXP(2,1,5),PREXP(3,1,5),PREXP(4,1,5)
20    FORMAT (5E10.3//)
      TYPE 22
22    FORMAT ('------------ GAS PHASE TEMPERATURES IN COLUMN --------'/)
      TYPE 21,TGASF,TGAS(1),TGAS(2),TGAS(3)
21    FORMAT (10X,4E10.3//)
      TYPE 17
17    FORMAT ('-------------- FROTH TEMPERATURES IN COLUMN ----------'/)
      TYPE 30,TFROTH(1),TFROTH(2),TFROTH(3)
30    FORMAT (20X,3E10.3/)
      TYPE 18
18    FORMAT ('           AIR FLOW  ','  HNO3 CONC','  HNO2 CONC', ' SPARGE
     *'/)
      TYPE 50,GAIR,MTHREE,MTWO,FSPARG
50    FORMAT (10X,4E10.3)
      TYPE 19
19    FORMAT ('           LIG HOLD UP'/)
      TYPE 23,RESLHT
23    FORMAT (10X,E10.3//)
      TYPE 24
24    FORMAT (' CALCULATED AND EXPERMENTAL NOX PROFILES IN COLUMN')
      TYPE 25
25    FORMAT ('                    NOX PARTIAL PRESSURES (IN ATM)'/)
      TYPE 26
26    FORMAT ('                  POSITION          EXP        CAL'/)
      TYPE 29,PREXP(1,1,5),PRCAL(1,1,5)
29    FORMAT (20X,'  FEED     ',2E10.3/)
      DO 27 I =2,NDATA
      ID=I-1
      TYPE 28,ID,PREXP(I,1,5),PRCAL(I-1,2,5)
28    FORMAT (20X,'STAGE-',I1,2X,2E10.3/)
27    CONTINUE
      TYPE 70
70    FORMAT ('----------- GAS FLOW RATE THROUGH COLUMN ------------'/)
      TYPE 71
71    FORMAT ('            FROTH   GAS SPACE'/)
      DO 60 I = 1,NPLAT
      TYPE 61,I,G(I,1),G(I,2)
61    FORMAT ('  STAGE-',I2,' ',2E10.3/)
60    CONTINUE
      TYPE 31
31    FORMAT ('--CAL. AND EXP. CONVERSIONS OF NO2 AND EXP. CONV. OF NO-
     *'/)
      TYPE 32
32    FORMAT (10X,' XNOX-EXP  XNOX-CAL  XNO2-CAL   XNO-CAL'/)
      DO 33 I = 1,NPLAT
      TYPE 34,I,XEXP(I),XNOX(I),X(I),XNO(I),XC3(I)
34    FORMAT (2X,'STAGE-',I2,5E10.3/)
33    CONTINUE
```

```
      TYPE 64
64    FORMAT ('-------- GAS COMPOSITION VERSES COLUMN LOCATION ------'/)
      TYPE 65
65    FORMAT ('            NO2*        NO            O2          N2          NO2*
     *       NO           O2        N2'/)
      DO 62 I= 1,NPLAT
      TYPE 63,I,PRCAL(I,1,1),PRCAL(I,1,2),PRCAL(I,1,4),PRCAL(I,1,3),
     *PRCAL(I,2,1),PRCAL(I,2,2),PRCAL(I,2,4),PRCAL(I,2,3)
63    FORMAT ('  STAGE-',I2,8E10.3/)
62    CONTINUE
      TYPE 102,CB(1)
102   FORMAT ('     NITROUS ACID CONC. LEAVING COLUMN IS',F5.3,/)
 4    CONTINUE
      STOP
      END
```

```
      SUBROUTINE PATERN(NP,P,STEP,NRD,IO,COST)
C       ***************************************************************
C       *                                                             *
C       *     PATERN IS A COMPLETE NUMERICAL SEARCH TECHNIQUE         *
C       *     EMPLOYING A PATTERN SEARCH STRATEGY                     *
C       *     BY C.F.MOORE,C.L.SMITH,AND P.W.MURRILL; L.S.U.          *
C       *     BATON ROUGE,LOUISIANA 70803                             *
C       *                                                             *
C       ***************************************************************
C-----THE SIZE OF B1,B2,T,AND S NEED ONLY BE EQUAL TO THE NUMBER OF PAR
      DIMENSION P(NP),STEP(NP),B1(10),B2(10),T(10),S(10)
C-----STARTING POINT
      L=1
      ICK=2
      ITTER=0
      DO5 I=1,NP
      B1(I)=P(I)
      B2(I)=P(I)
      T(I)=P(I)
  5   S(I)=STEP(I)*10.
C-----INITIAL BOUNDARY CHECK AND COST EVALUATION
      CALL BOUNDS(P,IOUT)
      IF(IOUT.LE.0)GOTO10
                    IF(IO.LE.0)GOTO6
                    TYPE 1005
                    WRITE(5,1000)(J,P(J),J=1,NP)
  6   RETURN
 10   CALL PROC(P,C1)
                    IF(IO.LE.1)GOTO11
                    WRITE(5,1001)ITTER,C1
                    WRITE(5,1000)(J,P(J),J=1,NP)
C-------BEGINNING OF PATTERN SEARCH STRATEGY
 11   DO99 INRD=1,NRD
      DO12 I=1,NP
 12   S(I)=S(I)/10.
                    IF(IO.LE.1)GOTO20
                    WRITE(5,1003)
                    WRITE(5,1000)(J,S(J),J=1,NP)
 20   IFAIL=0.0
C-----PRETURBATION ABOUT T
      DO30 I=1,NP
      IC=0
 21   P(I)=T(I)+S(I)
      IC=IC+1
      CALL BOUNDS(P,IOUT)
      IF(IOUT.GT.0)GOTO23
      CALL PROC(P,C2)
                    L=L+1
                    IF(IO.LT.3)GOTO22
                    WRITE(5,1002)L,C2
                    WRITE(5,1000)(J,P(J),J=1,NP)
 22   IF(C1-C2)23,23,25
 23   IF(IC.GE.2)GOTO24
      S(I)=-S(I)
      GOTO21
 24   IFAIL=IFAIL+1
```

```
      P(I)=T(I)
      GOTO30
 25   T(I)=P(I)
      C1=C2
 30   CONTINUE
      IF(IFAIL.LT.NP)GOTO35
      IF(ICK.EQ.2)GOTO90
      IF(ICK.EQ.1)GOTO35
      CALL PROC(T,C2)
                    L=L+1
                    IF(IO.LT.3)GOTO31
                    WRITE(5,1002)L,C2
                    WRITE(5,1000)(J,T(J),J=1,NP)
 31   IF(C1-C2)32,34,34
 32   ICK=1
      DO33 I=1,NP
      B1(I)=B2(I)
      P(I)=B2(I)
 33   T(I)=B2(I)
      GOTO20
 34   C1=C2
 35   IB1=0
      DO39 I=1,NP
      B2(I)=T(I)
      IF(ABS(B1(I)-B2(I)).LT..01*ABS(S(I))) IB1=IB1+1
 39   CONTINUE
      IF(IB1.EQ.NP)GOTO90
      ICK=0
                    ITTER=ITTER+1
                    IF(IO.LT.2)GOTO40
                    WRITE(5,1001)ITTER,C1
                    WRITE(5,1000)(J,T(J),J=1,NP)
C-----ACCELERATION STEP
 40   SJ=1.0
      DO45 II=1,11
      DO42 I=1,NP
      T(I)=B2(I)+SJ*(B2(I)-B1(I))
 42   P(I)=T(I)
      SJ=SJ-.1
      CALL BOUNDS(T,IOUT)
      IF(IOUT.LT.1)GOTO46
      IF(II.EQ.11)ICK=1
 45   CONTINUE
 46   DO47 I=1,NP
 47   B1(I)=B2(I)
      GOTO20
 90   DO91 I=1,NP
 91   T(I)=B2(I)
 99   CONTINUE
      DO100 I=1,NP
100   P(I)=T(I)
      COST=C1
                    IF(IO.LE.0)RETURN
                    WRITE(5,1004)L,C1
                    WRITE(5,1000)(J,P(J),J=1,NP)
      RETURN
```

```
1000  FORMAT(10X,5(I7,E13.6)/)
1001  FORMAT(//1X14HITTERATION NO.  ,I5/5X,5HCOST= ,E15.6,20X,
     1   10HPARAMETERS)
1002  FORMAT(10X3HNO.,I4, 8X5HCOST=,E15.6)
1003  FORMAT(/1X28HSTEP SIZE FOR EACH PARAMETER    )
1004  FORMAT(1H113HANSWERS AFTER ,I3,2X,23HFUNCTIONAL EVALUATIONS    //
     1   5X5HCOST=,E15.6,20X,18HOPTIMAL PARAMETERS  )
1005  FORMAT(1H135HINITIAL PARAMETERS OUT OF BOUNDS          )
      END
```

```
      SUBROUTINE PROC (P,COST)
C       ****************************************************************
C       *                                                              *
C       *     PROC CONTAINS THE OVERALL LOGIC USED IN CALCULATING      *
C       *     NOX SCRUBBING EFFIENCY PER PLATE IN A MULTISTAGE SIEVE   *
C       *     PLATE COLUMN                                             *
C       *                                                              *
C       ****************************************************************
      DIMENSION P(6),M(10,2,10),KCB(10),PRNOX(10)
      REAL MACID,KPCB,L,MSUM,KCB,KPABEL,MTWO,KKOB
        REAL*8 NOPROD,M
C------P(I,J,K) IS PARTIAL PRESSURE OF COMPONENT K IN I'TH STAGE,POSITION J
      COMMON TFROTH(10),PRCAL(10,2,10),XEXP(10),G(10,2),NPLAT,X(10)
     *,TGAS(10),PREXP(10,2,10),MACID,XNO(10),XNOX(10),Y(10),CA,L
     *,CB(10),GAIR,KPCB(10),CBEQ(10),KPABEL(10),MTWO,KKOB(6),FSTEAM
     *,XCB(10)
C*****NO2*IS COMPONENT 1
C*****NO  IS COMPONENT 2
C*****N2  IS COMPONENT 3
C*****O2  IS COMPONENT 4
C------NOX IS COMPONENT 5
C     CALCULATION OF RATE CONSTANT FOR NITROUS ACID DISAPPEARANCE
      DO 30 I=1,NPLAT
C       INITIAL GUESSES
        PRNOX(I)=0.0
        G(I,2)=.0002
        CB(I)=0.05
       KCB(I)=.01*EXP(1.2E5*((TFROTH(I)-273.)/(273.*TFROTH(I)))/8.314)
   30 CONTINUE
        R=.08205
      NPASS=0
      V=.00003988
  14  CONTINUE
      M(1,1,3)=.03882*GAIR
      M(1,1,4)=.01034*GAIR
      M(1,1,1)=(M(1,1,3)+M(1,1,4))*Y(1)/(1.-Y(1))
      M(1,1,2)=0.0D0
      M(1,1,5)=M(1,1,1)
      CONV=0.0
      COST=0.0
      I=1
      MSUM=M(I,1,1)+M(I,1,2)+M(I,1,3)+M(I,1,4)
      PRCAL(I,1,1)=1.1*M(I,1,1)/MSUM
      PRCAL(I,1,2)=1.1*M(I,1,2)/MSUM
      PRCAL(I,1,4)=1.1*M(I,1,4)/MSUM
      PRCAL(I,1,3)=1.1*M(I,1,3)/MSUM
      PRCAL(I,1,5)=1.1*(M(I,1,1)+M(I,1,2))/MSUM
      DO 2 I=1,NPLAT
        PT=1.1
      RATIO=FSTEAM/L
      J=1
      G(I,1)=.0745*MSUM*TFROTH(I)
      IF (PRCAL(I,1,1) .LE. .001) GO TO 41
C       IF (I .GT. 1) GO TO 888
C       IF (FSTEAM .EQ. 0.0) GO TO 888
C       X(1)=.7722+7967.43*L-131377500*L**2.
```

```
C         X(I)=X(I)-1000.*(G(I,1)-.0002)
C        GO TO 42
888     CONTINUE
        CALL FROTH (FSTEAM,P,MACID,PRCAL,TFROTH,G,I,L,X)
        GO TO 42
  41    X(I)=0.0
  42    CONTINUE
C-----CALCULATION OF GAS COMPOSITION LEAVING FROTH
        M(I,2,1)=M(I,1,1)*(1.-X(I))
        AFROTH=.00213
        HFROTH=.031+67.7*G(I,1)+177.1*(L-17.5E-6)
        VFROTH=AFROTH*HFROTH
          CB(NPLAT+1)=CB(1)
          CXXX=CB(I+1)+.5*M(I,1,1)*X(I)/L
          GSTAR=G(I,2)
        CALL NITRUS (L,GSTAR,CXXX,CA,KPABFL(I),PRCAL(I,1,2),
       *TFROTH(I),R,XCB(I))
 1011   FORMAT(6(2X,E10.3))
 223    CONTINUE
C         TYPE 51,XCB(I)
          NOPROD=.667*L*CXXX*XCB(I)
C        NOPROD=.667*R*TFROTH(I)*CXXX*XCB(I)
C         NOPROD=.333*M(I,1,1)*X(I)
 336    FORMAT (3X,E14.3)
C        IF (NOPROD .LE. 0.0) NOPROD=0.0
          CB(I)=CXXX*(1.-XCB(I))
  51    FORMAT (E10.4)
        M(I,2,2)=M(I,1,2) + NOPROD
        MSUM=M(I,2,1)+M(I,2,2)+M(I,1,3)+M(I,1,4)
        M(I,2,3)=M(I,1,3)
        M(I,2,4)=M(I,1,4)
        G(I,2)=.0745*MSUM*TGAS(I)
        PRCAL(I,2,1)=1.1*M(I,2,1)/MSUM
        PRCAL(I,2,2)=1.1*M(I,2,2)/MSUM
        PRCAL(I,2,3)=1.1*M(I,2,3)/MSUM
        PRCAL(I,2,4)=1.1*M(I,2,4)/MSUM
        PRCAL(I,2,5)=1.1*(M(I,2,1)+M(I,2,2))/MSUM
        IF (PRCAL(I,2,2) .LT. .001)GO TO 3
 203    FORMAT (3(4X,E10.3))
        CALL GAS (PRCAL,P,TGAS,G,I,XNO)
        GO TO 4
  3     CONTINUE
        XNO(I)=0.0
  4     CONTINUE
        M(I+1,1,1)=M(I,2,1)+M(I,2,2)*XNO(I)
        M(I+1,1,2)=M(I,2,2)*(1.-XNO(I))
        M(I+1,1,3)=M(I,2,3)
          B=M(I,2,2)/M(I,2,4)
        M(I+1,1,4)=M(I,2,4)*(1.-B*XNO(I))
        M(I+1,1,5)=M(I+1,1,1)+M(I+1,1,2)
        MSUM=M(I+1,1,1)+M(I+1,1,2)+M(I+1,1,3)+M(I+1,1,4)
        PRCAL(I+1,1,1)=1.1*M(I+1,1,1)/MSUM
        PRCAL(I+1,1,2)=1.1*M(I+1,1,2)/MSUM
        PRCAL(I+1,1,4)=1.1*M(I+1,1,4)/MSUM
        PRCAL(I+1,1,3)=1.1*M(I+1,1,3)/MSUM
        PRCAL(I+1,1,5)=1.1*(M(I+1,1,1)+M(I+1,1,2))/MSUM
```

```
C         TYPE 245,PRCAL(I+1,1,5)
          BB=PRCAL(I+1,1,5)/PRCAL(I,1,5)
  245     FORMAT (E10.4)
        XNOX(I)=(1.-BB)/(1.-PRCAL(I,1,5)*BB)
        CONV = CONV+ABS(PRNOX(I)-PRCAL(I,2,5))
          PRNOX(I)=PRCAL(I,2,5)
C-----XNOX( ) IS THE CALCULATED NOX CONVERSION
        XDIFF=PREXP(I+1,1,5)-PRCAL(I,2,5)
        XDIFF=ABS(XDIFF)
 303    FORMAT (30X,3E13.6)
        COST=COST+XDIFF
 2      CONTINUE
        NPASS=NPASS+1
C         TYPE 356,CB(1),CB(2),CB(3)
  356     FORMAT (3E14.6)
        IF (NPASS .GT. 500) GO TO 13
          IF (CONV .GT. .0001) GO TO 14
 13     CONTINUE
        IF (NPASS .GT. 500) TYPE 500
 500    FORMAT (' THE NITROUS ACID CONCENTRATION IS NOT CONV.')
        RETURN
        END
```

```
      SUBROUTINE BOUNDS (P,IOUT)
C       ***************************************************************
C       *                                                             *
C       *     BOUNDS CONTAINS THE BOUNDARIES OF THE VARIABLES         *
C       *     BEING OPTIMIZED                                         *
C       *                                                             *
C       ***************************************************************
      DIMENSION P(6)
      IOUT = 0
      IF (P(1) .LT. 0.0) IOUT = 1
C      IF (P(2) .LT. 0.0) IOUT = 1
C      IF (P(3) .LT. 0.0) IOUT = 1
      RETURN
      END
```

```
      SUBROUTINE GAS (PR,P,T,G,I,XNO)
C       ***************************************************************
C       *                                                             *
C       *     GAS USES THE BISECTION METHOD OF SOLVING FOR THE        *
C       *     CONVERSION OF NO TO NO2,XNO(I), IN A GIVEN GAS SPACE    *
C       *     BETWEEN THE SIEVE PLATES                                *
C       *                                                             *
C       ***************************************************************
C-----P(I,J,K) IS PARTIAL PRESSURE OF COMPONENT K IN I'TH STAGE,POSITION J
C-----POSITION J = 1 ENTERING A STAGE AND J = 2 LEAVING THE BUBBLE LAYER
C-----T IS TEMPERATURE DEGREES KELVIN
C-----K IS THIRD ORDER REACTION RATE CONSTATNT FOR NO OXIDATION
C-----V IS VOLUME OF FREE SPACE BETWEEN PLATES IN CUBIC METERS
C-----R IS IDEAL GAS LAW CONSTANT
C-----SOLUTION INVOLVES FINDING THE ROOT,XNO, OF A THIRD DEGREE POLYNOMIAL
C-----XNO IS CONVERSION OF NO
C-----THE BISECTION METHOD
      DIMENSION G(10,2),PR(10,2,10),T(10),P(5),XNO(10)
      REAL K
      NPASS = 0
      CXZ = 0
      XL = 0.0010
      XR = .9990
        B=PR(I,J,2)/(2.*PR(I,J,4))
      J=2
      EPI = .0000000001
      R = .082
      PT= 1.1
      VGAS=.000687
 27   FORMAT (F10.4,2X,F10.4/)
C       BODENSTEIN'S RATE CONSTANT
C      K=.2166*EXP(1399./T(I))
C       RATE CONSTANT BY GREIG AND HALL
        K=3.3364E+02-1.63025*T(I)+2.08146E-03*T(I)**2.
      TAW=VGAS/G(I,2)
      A = K*TAW *PR(I,J,2)*PR(I,J,4)
 101  FORMAT (2(4X,E10.3))
      CALL EVALG (B,A,XR,FXR)
      CALL EVALG (B,A,XL,FXL)
      AFXL = ABS(FXL)
      AFXR = ABS(FXR)
      IF(AFXL - EPI) 20,20,10
 10   IF(AFXR - EPI) 21,21,11
 11   IF (FXL * FXR .LT. 0.0) GO TO 12
      TYPE 13
 13   FORMAT(5X,' METHOD NOT APPLICABLE')
      XNO(I)=0.0
      GO TO 23
 12   IF(XR-XL) 14,14,15
 14   XZ = (XL - XR)/2
      CALL EVALG (B,A,XZ,FXZ)
      XNO(I)=XZ
      GO TO 23
 15   TXL = XL
      TXR = XR
 16   NPASS = NPASS + 1
```

```
      XZ = (TXL + TXR)/2
      XNO(I)=XZ
      CONV = ABS(XZ -CXZ)
      IF (CONV .LT. EPI) GO TO 40
      IF (NPASS .GT. 1000) GO TO 40
      GO TO 30
 40   CONTINUE
      GO TO 100
 30   CONTINUE
      CXZ = XZ
      CALL EVALG (B,A,XZ,FXZ)
      AFXZ = ABS (FXZ)
      ADXZ = ABS (TXL - TXR)
      IF (AFXZ .LE. EPI) GO TO 24
      IF (ADXZ .LE. EPI) GO TO 24
      IF (FXL * FXZ .LT. 0) GO TO 25
      TXL = XZ
      FXL=FXZ
      GO TO 16
 20   CONTINUE
      XNO(I)=XL
      GO TO 23
 21   CONTINUE
      XNO(I)=XR
      GO TO 23
 24   CONTINUE
 25   TXR = XZ
      FXR=FXZ
      XNO(I)=XZ
      GO TO 16
  23  CONTINUE
100   CONTINUE
      RETURN
      END
```

```
      SUBROUTINE EVALG (B,A,X,FX)
C       ***********************************************************
C       *                                                         *
C       *     EVALG CONTAINS THE FUNCTION WHOSE ROOT IS SOUGHT IN GAS  *
C       *                                                         *
C       ***********************************************************
C      IF NFLOW EQ 2,THE MODEL USED IS PLUG FLOW
C      IF NFLOW EQ 1, THE FLOW IS ASSUMED TO BE MIXED
      NFLOW=1
      IF (NFLOW .EQ. 2) GO TO 2
      FX=X-A*(1.-((B/2)+2.)*X+(B+1.)*X**2.-(B/2)*X**3.)
      GO TO 1
    2 CONTINUE
      FX=A-2.*(1./(1.-X)-ALOG((1.-B*X)/(1.-X))-1.)
    1 CONTINUE
      RETURN
      END
```

```
      SUBROUTINE NITRUS (L,G,CHNO2,CHNO3,K,PNO,T,R,X)
C     ***************************************************************
C     *                                                             *
C     *     NITRUS USES THE BISECTION METHOD FOR FINDING THE        *
C     *     CONVERSION OF HNO2,X, IN THE FROTH OF A GIVEN PLATE     *
C     *                                                             *
C     ***************************************************************
C-----THE BISECTION METHOD
      REAL K,L
      IF (CHNO2 .LE. 0.0) GO TO 100
      NPASS= 0
      CXZ = 0
      XL =-1E6
      A=.667*(L/G)*R*T*CHNO2*XL
      TEST=PNO*A
      IF (TEST .LT. 0.0) XL=(-1.5)*G*PNO/(L*R*T*CHNO2)
      XR =.99

      EPI = .000001
      CALL EVALN (L,G,CHNO2,CHNO3,K,PNO,T,R,XR,FXR)
      CALL EVALN (L,G,CHNO2,CHNO3,K,PNO,T,R,XL,FXL)
      AFXL = ABS(FXL)
      AFXR = ABS(FXR)
      IF(AFXL - EPI) 20,20,10
 10   IF(AFXR - EPI) 21,21,11
 11   IF (FXL * FXR .LT. 0.0) GO TO 12
      TYPE 13
 13   FORMAT(5X,' METHOD NOT APPLICABLE IN NIT')
      X=0.0
      GO TO 23
 12   IF(XR-XL) 14,14,15
 14   XZ = (XL - XR)/2
      CALL EVALN (L,G,CHNO2,CHNO3,K,PNO,T,R,XZ,FXZ)
      X = XZ
      GO TO 23
 15   TXL = XL
      TXR = XR
 16   NPASS = NPASS + 1
      XZ = (TXL + TXR)/2
      X=XZ
      CONV = ABS(XZ -CXZ)
      IF (CONV .LT. EPI) GO TO 40
      IF (NPASS .GT. 1000) GO TO 40
      GO TO 30
 40   CONTINUE
      GO TO 100
 30   CONTINUE
      CXZ = XZ
      CALL EVALN (L,G,CHNO2,CHNO3,K,PNO,T,R,XZ,FXZ)
      AFXZ = ABS (FXZ)
      ADXZ = ABS (TXL - TXR)
      IF (AFXZ .LE. EPI) GO TO 24
      IF (ADXZ .LE. EPI) GO TO 24
      IF (FXL * FXZ .LT. 0) GO TO 25
      TXL = XZ
      FXL=FXZ
```

```
      GO TO 16
 20   CONTINUE
      X=XL
      GO TO 23
 21   CONTINUE
      X=XR
      GO TO 23
 24   CONTINUE
 25   TXR = XZ
      FXR=FXZ
      X=XZ
      GO TO 16
  23  CONTINUE
100   CONTINUE
        IF (CHNO2 .LE. 0.0) X=0.0
C       TYPE 22,X
  22    FORMAT (E14.5)
      RETURN
      END
```

```
      SUBROUTINE EVALN (L,G,CHNO2,CHNO3,K,PNO,T,R,X,F)
C       ***************************************************************
C       *                                                             *
C       *      EVALN CONTAINS THE FUNCTION WHOSE ROOT IS SOUGHT       *
C       *      BY NITRUS                                              *
C       *                                                             *
C       ***************************************************************
      REAL K,L
 103  FORMAT ('  MADE IT TO EVALN')
 100  FORMAT (20X,E12.4)
C-----CALCULATION OF ACTIVITY COEFFICIENT FOR HNO3 (ABLE)
      ACA=EXP(-.34857+(CHNO3-1.)*.10213)
 23   FORMAT (E12.4)
        TEST=PNO+.667*(L/G)*R*T*CHNO2*X
        IF (TEST .LE. 0.0) GO TO 1
      F=K**.333*(CHNO2*(1.-X))-(ACA*CHNO3)**.667*(PNO
     **.667*(L/G)*R*T*CHNO2*X)**.667
        GO TO 2
  1           F=K*(CHNO2*(1.-X))**3
  2     CONTINUE
C       TYPE 101,ACA,CHNO3,CHNO2,L,G,K,R,F,PNO,T,X
 101  FORMAT (11(3X,E14.6))
      RETURN
      END
```

```
      SUBROUTINE FROTH (FSTEAM,P,MACID,PRCAL,T,G,I,L,X)
C       ****************************************************************
C       *                                                              *
C       *     FROTH USES THE BISECTION METHOD OF FINDING THE           *
C       *     CONVERSION OF NO2* (THE AMOUNT OF NO2* ABSORBED          *
C       *     PER PLATE), X(I), IN THE FROTH OF A GIVEN PLATE          *
C       *                                                              *
C       ****************************************************************
C-----PRCAL(I,J,K) IS PARTIAL PRESSURE OF COMPONENT K IN I'TH STAGE,POSITION J
      REAL KONE,PRCAL,KP,MU,MACID,L
      DIMENSION PRCAL(10,2,10),T(10),G(10,2),X(10),P(5)
C     CALCULATION OF EQUILIBERIUM CONSTANT FOR NO2 AND N2O4
      KP=.685E-9*EXP(6866./T(I))
      KP=1./KP
      J=1
C     VFROTH IS VOLUME OF FROTH ON SIEVE PLATE
C-----CALCULATION OF FROTH VOLUME
      AFROTH=.00213
      HFROTH=.031+67.7*G(I,1)+177.1*(L-17.5E-6)
      VFROTH=AFROTH*HFROTH
C     R IS IDEAL GAS LAW CONSTANT
      R = .082
      AREA=333.-1.025E6*G(I,1)+3.544E9*G(I,1)**2.

        IF (I .GT. 1) GO TO 112
 111   IF (FSTEAM .LE.0.0) GO TO 112
        AREA=AREA*(1.94254+2047.3*FSTEAM)
        AREA=AREA*(2.34-1.212E5*L+2.3119E9*L**2)
 112    CONTINUE
      FACTOR=4.*PRCAL(I,1,1)/KP
      A=1.+FACTOR
      B=1.+2.*FACTOR
      C=2.*FACTOR
      D=FACTOR
      EKL=SQRT(DI*KONE)
      EKLHE=10**(-.5198-745.31/T(I))*EXP((-1)*.0375*MACID)
      F=EKLHE*AREA*VFROTH*R*T(I)/(FACTOR*G(I,1))
      CXZ = 0
      XL = 0.0010
      XR = .9999
      EPI = .00000001
      NPASS = 0
C-----THE BISECTION METHOD
      CALL EVAL (A,B,C,D,F,XR,FXR)
      CALL EVAL (A,B,C,D,F,XL,FXL)
      AFXL = ABS(FXL)
      AFXR = ABS(FXR)
      IF(AFXL - EPI) 20,20,10
 10   IF(AFXR - EPI) 21,21,11
 11   IF (FXL * FXR .LT. 0.0) GO TO 12
      TYPE 13
 13   FORMAT(5X,' A ROOT IS NOT FOUND IN INTERVAL FOR FROTH MODEL')
      PRINT 2000,I
2000  FORMAT (  'THE PROGRAM HAS FAILED ON STAGE-',I2/)
1000  FORMAT (E14.8)
      PRINT 1000, FXL
```

```
      PRINT 1000, FXR
      IF (FXL .GT. 0.0) X(I)=0.0
      IF (FXL .LT. 0.0) X(I)=1.0
      GO TO 23
 12   IF(XR-XL) 14,14,15
 14   XZ = (XL - XR)/2
      CALL EVAL (A,B,C,D,F,XZ,FXZ)
      X(I)=XZ
      GO TO 23
 15   TXL = XL
      TXR = XR
 16   NPASS = NPASS + 1
      XZ = (TXL + TXR)/2
      X(I)=XZ
      CONV = ABS(XZ -CXZ)
      IF (CONV .LT. EPI) GO TO 40
      IF (NPASS .GT. 1000) GO TO 40
      GO TO 30
 40   CONTINUE
      GO TO 100
 30   CONTINUE
      CXZ = XZ
      CALL EVAL (A,B,C,D,F,XZ,FXZ)
      AFXZ = ABS (FXZ)
      ADXZ = ABS (TXL - TXR)
      IF (AFXZ .LE. EPI) GO TO 24
      IF (ADXZ .LE. EPI) GO TO 24
      IF (FXL * FXZ .LT. 0) GO TO 25
      TXL = XZ
      FXL=FXZ
      GO TO 16
 20   CONTINUE
      X(I)=XL
      GO TO 23
 21   CONTINUE
      X(I)=XR
      GO TO 23
 24   CONTINUE
 25   TXR = XZ
      FXR=FXZ
      X(I)=XZ
      GO TO 16
100   CONTINUE
 23   CONTINUE
      RETURN
      END
```

```
      SUBROUTINE EVAL (A,B,C,D,F,X,FX)
C       ***************************************************************
C       *                                                             *
C       *      EVAL CONTAINS THE FUNCTION WHOSE ROOT IS SOUGHT IN FROTH *
C       *                                                             *
C       ***************************************************************
      REAL KAPPA
      AA=B-C*X
      PHI=ALOG((SQRT(AA)-1.0)/(SQRT(B)-1.0))
      SIGMA=(SQRT(AA)-SQRT(B))/((SQRT(AA)-1.0)*(SQRT(B)-1.0))
      KAPPA=F*D/2.
      FX=PHI+SIGMA+KAPPA
      RETURN
      END
```

ORNL-5438
Dist. Category UC-79c

INTERNAL DISTRIBUTION

1. J. M. Begovich
2. M. R. Bennett
3. R. E. Blanco
4. J. O. Blomeke
5. W. D. Bond
6. B. F. Bottenfield
7. E. C. Bradley
8. N. C. Bradley
9. R. E. Brookbank
10. C. H. Brown, Jr.
11. K. B. Brown
12-16. W. D. Burch
17. D. O. Campbell
18. J. M. Chandler
19. H. E. Cochran, Jr.
20. D. A. Costanzo
21-30. R. M. Counce
31. D. J. Crouse
32. B. F. Crump
33. J. P. Drago
34. B. C. Duggins
35. M. J. Feldman
36. D. E. Ferguson
37. T. M. Gilliam
38. J. H. Goode
39. N. R. Grant
40-44. W. S. Groenier
45. W. R. Hamel
46. D. C. Hampson
47. B. A. Hannaford
48. W. O. Harms
49. J. N. Herndon
50. J. R. Hightower
51. D. W. Holliday
52. W. D. Holland
53. J. M. Holmes
54. A. R. Irvine
55. J. D. Jenkins
56. R. T. Jubin
57. A. D. Kelmers
58. L. J. King
59. J. Q. Kirkman
60. J. A. Klein
61. R. E. Leuze
62. B. E. Lewis
63. J. C. Mailen
64. J. D. McGaugh
65. L. E. McNeese
66. R. P. Milford
67. J. G. Morgan
68. E. L. Nicholson
69. E. D. North
70. F. L. Peishel
71. J. J. Perona
72. H. Postma
73. R. H. Rainey
75. A. D. Ryon
76. W. F. Shaffer, Jr.
77. C. D. Scott
78. B. B. Spencer
79. M. J. Stephenson
80. J. G. Stradley
81. J. B. Talbot
82. D. B. Trauger
83. W. E. Unger
84. V. C. A. Vaughen
85. B. L. Vondra
86. J. S. Watson
87. B. S. Weil
88. T. D. Welch
89. M. E. Whatley
90. J. R. White
91. R. G. Wymer
92. O. O. Yarbro
93. E. L. Youngblood
94. S. Beard (consultant)
95. L. Burris, Jr. (consultant)
96. A. B. Carson (consultant)
97. E. L. Gaden, Jr. (consultant)
98. C. H. Ice (consultant)
99. R. B. Richards (consultant)
100. A. Schneider (consultant)
101. L. E. Swabb, Jr. (consultant)
102. M. J. Szulinski (consultant)
103. J. S. Theilacker (consultant)
104. A. K. Williams (consultant)
105-106. Central Research Library
107. ORNL—Y-12 Technical Library, Document Reference Section
109. Laboratory Records

110. Laboratory Records, ORNL RC
111. ORNL Patent Office
112. Nuclear Safety Information Center

EXTERNAL DISTRIBUTION

113. Director, Reactor Division, DOE-ORO
114-115. Director, Division of Nuclear Fuel Cycle and Production, DOE, Washington, D.C. 20545
116-117. Division of Reactor Research and Development, DOE, Washington, D.C. 20545
118. F. A. Lijewski, Westinghouse Electric Corporation, Advanced Reactors Division, Waltz Mill Site, P. O. Box 158, Madison, PA 15563
119. Duane E. Clayton, Battelle Pacific Northwest Laboratory, P. O. Box 999, Richland, WA 99352
120. Martin Friedland, Gulf + Western Advanced Development and Engineering Center, 101 Chester Road, Swarthmore, PA 19081
121. Jerry M. Friedman, Sandia Laboratories, P. O. Box 5800, Albuquerque, NM 87115
122. Frank J. Jones, Bechtel Corporation, P. O. Box 3965, San Francisco, CA 94119
123. B. F. Judson, Vice-President & Mgr., GEUMCO-Engineering, 175 Curtner Avenue — Mail Code 858 San Jose, California 95125
124. R. S. Karinen, Programmed and Remote Systems Corporation, 3460 Lexington Avenue, St. Paul, MN 55112
125. Robert H. Karlsson, Rockwell International, Atomics International Division, Rocky Flats Plant, P. O. Box 464, Golden, CO 80401
126. R. E. Mullen, Aerojet Manufacturing Company, 601 South Placentia Avenue, P. O. Box 4210, Fullerton, CA 92634
127. D. E. Wood, Kaman Sciences Corporation, 1500 Garden of the Gods Road, P. O. Box 7463, Colorado Springs, CO 80933
128. Research and Technical Support Division, DOE-ORO
129-337. Given distribution as shown in TID-4500 under UC-79c, Fuel Recycle Category (Applied)

☆ U.S. GOVERNMENT PRINTING OFFICE: 1978-748-189/199